
Electronic Thesis and Dissertation Repository

11-7-2018 3:00 PM

Characterization Of The Coat Protein Of Turnip Mosaic Virus And Its Arabidopsis Interactors In The Virus Infection Process

Zhaoji Dai, *The University of Western Ontario*

Supervisor: Wang, Aiming, *The University of Western Ontario*

Co-Supervisor: Bernards, Mark, *The University of Western Ontario*

A thesis submitted in partial fulfillment of the requirements for the Doctor of Philosophy degree in Biology

© Zhaoji Dai 2018

Follow this and additional works at: <https://ir.lib.uwo.ca/etd>



Part of the [Plant Pathology Commons](#)

Recommended Citation

Dai, Zhaoji, "Characterization Of The Coat Protein Of Turnip Mosaic Virus And Its Arabidopsis Interactors In The Virus Infection Process" (2018). *Electronic Thesis and Dissertation Repository*. 5800.
<https://ir.lib.uwo.ca/etd/5800>

This Dissertation/Thesis is brought to you for free and open access by Scholarship@Western. It has been accepted for inclusion in Electronic Thesis and Dissertation Repository by an authorized administrator of Scholarship@Western. For more information, please contact wlsadmin@uwo.ca.

Abstract

Viruses are infectious and obligate intracellular parasites. *Turnip mosaic virus* (TuMV) is a member of the genus *Potyvirus* which comprises many agriculturally important viral pathogens that threaten crop production. Potyviruses are fully dependent on the host cellular machinery to fulfil their infection cycle in plant hosts. It is well accepted that viral coat protein (CP) is a multifunctional protein that plays key roles in virus propagation and host-virus interactions. This dissertation project aimed to investigate the role of CP in TuMV cell-to-cell movement, to identify the host interactors of TuMV CP, and further to characterize their roles in TuMV infection.

To examine the role of CP in viral cell-to-cell movement, a series of CP deletion and point mutations were introduced into a special TuMV infectious clone that allows for distinguishing primarily and secondarily infected cells. It was found that the core domain and C-terminus of CP are critical for TuMV cell-to-cell movement, but the N-terminal domain is dispensable for TuMV movement and virion assembly. Among cell-to-cell movement defective point mutants, R_{178A} and D_{222A} lost the ability to form detectable virions in protoplasts. The CP protein R_{178A} was not as stable as wild-type CP. Overall, the results revealed the CP determinants of TuMV cell-to-cell movement and suggested that there is a correlation between assembly defects and cell-to-cell movement defects in TuMV biology.

To identify the host interactors of TuMV CP, a yeast two-hybrid screening against *Arabidopsis* cDNA library was conducted. The screening resulted in the discovery of two novel host proteins, Patellin 3 (PATL3) and Patellin 6 (PATL6) that bind to CP in yeast. TuMV infection assay on *PATLs* knockout mutants and stable overexpression lines showed that PATL3 and PATL6 negatively regulate TuMV infection. Subcellular localization studies demonstrated that PATL3, but not PATL6, was partially redistributed to viral replication complexes (VRCs) upon TuMV infection. In addition, PATL3 also interacted with the viral protein cylindrical inclusion protein (CI), an essential component of VRCs, suggesting that PATL3 is recruited to the VRC likely through its interaction with CI. Overall, this study identified two host restriction proteins of TuMV that may be manipulated against TuMV and related viruses.

Keywords

plant virus, potyvirus, TuMV, coat protein, host protein, Patellin, cell-to-cell movement, assembly, viral replication complex, antiviral, host restriction factor, protoplasts.

Dedication

This thesis is dedicated to my parents, 毛菊香 (Juxiang Mao) and 戴海金 (Haijin Dai).

Acknowledgments

First, I am sincerely grateful to my supervisor Dr. Aiming Wang who accepted me as a student in the Department of Biology, the University of Western Ontario and for his excellent mentorship and financial support. During these years, I have received so much training and encouragement from him. He helped and encouraged me to develop various experimental skills, to be an independent researcher, and more importantly, to be dedicated to science. I have regained my self-confidence and the pleasure of doing research under his wings, and this will certainly benefit me for a lifetime.

I also would like to thank my co-supervisor Dr. Mark Bernards for his guidance, understanding and continuous support throughout these years. I am deeply grateful for his guidance on developing scientific writing skills, broaden biological knowledge as well as critical thinking. I would like to acknowledge my committee members Dr. Frédéric Marsolais and Dr. David Smith for the insightful discussion and feedback given to my project and my study plan. I am also thankful to Dr. Richard Gardiner for his guidance on transmission electron microscopy (TEM). I am grateful to the Department of Biology, the University of Western Ontario and the London Research and Development Centre (LoRDC), Agriculture and Agri-Food Canada for the funding support, facility and various training programs throughout these years.

I want to extend my acknowledgement to current and former members in Dr. Aiming Wang's lab for creating a supportive and enjoyable study and working environment. Thanks to Huangyu Wang, for sharing her life experiences with me and encouragement of dealing with hard times. Thanks to Jamie McNeil, for his sense of humor, his patience on helping with endless administrative requests, and TEM support. I am also grateful to the past and present postdocs in the Wang lab: Dr. Hui Chen, Dr. Hongguang Cui, Dr. Xiaofei Cheng, Dr. Andrej Adam Arsovski, Dr. Lingrui Zhang, Dr. Ruyi Xiong, Dr. Sang-Ho Park, Dr. Fangfang Li and Dr. Guanwei Wu for their insightful discussion on science and tremendous technical support. Thanks to the former and current graduate students in the Wang lab: Dr. Yinzi Li, Dr. Quyue Pan, Dr. Hong Hanh Tran, Aaron Simkovich, Shanwu Lyu, Bin Chen and Rongrong He for their friendship, the good laughs and enjoyable collaborations.

Lastly, thanks to my dearest parents, 毛菊香 (Juxiang Mao) and 戴海金 (Haijin Dai), my family members, 戴瑶琪 (Yaoqi Dai), 戴兆开 (Zhaokai Dai) and 邓萍 (Ping Deng) for their love and support.

Table of Contents

Abstract.....	i
Dedication.....	iii
Acknowledgments.....	iv
Table of Contents.....	vi
List of Tables.....	x
List of Figures.....	xi
List of Abbreviations.....	xiii
Chapter 1.....	1
1 General Introduction.....	1
1.1 Plant positive-strand RNA viruses.....	1
1.2 <i>Turnip mosaic virus</i> (TuMV).....	2
1.2.1 Taxonomy, host range and importance.....	2
1.2.2 Virions and Genome organization.....	3
1.2.3 Transmission and symptoms.....	5
1.2.4 Features of CI, 6K2 and NlB.....	5
1.2.5 The Potyvirus infection cycle.....	7
1.3 Functions of potyviral CPs.....	9
1.3.1 Structural features of potyviral CP.....	9
1.3.2 Multifunctional CP.....	10
1.4 Cell-to-cell movement of plant virus.....	10
1.4.1 Cell-to-cell movement of Plant viruses.....	10
1.4.2 Cell-to-cell movement of potyvirus.....	11
1.5 Virus-Host interactions.....	13
1.5.1 Virus-Host arms race.....	13

1.5.2	Host proteins involved in potyvirus infection.....	13
1.5.3	CP-host interaction in Potyvirus infection.....	14
1.5.4	Plasma membrane-associated protein and microbe interactions	15
1.5.5	The <i>Arabidopsis thaliana</i> PATL family	16
1.6	Research goals and objectives.....	16
1.7	References	19
Chapter 2.....		25
2	Identification of the determinants in TuMV CP essential for viral cell-to-cell movement, long-distance movement and virion assembly	25
2.1	Abstract.....	25
2.2	Introduction.....	26
2.3	Results.....	28
2.3.1	Construction of a plant expression vector that allows for visualization of TuMV-inoculated cells from secondarily infected cells.....	28
2.3.2	TuMV CP is dispensable for virus replication, but critical for cell-to-cell movement.....	31
2.3.3	The core domain and C-terminus of CP are critical for TuMV cell-to-cell movement, whereas the N-terminal amino acids 6-50 are dispensable for viral movement and virion assembly	35
2.3.4	Identification of amino acids in TuMV CP essential for virus cell-to-cell movement via point mutation analyses.....	40
2.3.5	Effects of point mutations in TuMV CP on virion assembly.....	46
2.3.6	Mapping the domains essential for CP self-interaction	49
2.3.7	Characterization of the CP point mutant R ₁₇₈ A	52
2.3.8	R ₁₇₈ A is less stable than wild-type CP.....	55
2.4	Discussion.....	56
2.5	Materials and Methods.....	60
2.5.1	Construction of two fluorescent protein-tagged TuMV infectious clone pCBTuMV-GFP//mCherry	60

2.5.2	Construction of CP mutants	60
2.5.3	Protoplast isolation and transfection	61
2.5.4	Cell-to-cell movement of TuMV CP mutants.....	61
2.5.5	Crude virion preparation and electron microscopy.....	61
2.5.6	qRT-PCR assay.....	62
2.5.7	Y2H and BiFC experiments.....	63
2.5.8	Electrophoretic gel mobility shift assay (EMSA).....	63
2.5.9	SDS-PAGE and Western blot analyses.....	64
2.6	References.....	65
Chapter 3.....		67
3	Patellin 3 and 6, two members of the Arabidopsis Sec14-GOLD proteins, interact with both the coat protein (CP) and cylindrical inclusion protein (CI) of <i>Turnip mosaic virus</i> and inhibit virus accumulation	67
3.1	Abstract.....	67
3.2	Introduction.....	68
3.3	Results.....	69
3.3.1	Identification of TuMV CP-interacting Arabidopsis proteins by Y2H screening	69
3.3.2	PATL3 and PATL6 interact with CP in <i>N. benthamiana</i> cells.....	73
3.3.3	Isolation of <i>patl3</i> and <i>patl6</i> single mutants and generation of <i>patl3patl6</i> double mutant.....	76
3.3.4	Knockout of <i>PATL3</i> or <i>PATL6</i> or both genes promotes TuMV infection in Arabidopsis	79
3.3.5	Knockout of <i>PATL3</i> or <i>PATL6</i> or both facilitates TuMV multiplication in protoplasts.....	81
3.3.6	Stable overexpression of PATL3 inhibits TuMV accumulation.....	84
3.3.7	Subcellular localization of AtPATL3 and AtPATL6 in uninfected and TuMV-infected <i>N. benthamiana</i> plants	86
3.3.8	PATL3, but not PATL6 co-localized with TuMV-induced VRCs.....	88

3.3.9	PATL3 targets the VRC likely through the interaction with CI	90
3.4	Discussion	92
3.5	Materials and Methods.....	94
3.5.1	Plant material and growth conditions	94
3.5.2	Y2H and BiFC Assay.....	94
3.5.3	BiFC and Subcellular Localization study	95
3.5.4	Coimmunoprecipitation (co-IP) assay	96
3.5.5	Characterization of T-DNA insertions.....	96
3.5.6	Generation of double knockout mutant.....	97
3.5.7	Generation of PATL3 transgenic plants	97
3.5.8	Protoplasts isolation and TuMV transfection	98
3.6	References	99
Chapter 4	101
4	General discussion and future directions	101
4.1	Requirement of coat protein (CP) for potyviral cell-to-cell movement.....	101
4.2	Role of CP in TuMV cell-to-cell movement.....	103
4.3	Role of Patellins in TuMV infection.....	104
4.4	Reference	106
Curriculum Vitae	108

List of Tables

Table 2.1 Effect of TuMV CP point mutants on systemic infection of *N. benthamiana*..... 45

Table 3.1 TuMV CP-interacting Arabidopsis protein candidates identified by Y2H screening
..... 71

List of Figures

Figure 1.1 Electron micrograph of TuMV virion stained with 2% phosphotungstic acid (PTA)	3
Figure 1.2 Genome organization of TuMV.	4
Figure 1.3 Confocal images on TuMV-induced vesicles in <i>N. benthamiana</i> epidermal cells..	6
Figure 1.4 The infection cycle of potyvirus.....	8
Figure 1.5 Near-atomic cryoEM structure of WMV virions.	9
Figure 2.1 Construction of a TuMV infectious clone suitable for monitoring viral cell-to-cell movement.....	30
Figure 2.2 CP is required for TuMV cell-to-cell movement but not for viral replication.	34
Figure 2.3 Effects of truncated mutations of CP on TuMV cell-to-cell movement and long-distant movement.	38
Figure 2.4 The N-terminus of CP is dispensable for TuMV virion assembly.	39
Figure 2.5 Effects of CP point mutants on TuMV cell-to-cell movement and systemic infection.	44
Figure 2.6 Effects of point mutations in TuMV CP on virion assembly.	48
Figure 2.7 Mapping the domains required for TuMV CP self-interaction.	51
Figure 2.8 The CP point mutant R ₁₇₈ A exhibits normal subcellular localization, self-interaction, CI interaction and binding ability with TuMV 5' UTR.....	54
Figure 2.9 R ₁₇₈ A is less stable than wild-type CP.	55
Figure 3.1 PATL3, PATL6 and LSM1B interact with TuMV CP in yeast.....	72
Figure 3.2 PATL3 and PATL6 interact with TuMV CP in <i>N. benthamiana</i> cells	75

Figure 3.3 Isolation of single and double <i>patls</i> T-DNA insertion mutants.....	78
Figure 3.4 TuMV accumulation is enhanced in Arabidopsis Patellin knockouts.....	80
Figure 3.5 Knockout of <i>PATL3</i> and <i>PATL6</i> promotes TuMV accumulation in Arabidopsis protoplasts.....	83
Figure 3.6 Stable overexpression of <i>PATL3</i> inhibits TuMV accumulation in Arabidopsis protoplasts.....	85
Figure 3.7 Subcellular localization of AtPATL3 and AtPATL6 in uninfected and TuMV-infected <i>N. benthamiana</i> epidermal cells.....	87
Figure 3.8 PATL3-GFP is recruited to the viral replication complex (VRC) in TuMV-infected <i>N. benthamiana</i> epidermal cells.....	89
Figure 3.9 PATL3 interacts with TuMV CI in yeast and <i>in planta</i>	91

List of Abbreviations

aa	amino acids
AAFC	Agriculture and Agri-Food Canada
ABRC	Arabidopsis Biological Resource Center
AD	activation domain
Ade	Adenine
Arg	Arginine
Asp	Aspartic acid
BiFC	bimolecular fluorescence complementation
BD	binding domain
BMV	<i>Brome mosaic virus</i>
bp	base pair
CaMV	<i>Cauliflower mosaic virus</i>
CBB	Coomassie Brilliant Blue
cDNA	complementary DNA
CI	the cylindrical inclusion protein
CMV	<i>Cucumber mosaic virus</i>
Col-0	ecotype Columbia
Co-IP	co-immunoprecipitation
CP	coat protein or capsid protein
CPIP	coat protein interacting-protein
C-terminal	carboxyl-terminal
DBP1	DNA-binding protein phosphatase 1
DIP2	DBP1 interacting-protein 2
DNA	deoxyribonucleic acid
DNase	deoxyribonuclease
DDO	double dropout
dsRNA	double-stranded RNA
EDTA	ethylenediaminetetraacetic acid
EM	electron microscope
EMSA	Electrophoretic gel mobility shift assay
eEF1A	eukaryotic elongation factor 1A
eIF4E	eukaryotic translation initiation factor 4E
eIF(iso)4E	eukaryotic translation initiation factor isoform 4E
ER	endoplasmic reticulum
ERESs	endoplasmic reticulum exit sites

EXPA1	α -expansin
FLAG	sequence motif DYKDDDDK (D, aspartic acid; Y, tyrosine; and K, lysine)
GDD	Glycine-Asparagine-Asparagine (GDD) motif
GFP	green fluorescent protein
GOLD	Golgi dynamics
HA	Human influenza hemagglutinin
HC-Pro	the helper component protease
HCV	<i>Hepatitis C virus</i>
His	histidine
HM	homozygous
Hsc70	heat shock cognate 70 kDa protein
Hsp70	The 70 kDa heat shock protein
ICTV	International Committee on Taxonomy of Viruses
6K1	the first 6 kDa protein
6K2	the second 6 kDa protein (also referred to as 6K)
kb	kilobase
kDa	kilodalton
LB	T-DNA left border
Leu	leucine
LiAc	lithium acetate
LP	left genomic primer
LSM1B	Small nuclear ribonucleoprotein family protein 1b
mRNA	messenger RNA
MP	movement protein
nt	nucleotide(s)
NCBI	National Center for Biotechnology Information
NIa	the nuclear inclusion a protein
NIa-Pro	the nuclear inclusion a protease
NIa-VPg	genome-linked protein–viral proteinase
NIb	the nuclear inclusion b protein
N-terminal	amino-terminal
OD	optical density (absorbance)
ORF	open reading frame
P1	the first protein
P24	a conserved family of 23- to 27-kDa transmembrane protein
P3	the third protein
P3N-PIPO	pipo as a translational fusion with the N-terminus of P3

PABP	poly(A)-binding protein
PATL	Patellin protein
PCaP1	plasma membrane associated cation-binding protein 1
PCR	polymerase chain reaction
PDs	plasmodesmata
PEG	polyethylene glycol
PIPO	pretty interesting <i>Potyviridae</i> ORF
PM	plasma membrane
Poly(A)	polyadenylate
PPV	<i>Plum pox virus</i>
PTA	phosphotungstic acid
PTMs	posttranslational modifications
PVA	<i>Potato virus A</i>
PVIP	potyvirus VPg-interacting protein
PVX	<i>Potato virus X</i>
PVY	<i>Potato virus Y</i>
QDO	quadruple dropout
qRT-PCR	real-time quantitative RT-PCR
RdRp	RNA-dependent RNA polymerase (virus)
RH8	an Arabidopsis DEAD-box RNA helicase-like protein
RNA	ribonucleic acid
RNP	ribonucleoprotein
(+) RNA	positive-sense RNA
(-) RNA	negative-sense RNA
RNase	ribonuclease
RP	right genomic primer
rpm	revolutions per minute
RSS	RNA silencing suppressor
RT-PCR	reverse transcription polymerase chain reaction
RTM	restricted TEV movement
RubisCO	ribulose-1,5-bisphosphate carboxylase/oxygenase
SCE1	SUMO conjugation enzyme 1
SEC	<i>Saccharomyces cerevisiae</i> secretory
SEL	size exclusion limit
SEs	sieve elements
SMV	<i>Soybean mosaic virus</i>
SNARE	soluble N-ethylmaleimide-sensitive-factor attachment protein receptors

ssRNA	single-stranded RNA
(+) ssRNA	positive-sense single-stranded RNA
SUMO	small ubiquitin-related modifier
TAIR	The Arabidopsis Information Resource
TBSV	<i>Tomato bushy stunt virus</i>
TCV	<i>Turnip crinkle virus</i>
T-DNA	transfer DNA
TEM	transmission electron microscopy
TEV	<i>Tobacco etch virus</i>
TMV	<i>Tobacco mosaic virus</i>
Trp	tryptophan
TuMV	<i>Turnip mosaic virus</i>
TVMV	<i>Tobacco vein mottling virus</i>
UTR	untranslated region
UWO	The University of Western Ontario
VPg	the viral genome-linked protein
VPg-Pro	VPg fused to a protease domain at the C terminus
VRC	viral replication complex
vRNA	viral RNA
WMV	<i>Watermelon mosaic virus</i>
WSMV	<i>Wheat streak mosaic virus</i>
WT	wild-type
Y2H	yeast two-hybrid
YC	C-terminal fragment of the YFP protein
YFP	yellow fluorescent protein
YN	N-terminal fragment of the YFP protein

Chapter 1

1 General Introduction

1.1 Plant positive-strand RNA viruses

Plant viruses are infectious and obligate intracellular parasites that comprise genetic material (DNA or RNA) surrounded by a protective protein coat and/or membrane. Positive-strand (+) RNA viruses account for the largest group of known plant viruses and comprise many economically important viruses in agriculture, including the so-called ‘Top ten’ economically important plant viruses such as *Tobacco mosaic virus* (TMV), *Potato virus Y* (PVY), *Cucumber mosaic virus* (CMV), *Brome mosaic virus* (BMV), *Potato virus X* (PVX) and *Plum pox virus* (PPV) (Sanfaçon, 2005; Rybicki, 2015). As their single-stranded RNA genome is of positive sense/polarity and can act like a messenger RNA (mRNA), it can be directly translated into viral proteins by the host translation machinery.

Plant (+) RNA viruses have relatively small genomes, typically between 4 and 15 kilobases (kb), encoding a very limited number of viral proteins. The typically encoded proteins include

- i. a protein that functions as an RNA dependent RNA polymerase (RdRp) for replication
- ii. a structural capsid/coat protein (CP) for encapsidating the viral genome
- iii. a protein or multiple proteins that function as movement protein (MP) to facilitate virus movement.
- iv. a protein that functions as an RNA silencing suppressor (RSS) to repress RNA silencing

A successful viral infection starts from its entry into the host cells. Unlike animal virus, plant virus can't enter cells via endocytosis due to the rigid plant cell wall, and the entry of plant virus is assisted by the wound resulting from vector bites (insects) or through mechanical rub/inoculation. Then, the viral (+) RNA genome is released from the virion

and acts as a template for translation and replication in the primary infected cells. Next, the newly synthesized progeny viral RNA and viral proteins form the ribonucleoprotein (RNP) complex or virion for cell-to-cell movement through the plasmodesmata (PDs) that connect two neighboring cells. After multiple rounds of cell-to-cell movement, the virus may reach the vascular tissue for long-distance movement, eventually invading the whole plant. Viral infection induces a variety of symptoms in the infected plants, including leaf yellowing, mosaicism and/or mottling, tissue necrosis, overall plant stunting or wilting, and in some cases death of the plant (Sanfaçon, 2005).

1.2 *Turnip mosaic virus* (TuMV)

1.2.1 Taxonomy, host range and importance

Turnip mosaic virus (TuMV) belongs to the genus *Potyvirus* in the Potyviridae. According to the Tenth Report of the International Committee on Taxonomy of Viruses (ICTV), *Potyvirus* comprises 160 species and accounts for around 80% of species in the Potyviridae. The Potyviridae is the largest family of RNA plant viruses (Wylie et al., 2017) and includes several agriculturally and economically important plant viruses such as *Plum pox virus* (PPV), *Potato virus Y* (PVY), *Potato virus A* (PVA), *Tobacco etch virus* (TEV), and *Soybean mosaic virus* (SMV) (Wang, 2013b).

Turnip mosaic virus is considered to be the second most important virus infecting field-grown vegetables after *Cucumber mosaic virus* (CMV) (Tomlinson, 1987). It infects a large number of economically important plants in the genus *Brassica*, such as turnip, cabbage, and cauliflower (Walsh and Jenner, 2002). TuMV has a very wide host range and can infect at least 318 species in over 43 dicot families as well as various monocots (Walsh and Jenner, 2002). Conveniently, TuMV can infect two well-studied model plants *Arabidopsis thaliana* and *Nicotiana benthamina*, and as a result, TuMV has become a model for host-potyvirus interaction studies.

1.2.2 Virions and Genome organization

Turnip mosaic virus virions are non-enveloped, flexuous filamentous particles. Typical TuMV virions range from around 600 to 1000 nm long and 15 to 20 nm wide under transmission electron microscopy (TEM) (Fig 1.1).

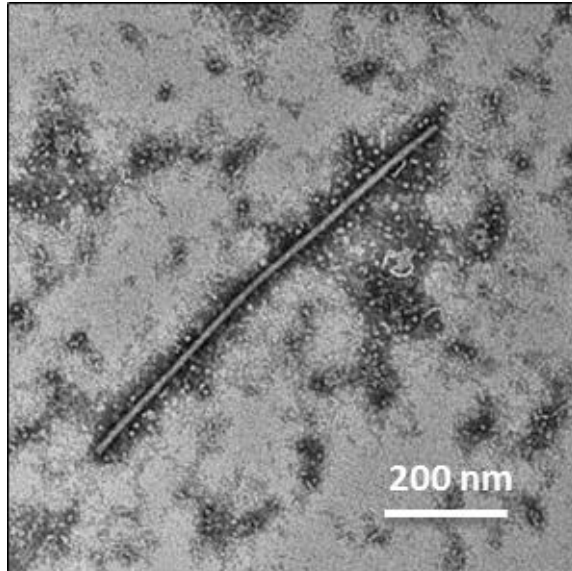


Figure 1.1 Electron micrograph of TuMV virion stained with 2% phosphotungstic acid (PTA)

The TuMV genome is a positive-sense single stranded RNA (ssRNA) of about 10 kb in length that has a viral-encoded, viral genome-linked protein (VPg) covalently linked to its 5' end and a poly (A) tail at the 3' end (Olivier and Laliberté, 1992). The viral genome contains one large open reading frame (ORF) and a relatively short ORF (Pretty Interesting Potyviridae ORF, *pipo*) resulting from transcriptional slippage in the P3-coding sequence (Revers and Gracia, 2015). These two ORFs encode two polyproteins that are processed by three proteinase domains into eleven mature proteins. These mature proteins are from the N- to the C-terminus: P1 (the first protein), HC-Pro (the helper component/protease), P3 (the third protein), P3N-PIPO (the N terminal region of P3 fused with the peptide encoded by the pretty interesting Potyviridae ORF), 6K1 (the first 6 kDa peptide), CI (the cylindrical inclusion protein), 6K2 (the second 6 kDa peptide), NIa-VPg (nuclear inclusion 'a'-viral genome-linked protein; also VPg), NIa-Pro (nuclear inclusion 'a' protein-the protease), NIb (the nuclear inclusion 'b' protein), and CP (coat protein) (Chung et al., 2008; Wang, 2013b; Revers and Garcia, 2015) (Fig 1.2).

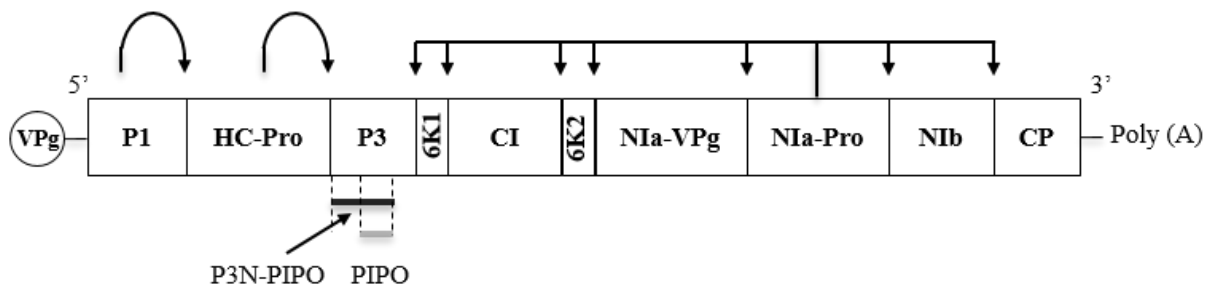


Figure 1.2 Genome organization of TuMV.

The genome is translated into a single large polyprotein and another small one, which is subsequently processed by virus-encoded proteases into individual proteins. Potyvirus encodes three different proteases (P1, HC-Pro and NIa-Pro proteases). Proteolytic cleavage sites are marked with arrows indicating the names of the corresponding proteases.

1.2.3 Transmission and symptoms

TuMV is transmitted between plants by *Myzus persicae* (green peach aphid) and more than 80 other aphid species in a non-persistent manner (Walsh and Jenner, 2002; Casteel et al., 2014). Casteel (2014) reported that TuMV improves growth and reproduction of the aphid vector on both *N. benthamiana* and *A. thaliana* (Casteel et al., 2014). TuMV infection results in various symptoms depending on plants such as leaf mottling, mosaicism, chlorosis, puckering and distortion. The disease caused by TuMV can lead to severe stunting of young plants and significant loss of yield.

1.2.4 Features of CI, 6K2 and NIb

CI is named after its abundant aggregation in the cytoplasm of potyvirus-infected plant cells known as laminate or pinwheel-shaped cytoplasmic inclusion bodies (Edwardson, 1966; Carrington et al., 1998). The CI protein has been demonstrated to be a key factor of potyvirus replication and movement. CI has helicase activity that unwinds double-stranded RNA (dsRNA) in a 3' to 5' direction (Lafn et al., 1990; Fernandez et al., 1995). Moreover, CI is present in the ER-derived vesicles that have been generally accepted as the viral replication complex (VRC) (Cotton et al., 2009). Early ultrastructural analyses through TEM revealed that cylindrical inclusions are localized in the vicinity of PD. CI, CP and viral RNA are associated with cone-shaped structures close to the PD (Sorel et al., 2014). More recently, it has been reported that CI is involved in intercellular movement likely through the formation of conical structures anchored to and extending through PD thanks to the interaction with P3N-PIPO, a PD localized viral protein (Wei et al., 2010b; Wang, 2013b). Moreover, reverse genetics approaches such as alanine-scanning mutagenesis experiments on TuMV, PPV and TEV demonstrated that CI is critical for potyviral cell-to-cell movement (Carrington et al., 1998; Gomez de Cedron et al., 2006; Deng et al., 2015).

6K2 is an integral membrane protein and can induce the formation of membranous vesicles derived from the ER in the presence or absence of potyviral infection (Schaad et al., 1997; Cotton et al., 2009). TuMV infection is associated with the formation of at least two different types of subcellular compartments induced by 6K2 protein: a perinuclear

globular structure and motile cortical vesicular structures (Fig 1.3). These vesicles contain viral RNA, viral proteins (NIb, CI, NIa, 6K2) and various host proteins, and have been generally referred as the VRC for potyvirus replication and translation sites. 6K2-induced vesicles are highly mobile and align with microfilaments in the infected plant cells (Wei and Wang, 2008; Cotton et al., 2009; Grangeon et al., 2012b).

NIb is the RNA-dependent RNA polymerase (RNA replicase) that catalyze the synthesis of RNA (Hong and Hunt, 1996). The highly conserved Glycine-Asparagine-Asparagine (GDD) motif in the RdRps across plant viruses and animal viruses is critical for RdRp enzyme activity (Kamer and Argos, 1984; Jablonski et al., 1991). For potyvirus, deletion or mutation of the GDD motif in NIb leads to deficient potyvirus replication and abolished virus movement (Dolja et al., 1994; Carrington et al., 1998).

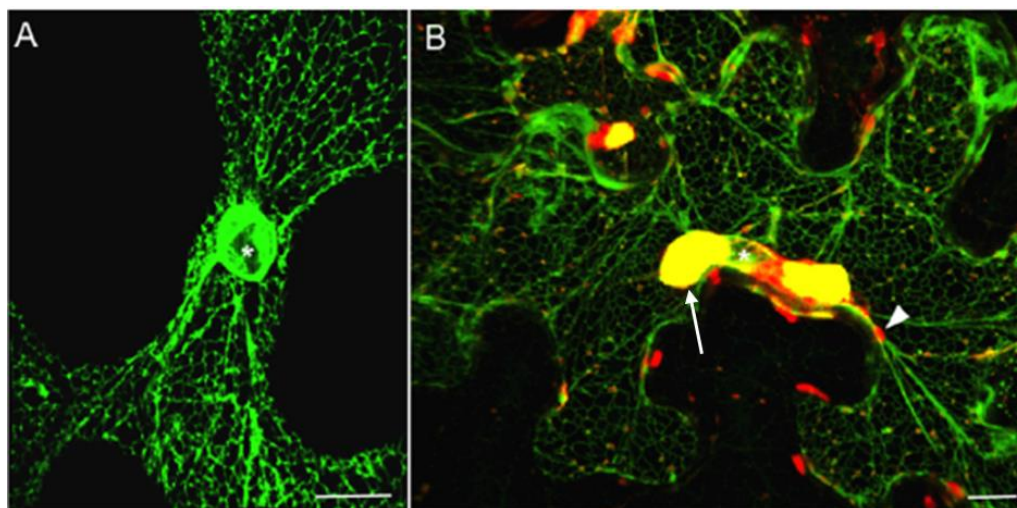


Figure 1.3 Confocal images on TuMV-induced vesicles in *N. benthamiana* epidermal cells.

(A) Confocal image of uninfected *N. benthamiana* cell expressing GFP-HDEL, a luminal ER marker. (B) Confocal image of TuMV-infected *N. benthamiana* cell expressing both GFP-HDEL and 6K2-mCherry. A white asterisk shows the position of the nucleus, the white arrow indicates the perinuclear globular structure and the white arrowhead points to the cortical vesicular structure. Bars = 10 μ m (Grangeon et al., 2012b). Copyright © 2012 by American Society for Microbiology. Adapted by permission.

1.2.5 The Potyvirus infection cycle

The viral infection cycle in the host plants starts from the entry of an invading virus into a plant cell. To facilitate the study on the viral infection cycle, virologists artificially divide this process into various steps including entry, disassembly/uncoating, translation, replication, assembly, intracellular movement and cell-to-cell movement (Fig 1.4).

Potyvirus enters the plant cells through aphid-mediated wounds or mechanical transmissions. Then, virions disassemble and viral RNA is translated by the host translational machinery into two polyproteins that are subsequently processed into 11 mature proteins by three virus-encoded proteases (P1, HC-Pro and NIa-Pro) (Wang, 2013b). Next, viruses assemble VRCs at ER exit sites (ERESs), recruiting various host proteins together with certain viral proteins, including NIb, CI, 6K2 and NIa (Cotton et al., 2009; Wang, 2013b). Those vesicles can travel along actin microfilaments and reach PDs for cell-to-cell movement (Cotton et al., 2009; Grangeon et al., 2013). Moreover, vesicles can also target chloroplasts for robust replication and further move towards PD for intercellular movement (Wei et al., 2010a). Alternatively, progeny RNA synthesized in VRCs can be further assembly into virions or RNPs, and subjected to cell-to-cell movement; however, the assembly sites for those virions or RNPs are not known yet. Once the virions, RNPs or vesicles are mounted on PD, they pass through the PD to the adjacent cells for new rounds of infection. But, the mechanism of this intercellular movement is not well studied.

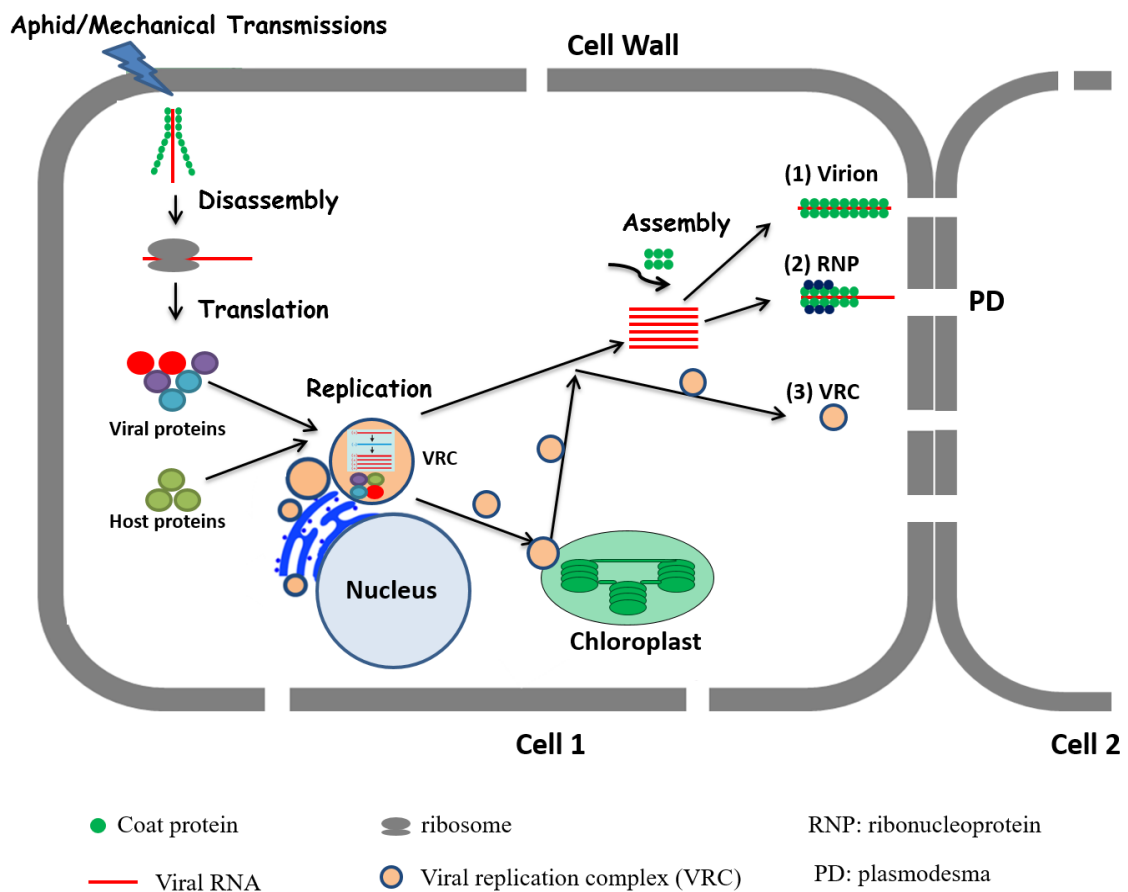


Figure 1.4 The infection cycle of potyvirus.

Potyvirus virions are disassembled after the entry through aphid or mechanical transmission, and the viral RNAs are further used as templates for both viral translation and replication. The new progeny forms virions or RNP or VRC for transporting virus to the neighboring cells for new rounds of infection.

1.3 Functions of potyviral CPs

1.3.1 Structural features of potyviral CP

The principal function of CP is the encapsidation of viral RNA. It was estimated that potyvirus particles are encapsidated by ~ 2000 CP subunits (Revers and Garcia, 2015). Using negative staining, transmission electron microscopy and diffraction technologies, it was shown that PVY particle is 730 nm long with a width of 105 Å, and the pitch (the axial distance between turns of the basic helix) is 33 Å in average (Varma et al., 1968). Recently, the cryo-electron microscopy (cryoEM) structure of potyvirus was determined at a high resolution of 4.0 Å for *Watermelon mosaic virus* (WMV). WMV displays a left-handed helix with a diameter of 130 Å, contains about 8.8 CP subunits per turn and a pitch of 35.2 Å. The WMV CP contains a core domain rich in α -helices and two long N- and C-terminal arms (Fig 1.5) (Wylie et al., 2017; Zamora et al., 2017).

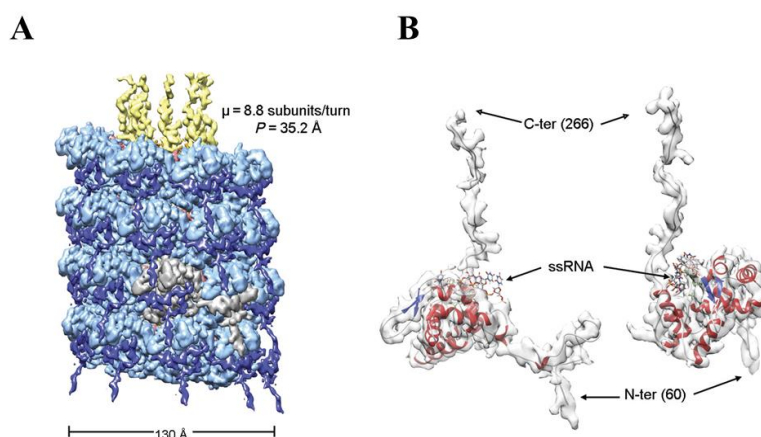


Figure 1.5 Near-atomic cryoEM structure of WMV virions.

(A) Renderings of the 3D cryoEM map calculated for WMV. Segmented densities are depicted as follows: WMV CP core region (light blue), N-terminal arm (dark blue), C-terminal arm (yellow), scattered densities at the inner side of the helix (orange), and density for the ssRNA (red). (B) Two views of the atomic model calculated for WMV CP within the semitransparent density for a subunit segmented from the cryoEM map (Zamora et al., 2017). An open-access article published by American Association for the Advancement of Science.

1.3.2 Multifunctional CP

It is well accepted that the potyviral CP is a three-domain protein with variable N- and C-terminal regions exposed on the particle surface that can be removed by treatment of virions with trypsin and a conserved core domain that interacts with viral RNA (Allison et al., 1985b; Shukla et al., 1988). The N-terminus of CP is involved in aphid transmission (Atreya et al., 1991) and systemic movement (Dolja et al., 1994). The core domain of potyviral CP is highly conserved among potyviral species and forms the core of potyvirus particles (Dolja et al., 1991). Several studies have revealed that the core domain of CP is critical for potyvirus assembly and cell-to-cell movement (Dolja et al., 1994; Dolja et al., 1995). The C-terminus of CP is important for SMV cell-to-cell movement (Seo et al., 2013), TEV and SMV systemic movement (Dolja et al., 1995; Seo et al., 2013). In addition, the C-terminus of SMV CP is required for the CP-CP self-interaction and virus assembly (Kang et al., 2006).

Viral protein modification is well known to be critical for virus infection processes (Wang, 2015). The potyviral CPs also undergo posttranslational modifications (PTMs) for regulating virus infection processes. The CP of PVA was shown to be phosphorylated both in virus infected plants and *in vivo*, and as a result, reduce its affinity to the viral RNA. The phosphorylated amino acid residue was mapped at the end of the core region of PVA CP (Ivanov et al., 2003). It has been shown that the PPV CP is not only phosphorylated but also O-GlcNAcylated (Fernandez-Fernandez et al., 2002; de Jesus Perez et al., 2006).

1.4 Cell-to-cell movement of plant virus

1.4.1 Cell-to-cell movement of Plant viruses

To establish a successful systemic infection, plant viruses need to move from the primarily infected cells through the PD, the cytoplasmic bridges between adjacent plant cells, to neighbouring cells (Lucas, 2006; Lucas et al., 2009). Then, the plant virus may undergoes several cycles of cell-to-cell movement until reaching the vascular tissue,

followed by loading into phloem tissues for long-distance movement, eventually invading the whole plant (Benitez-Alfonso et al., 2010; Hipper et al., 2013).

Cell-to-cell movement of plant viruses is mediated by virus-encoded movement proteins (MPs) through their interactions with host factors (Benitez-Alfonso et al., 2010; Harries et al., 2010). Generally, plant viruses can be classified into three groups on the characteristics of cell-to-cell movement. The first group, dominated by tobamoviruses, encodes a single dedicated 30 KDa MP that can interact with and increase the size exclusion limit (SEL) of PD to allow virions or ribonucleoprotein (RNP) complexes to pass through (Kawakami et al., 2004; Wei et al., 2010b). The second group of plant viruses includes some icosahedral viruses, such as bromoviruses, caulimoviruses, nepo- and comoviruses, which need both MPs and CPs to mediate virus passage through PD via tubule-like structures (Laporte et al., 2003; Pouwels et al., 2004; Benitez-Alfonso et al., 2010). The third group of viruses includes some viruses with flexuous, filamentous or rod-shaped particles such as potexviruses, hordeiviruses, pomoviruses and benyviruses, and these viruses encode the triple-gene-block proteins that function collectively to mediate virus passage through PD without forming tubule-like structures (Verchot-Lubicz, 2005; Jackson et al., 2009; Lim et al., 2009; Verchot-Lubicz et al., 2010).

1.4.2 Cell-to-cell movement of potyvirus

As described earlier, potyvirus has to move intracellularly from replication sites towards the PD, cross it and enter to adjacent cells for new rounds of infection. However, potyviruses have not been assigned to any of the groups of cell-to-cell movement described above. It appears the mechanism of cell-to-cell movement of potyvirus is very complicated that it's still not clear whether potyvirus moves as virions or RNPs or VRCs to pass through PD.

Currently, we do know that potyviruses encode one dedicated MP (P3N-PIPO) (Cui et al., 2017), and several additional potyviral proteins including CP, VPg, HC-Pro, and CI have also been implicated in potyvirus cell-to-cell movement (Wang, 2013b; Revers and Garcia, 2015).

Historically, several ultrastructural studies revealed that CI conical structures are present at the PD and sometimes can penetrate the cell wall, also CP is associated with the CI-induced structures at the PD (Rodríguez-Cerezo et al., 1997; Robert et al., 1998). These studies suggest a possible role of CP and CI in potyviral cell-to-cell movement. Indeed, reverse genetics studies using various TEV CI or CP mutants further support that CI and CP are crucial for potyviral movement (Dolja et al., 1994; Dolja et al., 1995; Carrington et al., 1998).

A microinjection study performed by Rojas and colleagues demonstrated that both CP and HC-Pro can increase in plasmodesmal SEL and spread intercellularly (Rojas et al., 1997). In 2008, the discovery of the P3N-PIPO protein encoded by the potyvirus genome significantly boosted the study of the mechanism of potyviral cell-to-cell movement. Shortly after its discovery, our lab demonstrated that TuMV P3N-PIPO is a PD localized protein and can physically interact with CI and direct CI to the PD (Wei et al., 2010b). More recently, the Laliberte group has suggested that TuMV might move as VRCs for cell-to-cell movement. This suggestion is based on observations that the motile 6K2-containing vesicles (VRCs) enable vRNA transport to PDs by trafficking along ER/microfilaments and can even pass PD to the neighboring cells (Grangeon et al., 2012a; Grangeon et al., 2013).

It is well accepted that plant viruses hijack host proteins for successful cell-to-cell movement (Wang, 2015). However, very limited studies are available for host proteins required for potyvirus cell-to-cell movement. Recently, a plasma membrane-associated cation-binding protein 1 (PCaP1) that can directly interact with P3N-PIPO to positively regulate TuMV cell-to-cell movement was identified by a yeast two-hybrid screening against an Arabidopsis cDNA library using P3N-PIPO as bait. The authors speculated that PCaP1 can enable the complex of viral proteins and viral RNA to the plasma membrane by binding P3N-PIPO (Vijayapalani et al., 2012)

Based on the studies above, a model for the cell-to-cell movement of potyvirus can be suggested. The complex including CI, P3N-PIPO, CP, viral RNA and other essential viral elements are anchored to the PD through the interaction of P3N-PIPO/PCaP1, and

subsequently, the virus-containing complex (either virions, RNPs or VRCs) passes through the CI conical structures and PD to enter the neighboring cells.

Despite studies showing that CI and P3N-PIPO are critical for TuMV cell-to-cell movement (Wei et al., 2010b; Deng et al., 2015), it is still not clear whether CP is required for TuMV cell-to-cell movement, and the mechanism by which CP mediates TuMV cell-to-cell movement needs to be investigated.

1.5 Virus-Host interactions

1.5.1 Virus-Host arms race

Plant viruses possess relatively small genomes and typically encode no more than a dozen proteins. As an intracellular parasite, viruses are fully dependent on host cell machinery to fulfill their survival and propagation in the host cells. In other words, viruses have to recruit certain host proteins (termed host factors) to facilitate their life cycle including disassembly, viral genome translation, viral genome multiplication, assembly and virus movement. As part of its resistance response to viral infection, hosts need to sense the presence of viruses rapidly at almost every step of the viral infection process and employ host proteins (termed as restriction factors) to interfere with viral infection (Daugherty and Malik, 2012; Coffin, 2013). In the past decade, molecular identification and characterization of those host proteins involved in virus-host arms race have been a research focus in the field of virology.

1.5.2 Host proteins involved in potyvirus infection

Considering the significant importance of potyvirus in damaging crops and vegetables in agriculture, extensive studies have been conducted to identify and characterize the host proteins that are involved in potyvirus infection processes. Several host proteins have been reported to be recruited to the VRCs for promoting virus multiplication, including heat shock protein 70 (HSP70), poly (A) binding-protein (PABP), eukaryotic initiation factor 4E (eIF4E), elongation factor 1A (eEF1A), DEAD-box RNA helicase RH8 (Ivanov and Makinen, 2012) and α -expansin (EXPA1). In addition, SNARE (soluble N-

ethylmaleimide-sensitive-factor attachment protein receptors) protein Syp71 was found to co-localize with the chloroplast-bound 6K2 complex. Wei and coworkers concluded that Syp71 is a host factor essential for successful virus infection by mediating the fusion of the virus-induced vesicles with chloroplasts during TuMV infection (Wei et al., 2013). DNA-binding protein1 (DBP1) was also identified as a host factor that contributes to potyvirus infection, in spite of an unclear mechanism (Castello et al., 2010).

Some host proteins may regulate viral movement. Documented examples include the cation-binding protein (PCaP1), a cysteine-rich protein named potyvirus VPg-interacting protein (PVIP), and RTM1, RTM2, and RTM3 (restricted TEV movement 1, 2 and 3, respectively) (Whitham et al., 2000; Chisholm et al., 2001; Dunoyer et al., 2004; Cosson et al., 2010; Vijayapalani et al., 2012).

Posttranslational modifications (PTMs) are implicated in potyvirus infection. For instance, the SUMO-conjugating enzyme (SCE1) was shown to interact with TuMV RdRp and play an essential role in TuMV infection (Xiong and Wang, 2013). Furthermore, TuMV RdRp was demonstrated to interact with and is sumoylated by small ubiquitin-like modifier 3 (SUMO3), and as a result, promoting TuMV infection (Cheng et al., 2017).

Not surprisingly, to fight back, plant hosts also employ restriction factors to interfere/restrict virus. For example, Beclin1, a core component of autophagy was demonstrated to restrict potyvirus infection through suppression and autophagic degradation of viral RdRp (Li et al., 2018). In addition, another restriction factor DIP2 (DBP interacting protein 2) was identified to inhibit PPV infection with an unrevealed mechanism (Castello et al., 2011)

1.5.3 CP-host interaction in Potyvirus infection

Although CP is a multifunctional viral protein that is involved in various steps of the potyvirus infection process, mechanistic details as to how the CP-host interactions regulate potyvirus infection are lacking. There are at least five host proteins that have been identified to be CP interacting partners.

The Chloroplastic 37 kDa protein of lettuce (*Lactuca sativa*) interacts with TuMV CP (McClintock et al., 1998), whereas PVY CP binds to the large subunit of the ribulose-1,5-biphosphate carboxylase/oxygenase (RubisCO-LSU) of tobacco (*N. tabacum cv. Xanthi*) (Feki et al., 2005). Unfortunately, the functional role of these interactions on virus infection still remains unknown. In a different study using a yeast two-hybrid approach, Hofius and colleagues identified a subset of DnaJ-like proteins from tobacco (NtCPIP1 and NtCPIP2a) that also interact with PVY CP (Hofius et al., 2007). Both transient expression and stable overexpression of truncated dominant-interfering NtCPIP strongly reduce PPV accumulation. NtCPIPs seem to act as important susceptibility factors during PVY infection (Hofius et al., 2007).

Interestingly, heat shock protein 70 (HSP70) was identified as a component of a membrane-associated viral ribonucleoprotein (RNP) complex by using an affinity purification approach and was co-immunoprecipitated with PVA CP in *N. benthamiana* plants. The study demonstrated that HSP70 together with its cochaperone CPIP regulates PVA CP function, which in turn can interfere with viral gene expression (Hafren et al., 2010).

1.5.4 Plasma membrane-associated protein and microbe interactions

It is well known that infection by bacteria, fungi and viruses is characterized by a significant morphological rearrangement of the host plasma membrane favoring microbe survival (Dormann et al., 2014). Despite a great number of plasma membrane-associated proteins having been identified to be regulators of host-bacteria and/or host-fungi interactions by recognizing microbes and activating subsequent signal transduction cascades leading to defense, very limited work has been done to elucidate of the roles of PM-associated proteins in virus-host interactions (Lefebvre et al., 2010; Dormann et al., 2014; Nathalie and Bouhidel, 2014). A PM associated protein, Remorin (from remora, smaller fish adhering to larger fishes and ships) in relation to its hydrophilicity and membrane location was identified to be a regulator of host-virus interaction and can inhibit *Potato virus X* (PVX) movement (Raffaele et al., 2009).

1.5.5 The *Arabidopsis thaliana* PATL family

The PATL family comprise six members (PATL1, PATL2, PATL3, PATL4, PATL5 and PATL6). All six PATLs possess a variable N-terminal domain, a Sec14-like domain (homologue to yeast Sec14p) and a C-terminal GOLD domain (Golgi dynamics) (Peterman et al., 2004).

Sec14p was originally identified using a *Saccharomyces cerevisiae* secretory (*Sec*) mutant by demonstrating its essential functions in the formation and exit of vesicles from the trans-Golgi network (Tejosa et al., 2017). To date, proteins with a Sec14 domain are reported to be involved in membrane trafficking, cytoskeleton dynamics, lipid metabolism and lipid-mediated regulatory functions (Peterman et al., 2004; Peiro et al., 2014; Tejosa et al., 2017). The GOLD domain is a conserved domain among p24 protein family that has been shown to be critical for cargo selection and cargo transportation from the ER to the Golgi complex. It is also presumably responsible for protein-protein interactions (Anantharaman and Aravind, 2002). However, the biological function of the N-terminal domain of PATLs remains unknown.

PATL family proteins have been found to be putative factors associated with diverse signalling pathways such as response to the hormones brassinosteroids and cytokinins through several proteomics studies (Deng et al., 2007; Cerny et al., 2011). In addition, PATLs are also implicated in response to biotic stresses (Kiba et al., 2012; Peiro et al., 2014). However, it is not clear if PATLs are involved in potyvirus infection.

1.6 Research goals and objectives

Potyriviruses are the major viral pathogens that threaten global crop security. Extensive studies have been conducted to better understanding potyviral infection processes as well as potyvirus-host interplays. However, how potyriviruses move intercellularly is still not well understood. It is well accepted that plant viral coat proteins (CPs) play key roles in virus propagation and virus-host interplays. My PhD project aimed to firstly, investigate the role of TuMV CP in viral cell-to-cell movement, and to identify host proteins that interact with TuMV CP and further characterize their biological effects in viral infection.

The hypotheses of my study are that (1) The CP of TuMV is critical for viral cell-to-cell movement through its role in virion assembly, RNA binding, interactions with viral proteins and host factors, and (2) The CP-interacting host proteins play an essential role in TuMV infection. To test these hypotheses, I proposed to address the following specific objectives:

1. To determine whether CP is required for TuMV cell-to-cell movement. A green fluorescent and mCherry fluorescent protein-tagged TuMV infectious clone was constructed that allows for distinguishing primarily and secondarily infected cells. Further, a series of CP deletion mutations were generated to examine viral cell-to-cell movement ability by confocal microscopy.
2. To identify CP determinants in TuMV cell-to-cell movement. A series of CP point mutants were introduced into TuMV infectious clone and the effects on viral cell-to-cell movement were examined.
3. To characterize the defective cell-to-cell mutants on subcellular localization, virion assembly, RNA binding ability and self-interaction or CI interaction ability. This was achieved by comparison between wild-type CP and CP point mutants using multiple techniques including transient expression, transmission electron microscopy (TEM), electrophoretic gel mobility shift assay (EMSA), yeast two-hybrid (Y2H) and bimolecular fluorescence complementation (BiFC).
4. To identify CP-interacting host proteins in Arabidopsis. A yeast two-hybrid screening against Arabidopsis cDNA library by using TuMV CP as bait was conducted.
5. To validate the interactions between CP and candidate host proteins identified in Y2H screening. Multiple methods including Y2H, BiFC and co-immunoprecipitation (co-IP) assays were applied for protein-protein interaction validation.

6. To test the biological impact of CP-interacting Arabidopsis protein in TuMV infection. The knockout and stable overexpression line of corresponding Arabidopsis protein were generated and inoculated by TuMV followed by quantification of viral RNA and viral protein accumulation by qRT-PCR and western blot, respectively.
7. To investigate the possible mechanism by which CP-interactors regulate TuMV multiplication. Subcellular localization of Arabidopsis protein was examined both in the absence and presence of TuMV infection. The involvement of VRCs in the virus-host interplays are assessed by co-infiltration agrobacterium harboring host proteins and 6K2mCherry-tagged TuMV infectious clone.

1.7 References

- Agbeci, M., Grangeon, R., Nelson, R.S., Zheng, H., and Laliberte, J.F.** (2013). Contribution of host intracellular transport machineries to intercellular movement of turnip mosaic virus. *PLoS Pathog* **9**, e1003683.
- Allison, R.F., Dougherty, W.G., Parks, T.D., Willis, L., Johnston, R.E., Kelly, M., and Armstrong, F.B.** (1985). Biochemical analysis of the capsid protein gene and capsid protein of tobacco etch virus: N-terminal amino acids are located on the virion's surface. *Virology* **147**, 309-316.
- Anantharaman, R., and Aravind, L.** (2002). The GOLD domain, a novel protein module involved in Golgi function and secretion. *Genome Biology* **3**.
- Atreya, P.L., Atreya, C.D., and Pirone, T.P.** (1991). Amino acid substitutions in the coat protein result in loss of insect transmissibility of a plant virus. *Proceedings of the National Academy of Sciences* **88**, 7887-7891.
- Benitez-Alfonso, Y., Faulkner, C., Ritzenthaler, C., and Maule, A.J.** (2010). Plasmodesmata: Gateways to Local and Systemic Virus Infection. *Molecular Plant-Microbe Interactions* **23**, 1403-1412.
- Carrington, J.C., Jensen, P.E., and Schaad, M.C.** (1998). Genetic evidence for an essential role for potyvirus CI protein in cell-to-cell movement. *The Plant Journal* **14**, 393-400.
- Casteel, C.L., Yang, C., Nanduri, A.C., De Jong, H.N., Whitham, S.A., and Jander, G.** (2014). The NIa-Pro protein of Turnip mosaic virus improves growth and reproduction of the aphid vector, *Myzus persicae* (green peach aphid). *Plant J* **77**, 653-663.
- Castello, M.J., Carrasco, J.L., and Vera, P.** (2010). DNA-binding protein phosphatase AtDBP1 mediates susceptibility to two potyviruses in Arabidopsis. *Plant Physiol* **153**, 1521-1525.
- Castello, M.J., Carrasco, J.L., Navarrete-Gomez, M., Daniel, J., Granot, D., and Vera, P.** (2011). A plant small polypeptide is a novel component of DNA-binding protein phosphatase 1-mediated resistance to plum pox virus in Arabidopsis. *Plant Physiol* **157**, 2206-2215.
- Cerny, M., Dycka, F., Bobal'ova, J., and Brzobohaty, B.** (2011). Early cytokinin response proteins and phosphoproteins of Arabidopsis thaliana identified by proteome and phosphoproteome profiling. *J Exp Bot* **62**, 921-937.
- Cheng, X., Xiong, R., Li, Y., Li, F., Zhou, X., and Wang, A.** (2017). Sumoylation of Turnip mosaic virus RNA Polymerase Promotes Viral Infection by Counteracting the Host NPR1-Mediated Immune Response. *Plant Cell* **29**, 508-525.
- Chisholm, S.T., Parra, M.A., Anderberg, R.J., and Carrington, J.C.** (2001). Arabidopsis RTM1 and RTM2 Genes Function in Phloem to Restrict Long-Distance Movement of Tobacco Etch Virus. *Plant Physiology* **127**, 1667-1675.
- Chung, B.Y.-W., Miller, W.A., Atkins, J.F., and Firth, A.E.** (2008). An overlapping essential gene in the Potyviridae. *Proceedings of the National Academy of Sciences* **105**, 5897-5902.
- Coffin, J.M.** (2013). Virions at the gates: receptors and the host-virus arms race. *PLoS Biol* **11**, e1001574.
- Cosson, P., Sofer, L., Le, Q.H., Leger, V., Schurdi-Levraud, V., Whitham, S.A., Yamamoto, M.L., Gopalan, S., Le Gall, O., Candresse, T., Carrington, J.C., and Revers, F.** (2010). RTM3, which controls long-distance movement of potyviruses, is a member of a new plant gene family encoding a meprin and TRAF homology domain-containing protein. *Plant Physiol* **154**, 222-232.
- Cotton, S., Grangeon, R., Thivierge, K., Mathieu, I., Ide, C., Wei, T., Wang, A., and Laliberte, J.F.** (2009). Turnip mosaic virus RNA replication complex vesicles are

- mobile, align with microfilaments, and are each derived from a single viral genome. *J Virol* **83**, 10460-10471.
- Daugherty, M.D., and Malik, H.S.** (2012). Rules of engagement: molecular insights from host-virus arms races. *Annu Rev Genet* **46**, 677-700.
- de Jesus Perez, J., Juarez, S., Chen, D., Scott, C.L., Hartweck, L.M., Olszewski, N.E., and Garcia, J.A.** (2006). Mapping of two O-GlcNAc modification sites in the capsid protein of the potyvirus Plum pox virus. *FEBS Lett* **580**, 5822-5828.
- Deng, P., Wu, Z., and Wang, A.** (2015). The multifunctional protein CI of potyviruses plays interlinked and distinct roles in viral genome replication and intercellular movement. *Virol J* **12**, 141.
- Deng, Z., Zhang, X., Tang, W., Osés-Prieto, J.A., Suzuki, N., Gendron, J.M., Chen, H., Guan, S., Chalkley, R.J., Peterman, T.K., Burlingame, A.L., and Wang, Z.Y.** (2007). A proteomics study of brassinosteroid response in Arabidopsis. *Mol Cell Proteomics* **6**, 2058-2071.
- Dolja, V.V., Boyko, V.P., Agranovsky, A.A., and Koonin, E., V.** (1991). Phylogeny of capsid proteins of rod-shaped and filamentous RNA plant viruses: Two families with distinct patterns of sequence and probably structure conservation. *Virology* **184**, 79-86.
- Dolja, V.V., Haldeman, R., Robertson, N.L., Dougherty, W.G., and Carrington, J.C.** (1994). Distinct functions of capsid protein in assembly and movement of tobacco etch potyvirus in plants. *The EMBO Journal* **13**, 1482-1491.
- Dolja, V.V., Haldeman-Cahill, R., Montgomery, A.E., Vandenbosch, K.A., and Carrington, J.C.** (1995). Capsid Protein Determinants Involved in Cell-to-Cell and Long Distance Movement of Tobacco Etch Potyvirus. *Virology* **206**, 1007-1016.
- Dormann, P., Kim, H., Ott, T., Schulze-Lefert, P., Trujillo, M., Wewer, V., and Huckelhoven, R.** (2014). Cell-autonomous defense, re-organization and trafficking of membranes in plant-microbe interactions. *New Phytol* **204**, 815-822.
- Dunoyer, P., Thomas, C., Harrison, S., Revers, F., and Maule, A.** (2004). A Cysteine-Rich Plant Protein Potentiates Potyvirus Movement through an Interaction with the Virus Genome-Linked Protein VPg. *Journal of Virology* **78**, 2301-2309.
- Edwardson, J.R.** (1966). Cylindrical Inclusions in the Cytoplasm of Leaf Cells Infected with Tobacco Etch Virus. *Science Advances* **Vol. 153**, pp. 883-884.
- Feki, S., Loukili, M.J., Triki-Marrakchi, R., Karimova, G., Old, I., Ounouna, H., Nato, A., Nato, F., Guesdon, J.L., Lafaye, P., and Elgaaied, A.B.A.** (2005). Interaction between tobacco Ribulose-1,5-biphosphate Carboxylase/Oxygenase large subunit (RubisCO-LSU) and the PVY Coat Protein (PVY-CP). *European Journal of Plant Pathology* **112**, 221-234.
- Fernandez-Fernandez, M.R., Camafeita, E., Bonay, P., Mendez, E., Albar, J.P., and Garcia, J.A.** (2002). The capsid protein of a plant single-stranded RNA virus is modified by O-linked N-acetylglucosamine. *J Biol Chem* **277**, 135-140.
- Fernandez, A., Lain, S., and Garcia, J.A.** (1995). RNA helicase activity of the plum pox potyvirus CI protein expressed in *Escherichia coli* Mapping of an RNA binding domain. *Nucleic Acids Research* **23**, 1327-1332.
- Gomez de Cedron, M., Osaba, L., Lopez, L., and Garcia, J.A.** (2006). Genetic analysis of the function of the plum pox virus CI RNA helicase in virus movement. *Virus Res* **116**, 136-145.
- Grangeon, R., Jiang, J., and Laliberte, J.F.** (2012a). Host endomembrane recruitment for plant RNA virus replication. *Curr Opin Virol* **2**, 683-690.
- Grangeon, R., Agbeci, M., Chen, J., Grondin, G., Zheng, H., and Laliberte, J.F.** (2012b). Impact on the endoplasmic reticulum and Golgi apparatus of turnip mosaic virus infection. *J Virol* **86**, 9255-9265.

- Grangeon, R., Jiang, J., Wan, J., Agbeci, M., Zheng, H., and Laliberte, J.F.** (2013). 6K2-induced vesicles can move cell to cell during turnip mosaic virus infection. *Front Microbiol* **4**, 351.
- Hafren, A., Hofius, D., Ronnholm, G., Sonnewald, U., and Makinen, K.** (2010). HSP70 and its cochaperone CPIP promote potyvirus infection in *Nicotiana benthamiana* by regulating viral coat protein functions. *Plant Cell* **22**, 523-535.
- Harries, P.A., Schoelz, J.E., and Nelson, R.S.** (2010). Intracellular Transport of Viruses and Their Components: Utilizing the Cytoskeleton and Membrane Highways. *MPMI* **23**, 1381-1393.
- Hipper, C., Brault, V., Ziegler-Graff, V., and Revers, F.** (2013). Viral and cellular factors involved in Phloem transport of plant viruses. *Front Plant Sci* **4**, 154.
- Hofius, D., Maier, A.T., Dietrich, C., Jungkunz, I., Bornke, F., Maiss, E., and Sonnewald, U.** (2007). Capsid protein-mediated recruitment of host DnaJ-like proteins is required for Potato virus Y infection in tobacco plants. *J Virol* **81**, 11870-11880.
- Hong, Y., and Hunt, A.G.** (1996). RNA Polymerase Activity Catalyzed by a Potyvirus-Encoded RNA-Dependent RNA Polymerase. *VIROLOGY* **226**, 146-151.
- Ivanov, K.I., and Makinen, K.** (2012). Coat proteins, host factors and plant viral replication. *Curr Opin Virol* **2**, 712-718.
- Ivanov, K.I., Puustinen, P., Gabrenaite, R., Vihinen, H., Rönstrand, L., Valmu, L., Kalkkinen, N., and Mäkinen, K.** (2003). Phosphorylation of the Potyvirus Capsid Protein by Protein Kinase CK2 and Its Relevance for Virus Infection. *The Plant Cell Online* **15**, 2124-2139.
- Jablonski, S.A., Luo, M., and Morrow, C.D.** (1991). Enzymatic Activity of Poliovirus RNA Polymerase Mutants with Single Amino Acid Changes in the Conserved YGDD Amino Acid Motif. *JOURNAL OF VIROLOGY*, 4565-4572.
- Jackson, A.O., Lim, H.S., Bragg, J., Ganesan, U., and Lee, M.Y.** (2009). Hordeivirus replication, movement, and pathogenesis. *Annu Rev Phytopathol* **47**, 385-422.
- Kamer, G., and Argos, P.** (1984). Primary structural comparison of RNA-dependent polymerases from plant, animal and bacterial viruses. *Nucleic Acids Research* **12**.
- Kang, S.H., Lim, W.S., Hwang, S.H., Park, J.W., Choi, H.S., and Kim, K.H.** (2006). Importance of the C-terminal domain of soybean mosaic virus coat protein for subunit interactions. *J Gen Virol* **87**, 225-229.
- Kawakami, S., Watanabe, Y., and Beachy, R.N.** (2004). Tobacco mosaic virus infection spreads cell to cell as intact replication complexes. *PNAS* **101**, 6291-6296.
- Kiba, A., Nakano, M., Vincent-Pope, P., Takahashi, H., Sawasaki, T., Endo, Y., Ohnishi, K., Yoshioka, H., and Hikichi, Y.** (2012). A novel Sec14 phospholipid transfer protein from *Nicotiana benthamiana* is up-regulated in response to *Ralstonia solanacearum* infection, pathogen associated molecular patterns and effector molecules and involved in plant immunity. *J Plant Physiol* **169**, 1017-1022.
- Lafn, S., Riechmann, J.L., and Garcfa, J.A.** (1990). RNA helicase: a novel activity associated with a protein encoded by a positive strand RNA virus. *Nucleic Acids Research* **18**, 7003.
- Laporte, C., Vetter, G., Loudes, A., Robinson, D.G., Hillmer, S., Stussi-Garaud, C., and Ritzenthaler, C.** (2003). Involvement of the Secretory Pathway and the Cytoskeleton in Intracellular Targeting and Tubule Assembly of Grapevine fanleaf virus Movement Protein in Tobacco BY-2 Cells. *The Plant Cell Online* **15**, 2058-2075.
- Lefebvre, B., Timmers, T., Mbengue, M., Moreau, S., Herve, C., Toth, K., Bittencourt-Silvestre, J., Klaus, D., Deslandes, L., Godiard, L., Murray, J.D., Udvardi, M.K., Raffaele, S., Mongrand, S., Cullimore, J., Gamas, P., Niebel, A., and Ott, T.** (2010). A remorin protein interacts with symbiotic receptors and regulates bacterial infection. *Proc Natl Acad Sci U S A* **107**, 2343-2348.

- Li, F., Zhang, C., Li, Y., Wu, G., Hou, X., Zhou, X., and Wang, A.** (2018). Beclin1 restricts RNA virus infection in plants through suppression and degradation of the viral polymerase. *Nat Commun* **9**, 1268.
- Lim, H.S., Bragg, J.N., Ganesan, U., Ruzin, S., Schichnes, D., Lee, M.Y., Vaira, A.M., Ryu, K.H., Hammond, J., and Jackson, A.O.** (2009). Subcellular localization of the barley stripe mosaic virus triple gene block proteins. *J Virol* **83**, 9432-9448.
- Lucas, W.J.** (2006). Plant viral movement proteins: agents for cell-to-cell trafficking of viral genomes. *Virology* **344**, 169-184.
- Lucas, W.J., Ham, B.K., and Kim, J.Y.** (2009). Plasmodesmata - bridging the gap between neighboring plant cells. *Trends Cell Biol* **19**, 495-503.
- McClintock, K., Lamarre, A., Parsons, V., Laliberté, J.F., and Fortin, M.J.** (1998). Identification of a 37 kDa plant protein that interacts with the turnip mosaic potyvirus capsid protein using anti-idiotypic-antibodies. *Plant Molecular Biology* **37**, 197-204.
- Nathalie, L.-C., and Bouhidel, K.** (2014). Plasma membrane protein trafficking in plant-microbe interactions: a plant cell point of view. *Front Plant Sci* **5**, 735.
- Olivier, N., and Laliberté, J.F.** (1992). The complete nucleotide sequence of turnip mosaic potyvirus RNA. *Journal of General Virology* **73**, 2785-2793.
- Park, S.H., Li, F., Renaud, J., Shen, W., Li, Y., Guo, L., Cui, H., Sumarah, M., and Wang, A.** (2017). NbEXPA1, an alpha-expansin, is plasmodesmata-specific and a novel host factor for potyviral infection. *Plant J* **92**, 846-861.
- Peiro, A., Izquierdo-Garcia, A.C., Sanchez-Navarro, J.A., Pallas, V., Mulet, J.M., and Aparicio, F.** (2014). Patellins 3 and 6, two members of the Plant Patellin family, interact with the movement protein of Alfalfa mosaic virus and interfere with viral movement. *Mol Plant Pathol* **15**, 881-891.
- Peterman, T.K., Ohol, Y.M., McReynolds, L.J., and Luna, E.J.** (2004). Patellin1, a novel Sec14-like protein, localizes to the cell plate and binds phosphoinositides. *Plant Physiol* **136**, 3080-3094; discussion 3001-3082.
- Pouwels, J., van der Velden, T., Willemse, J., Borst, J.W., van Lent, J., Bisseling, T., and Wellink, J.** (2004). Studies on the origin and structure of tubules made by the movement protein of Cowpea mosaic virus. *J Gen Virol* **85**, 3787-3796.
- Raffaele, S., Bayer, E., Lafarge, D., Cluzet, S., German Retana, S., Boubekour, T., Leborgne-Castel, N., Carde, J.P., Lherminier, J., Noirot, E., Satiat-Jeuemaitre, B., Laroche-Traineau, J., Moreau, P., Ott, T., Maule, A.J., Reymond, P., Simon-Plas, F., Farmer, E.E., Bessoule, J.J., and Mongrand, S.** (2009). Remorin, a solanaceae protein resident in membrane rafts and plasmodesmata, impairs potato virus X movement. *Plant Cell* **21**, 1541-1555.
- Revers, F., and Garcia, J.A.** (2015). Molecular biology of potyviruses. *Adv Virus Res* **92**, 101-199.
- Robert, I.M., Wang, K., Findlay, K., and Maule, A.J.** (1998). Ultrastructural and Temporal Observations of the Potyvirus Cylindrical Inclusions (CIs) Show That the CI Protein Acts Transiently in Aiding Virus Movement. *VIROLOGY*, 173-181.
- Rodríguez-Cerezo, E., Findlay, K., Shaw, J.G., Lomonosoff, G., P., Qiu, S.G., Linstead, P., Shanks, M., and Risco, C.** (1997). The Coat and Cylindrical Inclusion Proteins of a Potyvirus Are Associated with Connections between Plant Cells. *VIROLOGY*, 296-306.
- Rojas, M.R., Zerbini, F.M., Allison, R.F., Gilbertson, R.L., and Lucas, W.J.** (1997). Capsid Protein and Helper Component-Proteinase Function as Potyvirus Cell-to-Cell Movement Proteins. *VIROLOGY* **237**, 283-295.
- Rybicki, E.P.** (2015). A Top Ten list for economically important plant viruses. *Arch Virol* **160**, 17-20.
- Sanfaçon, H.** (2005). Replication of positive-strand RNA viruses in plants: contact points between plant and virus components. *Canadian Journal of Botany* **83**, 1529-1549.

- Schaad, M.C., Jensen, P.E., and Carrington, J.C.** (1997). Formation of plant RNA virus replication complexes on membranes: role of an endoplasmic reticulum-targeted viral protein. *The EMBO Journal* **16**, 4049–4059.
- Seo, J.K., Vo Phan, M.S., Kang, S.H., Choi, H.S., and Kim, K.H.** (2013). The charged residues in the surface-exposed C-terminus of the Soybean mosaic virus coat protein are critical for cell-to-cell movement. *Virology* **446**, 95-101.
- Shukla, D.D., Strike, P.M., Tracy, S.L., Gough, K.H., and Ward, C.W.** (1988). The N and C Termini of the Coat Proteins of Potyviruses Are Surface-located and the N Terminus Contains the Major Virus-specific Epitopes. *Journal of General Virology* **69**, 1497-1508.
- Sorel, M., Garcia, J.A., and German-Retana, S.** (2014). The Potyviridae cylindrical inclusion helicase: a key multipartner and multifunctional protein. *Mol Plant Microbe Interact* **27**, 215-226.
- Tejosa, R., Rodriguez-Furlanb, C., Adamowskic, M., Sauerd, M., Norambuenab, L., and Frimlc, J.** (2017). PATELLINS are regulators of auxin-mediated PIN1 relocation and plant development in *Arabidopsis thaliana*. *J Cell Sci* **jcs-204198**.
- Tomlinson, J.A.** (1987). Epidemiology and control of virus diseases of vegetables. *Annals of Applied Biology* **110**, 661-681.
- Varma, A., Gibbs, A.J., Woods, R.D., and Finch, J.T.** (1968). Some Observations on the Structure of the Filamentous Particles of Several Plant Viruses *Journal of General Virology* **2**, 107-114.
- Verchot-Lubicz, J.** (2005). A New Cell-to-Cell Transport Model for Potexviruses. *MPMI* **18**, 283–290.
- Verchot-Lubicz, J., Torrance, L., Solovyev, A.G., Morozov, S.Y., Jackson, A.O., and Gilmer, D.** (2010). Varied Movement Strategies Employed by Triple Gene Block–Encoding Viruses. *MPMI* **23**, 1231–1247.
- Vijayapalani, P., Maeshima, M., Nagasaki-Takekuchi, N., and Miller, W.A.** (2012). Interaction of the trans-frame potyvirus protein P3N-PIPO with host protein PCaP1 facilitates potyvirus movement. *PLoS Pathog* **8**, e1002639.
- Walsh, J.A., and Jenner, C.E.** (2002). Turnip mosaic virus and the quest for durable resistance. *MOLECULAR PLANT PATHOLOGY* **3**, 289–300.
- Wang, A.** (2013). Molecular isolation and functional characterization of host factors required in the virus infection cycle for disease control in plants. *CAB Reviews* **8**.
- Wang, A.** (2015). Dissecting the molecular network of virus-plant interactions: the complex roles of host factors. *Annu Rev Phytopathol* **53**, 45-66.
- Wei, T., and Wang, A.** (2008). Biogenesis of cytoplasmic membranous vesicles for plant potyvirus replication occurs at endoplasmic reticulum exit sites in a COPI- and COPII-dependent manner. *J Virol* **82**, 12252-12264.
- Wei, T., Zhang, C., Hou, X., Sanfacon, H., and Wang, A.** (2013). The SNARE protein Syp71 is essential for turnip mosaic virus infection by mediating fusion of virus-induced vesicles with chloroplasts. *PLoS Pathog* **9**, e1003378.
- Wei, T., Huang, T.S., McNeil, J., Laliberte, J.F., Hong, J., Nelson, R.S., and Wang, A.** (2010a). Sequential recruitment of the endoplasmic reticulum and chloroplasts for plant potyvirus replication. *J Virol* **84**, 799-809.
- Wei, T., Zhang, C., Hong, J., Xiong, R., Kasschau, K.D., Zhou, X., Carrington, J.C., and Wang, A.** (2010b). Formation of complexes at plasmodesmata for potyvirus intercellular movement is mediated by the viral protein P3N-PIPO. *PLoS Pathog* **6**, e1000962.
- Whitham, S.A., Anderberg, R.J., Chisholm, S.T., and Carrington, J.C.** (2000). *Arabidopsis* RTM2 Gene Is Necessary for Specific Restriction of Tobacco Etch Virus and Encodes an Unusual Small Heat Shock–like Protein. *The Plant Cell* **12**, 569–582.

- Wylie, S.J., Adams, M., Chalam, C., Kreuze, J., Lopez-Moya, J.J., Ohshima, K., Praveen, S., Rabenstein, F., Stenger, D., Wang, A., Zerbini, F.M., and Ictv Report, C.** (2017). ICTV Virus Taxonomy Profile: Potyviridae. *J Gen Virol* **98**, 352-354.
- Xiong, R., and Wang, A.** (2013). SCE1, the SUMO-conjugating enzyme in plants that interacts with NIb, the RNA-dependent RNA polymerase of Turnip mosaic virus, is required for viral infection. *J Virol* **87**, 4704-4715.
- Zamora, M., Méndez-López, E., Agirrezabala, X., Cuesta, R., Lavín, J.L., Sánchez-Pina, M.A., Aranda, M.A., and Valle, M.** (2017). Potyvirus virion structure shows conserved protein fold and RNA binding site in ssRNA viruses. *Science Advances* **3**.

Chapter 2

2 Identification of the determinants in TuMV CP essential for viral cell-to-cell movement, long-distance movement and virion assembly

2.1 Abstract

Plant viral coat proteins (CPs) are multifunctional proteins that play key roles in the virus infection cycle. To date, little is known about the role of *Turnip mosaic virus* (TuMV; the genus *Potyvirus*, the family *Potyviridae*) CP in viral movement and virion assembly. The coat protein of TuMV comprises 288 amino acids. Here I determined the domains and specific amino acids of CP that are critical for TuMV movement and virion assembly. A series of deletion and point mutations were introduced into the CP cDNA in a green fluorescent and mCherry fluorescent protein-tagged TuMV infectious clone, and the effects of these mutations on viral cell-to-cell, long-distance movement, and virion assembly were examined. The mutant with a deletion of the N-terminal amino acids 6-50 of CP showed normal cell-to-cell and long-distance movement, and morphologically typical virions, suggesting that the N-terminus of CP is dispensable for TuMV movement and virion assembly. However, mutants missing the core domain amino acids 51 to 199, or the C-terminal amino acids 200 to 288 or 265 to 274 abolished viral cell-to-cell movement, suggesting that the core domain and C-terminus of CP are critical for TuMV cell-to-cell movement. Additionally, twelve point mutants were generated in the core domain and C-terminus of CP and among them, the point mutants E₂₆₈A and R₂₆₉A and the double mutant ER_{268/269}AA exhibited slow cell-to-cell movement with a delayed onset of systemic infection independent of virion assembly. R₁₇₈A and D₂₂₂A abolished cell-to-cell movement and failed to form virions in protoplasts. We further found that the CP protein R₁₇₈A is less stable than wild-type CP. My studies identified the determinants of TuMV cell-to-cell movement, long-distance movement and virion assembly, revealing that TuMV CPs act as multifunctional proteins by bearing specific amino acids required for TuMV movement and assembly.

2.2 Introduction

Plant viral coat proteins (CPs) are structural proteins and form the protective shell that encapsidates and protects the viral genome. In addition to this conserved function, CPs play diverse roles at different stages of the infection process, such as virus entry, viral RNA transcription, replication, virus movement, virus transmission, activation or suppression of host defenses and symptom development (Callaway et al., 2001; Ni and Cheng Kao, 2013). From a molecular biology perspective, the CPs must possess multiple determinants (specific amino acids and/or motifs) to fulfill these multiple tasks. Thus, the molecular identification of the functional determinants of CPs involved in various steps of the viral infection cycle will certainly advance knowledge of virology.

To establish successful systemic infection, a plant virus needs to move from the primarily infected cells through plasmodesmata (PDs), the cytoplasmic bridges between adjacent plant cells, to the neighbouring cells (Lucas, 2006; Lucas et al., 2009). Then, plant viruses undergo several cycles of cell-to-cell movement until reaching the vascular tissue, followed by loading into phloem tissues for long-distance movement, eventually invading the whole plant (Benitez-Alfonso et al., 2010; Hipper et al., 2013). It is now well established that many plant viruses, such as tobamoviruses, cucumoviruses and geminiviruses, encode dedicated movement proteins (MPs) allowing viruses to pass through PDs to the neighboring cells in the form of virion or ribonucleoprotein (RNP) complex. For potyviruses, P3N-PIPO has recently been suggested to be a dedicated MP (Cui et al., 2017). In addition, several potyviral proteins have been implicated in potyviral cell-to-cell movement, including HC-Pro (the helper component protease), P3 (the third protein), CI (the cylindrical inclusion protein), VPg (viral genome-linked protein) and CP. The potyviral CP has variable N- and C-terminal domains exposed on the virion surface that are susceptible to trypsin treatment and a conserved core domain that interacts with viral RNA and forms the core subunit structure of the virion (Allison et al., 1985a; Shukla and Ward, 1988; Zamora et al., 2017).

The TuMV CP comprises 288 amino acid residues with a molecular mass of approximately 34 kDa. Among members of the *Potyvirus* genus, although the CP of

Tobacco etch virus (TEV) and *Soybean mosaic virus* (SMV) have been demonstrated to be critical for viral movement and virion assembly, very limited studies have been carried out to investigate the molecular mechanisms underlying the multiple functions of the CP.

The aim of the present study was to identify the determinants of TuMV CP in viral cell-to-cell movement and virion assembly using a series of CP deletion and point mutants tagged with green and mCherry fluorescent protein. This double fluorescent protein-tagged TuMV system allows to discriminate primarily and secondarily infected cells via agroinfiltration. I found that the C-terminal amino acids 265 to 274 are crucial for TuMV cell-to-cell movement. We further discovered that substitution of the C-terminal amino acid residue E₂₆₈ or R₂₆₉ with an alanine results in slow intercellular movement, which is independent of encapsidation, and substitution of the amino acid residue R₁₇₈ or D₂₂₂ with an alanine in the core domain abolishes viral cell-to-cell movement. Moreover, a stretch of 45 amino acid residues comprising amino acids 6-50 of CP is dispensable for TuMV cell-to-cell movement and virion assembly. I also demonstrated that the movement-deficient R₁₇₈A CP exhibits similar subcellular localization, interaction with other viral proteins and binding ability to TuMV genomic RNA as the wild-type CP. However, R₁₇₈A and D₂₂₂A fail to form virions in protoplasts and R₁₇₈A is less stable than wild-type CP.

2.3 Results

2.3.1 Construction of a plant expression vector that allows for visualization of TuMV-inoculated cells from secondarily infected cells

To discriminate virus-inoculated cells from secondarily infected cells in plants, we generated a plant expression vector (designated pCBTuMV-GFP//mCherry, WT) that contains two separate expression cassette: one containing a GFP coding sequence embedded in the TuMV genome and the other encoded mCherry fluorescent protein fused with a luminal ER retention signal (HDEL) (Fig 2.1A). Both GFP and mCherry fluorescent protein are expressed in the agroinfiltrated cells (or primarily infected cells), leading to the emission of both green and red fluorescence. As the virus tagged by GFP replicates and moves to the neighboring cells, the secondarily infected cells emit only green fluorescence.

To test the infectivity of pCBTuMV-GFP//mCherry (WT), the plasmid WT was transformed into *Agrobacterium tumefaciens* GV3101 and agroinfiltrated into three-week-old *Nicotiana benthamina* leaves with a very low concentration of agrobacterial cells (OD_{600} 0.001). TuMV cell-to-cell movement did not initiate until approximately three days post inoculation (dpi). The optimal time point for observation of viral cell-to-cell movement was 4 dpi when secondarily infected cells emitted strong green fluorescence whereas inoculated cells emitted green and red fluorescence (Fig 2.1B). Virus systemic infection was observed at five to seven dpi in the newly emerging leaves showing strong green fluorescence under UV light (Fig 2.1C). As expected, no detectable green fluorescence was observed in the buffer-inoculated leaf tissues of the plants (mock) (Fig 2.1C). Typical symptoms such as mosaic, chlorosis, and stunting were observed on WT-inoculated plants and no symptoms developed on the mock plants (data not shown). Viral infection was further confirmed on systemic leaves of WT-inoculated plants by RT-PCR using specific primers for the amplification of the coding sequence for CP, and by Western blot (WB) for the detection of TuMV CP using anti-TuMV antibodies at 7 dpi (Fig 2.1D).

Our results indicate that pCBTuMV-GFP//mCherry is a TuMV infectious clone that may serve as a powerful system for studying viral intercellular movement.

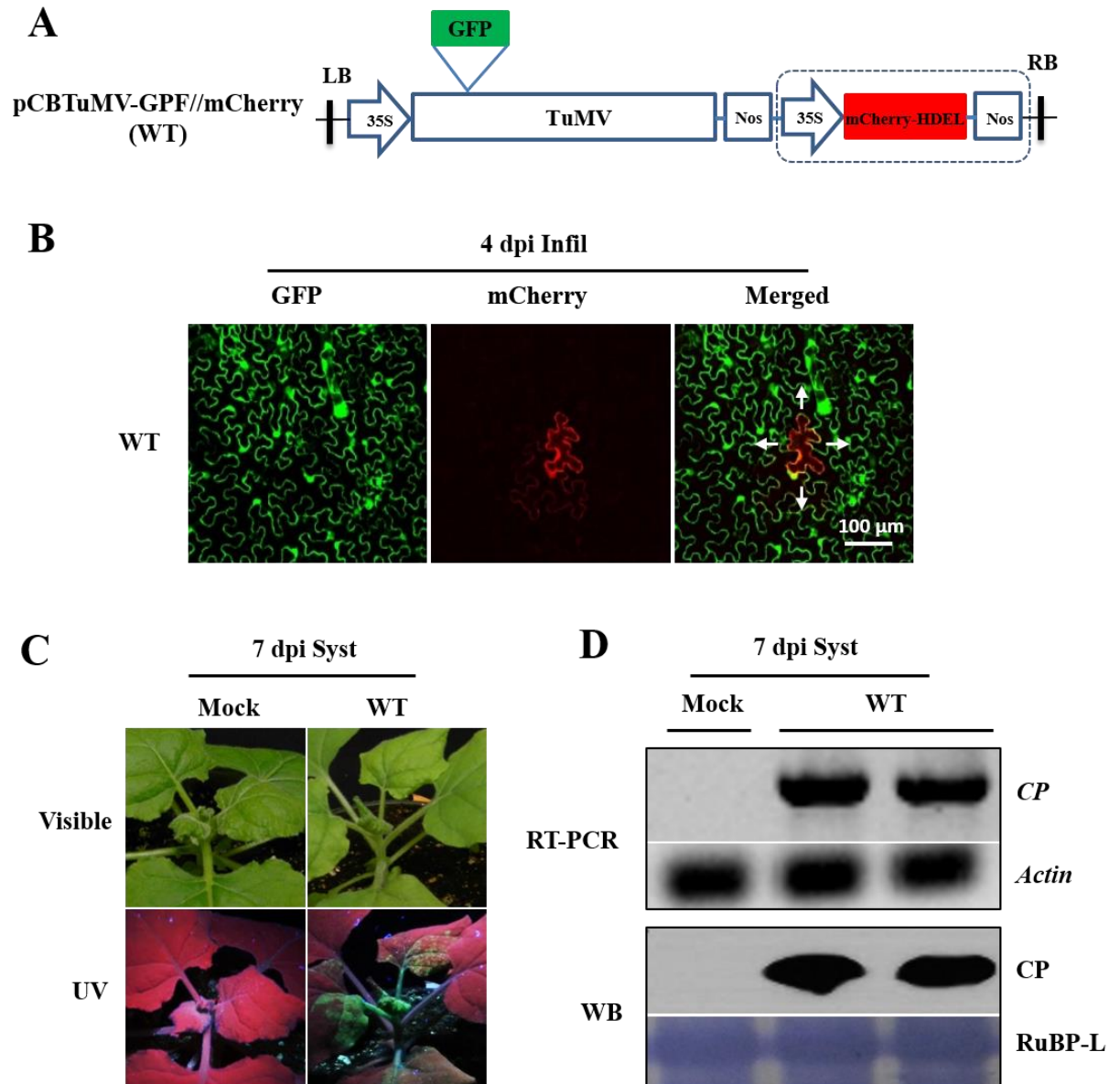


Figure 2.1 Construction of a TuMV infectious clone suitable for monitoring viral cell-to-cell movement.

(A) Schematic representation of the infectious clone pCBTuMV-GFP//mCherry (WT) for distinguishing between primary and secondary infection sites. GFP was inserted between P1 and HC-Pro cistrons of the TuMV genome. (B) Confocal images of pCBTuMV-GFP//mCherry agroinfiltrated into *N. benthamiana* leaf epidermal cells. The recombinant TuMV virus tagged by GFP moved from the primarily infected cells (emitting both green and red fluorescence) to the secondarily infected cells (emitting only green fluorescence) at 4 dpi. Arrows illustrate TuMV intercellular movement. Scale bar, 100 μ m. (C) WT established successful systemic infection on *N. benthamiana* plant. Infection was monitored by visualization of GFP fluorescence under UV light at 7 dpi. (D) RT-PCR and Western blot analysis of systemic leaves of *N. benthamiana* plant at 7 dpi. TuMV-specific primers were used for detection of positive-strand viral RNA. *NbActin* served as a control. Total proteins extracts were probed with TuMV CP antibodies. The Coomassie Brilliant Blue-stained rubisco large subunit (RuBP-L) served as a loading control.

2.3.2 TuMV CP is dispensable for virus replication, but critical for cell-to-cell movement

Previously, CP has been shown to be critical for TEV and SMV cell-to-cell movement (Dolja et al., 1994; Dolja et al., 1995; Seo et al., 2013). To determine if CP is required for TuMV intercellular movement, a CP deletion mutant (Δ CP) was constructed by deleting the CP coding sequence except for five amino acids at the N and C termini (Fig 2.2A). In addition, a replication-defective GDD deletion mutant (Δ GDD) was also generated by deletion of the highly conserved GDD motif of the viral RNA-dependent RNA polymerase N1b (Fig 2.2A). Agrobacterial cells harboring WT, Δ CP, and Δ GDD respectively, were infiltrated into *N. benthamina* leaf cells. At 4 dpi, a cluster of cells emitting only green fluorescence in WT-inoculated *N. benthamina* leaf, indicating viral intercellular movement. However, both Δ CP and Δ GDD were restricted to single cells that emitted both green and red fluorescence under confocal microscope (Fig 2.2B), suggesting Δ CP and Δ GDD mutants failed to move from the primarily infected cell to the neighboring cells. No intercellular movement for Δ CP and Δ GDD mutants was observed even at 5, 6 and 7 dpi by confocal microscopy (data not shown). In plants agroinfiltrated with the Δ CP mutant, no green fluorescence was detectable in the upper new leaves under UV light at 9 dpi (Fig 2.2B). Consistently, viral RNA was not detected by RT-PCR in these new leaves (Fig 2.2C). No typical symptoms and viral RNA were detected in Δ CP-inoculated plants over 35 dpi (data not shown).

As described above, virus intercellular movement does not occur approximately until 72 dpi. Therefore, TuMV replication in the primarily infected cells may be evaluated by quantification of viral RNA accumulation in the inoculated leaves at 54 hpi using RT-PCR. Quantitative RT-PCR (qRT-PCR) detected a comparable level of viral genomic RNA in Δ CP-inoculated leaves to that of WT-inoculated leaves (Fig 2.2D), indicating Δ CP mutant exhibits normal RNA amplification compared to WT.

I further carried out a protoplast transfection assay. Since transfection efficiency with pCBTuMV-GFP//mcherry by the PEG method was low (data not shown), I used pCambiaGFP-TuMV (pCam-WT) as a parental clone and constructed two mutants named

pCambiaGFP- Δ CP (pCam- Δ CP) and pCambiaGFP- Δ GDD (pCam- Δ GDD) where CP and GDD were deleted, respectively. *N. benthamiana* mesophyll protoplasts were isolated and transfected with pCam-WT, pCam- Δ GDD and pCam- Δ CP, respectively. qRT-PCR was performed to quantify TuMV genomic RNA at 24 hours post transfection (hpt). As expected, the negative control pCam- Δ GDD mutant showed a dramatically decreased viral RNA accumulation level in comparison with pCam-WT (Fig 2.2E). However, the pCam- Δ CP mutant showed a similar viral RNA accumulation level to that of pCam-WT (Fig 2.2E), suggesting that deletion of CP had no significant effect on TuMV replication in *N. benthamiana* protoplasts. Taken together, these data suggest that CP is dispensable for TuMV replication but is required for TuMV cell-to-cell movement.

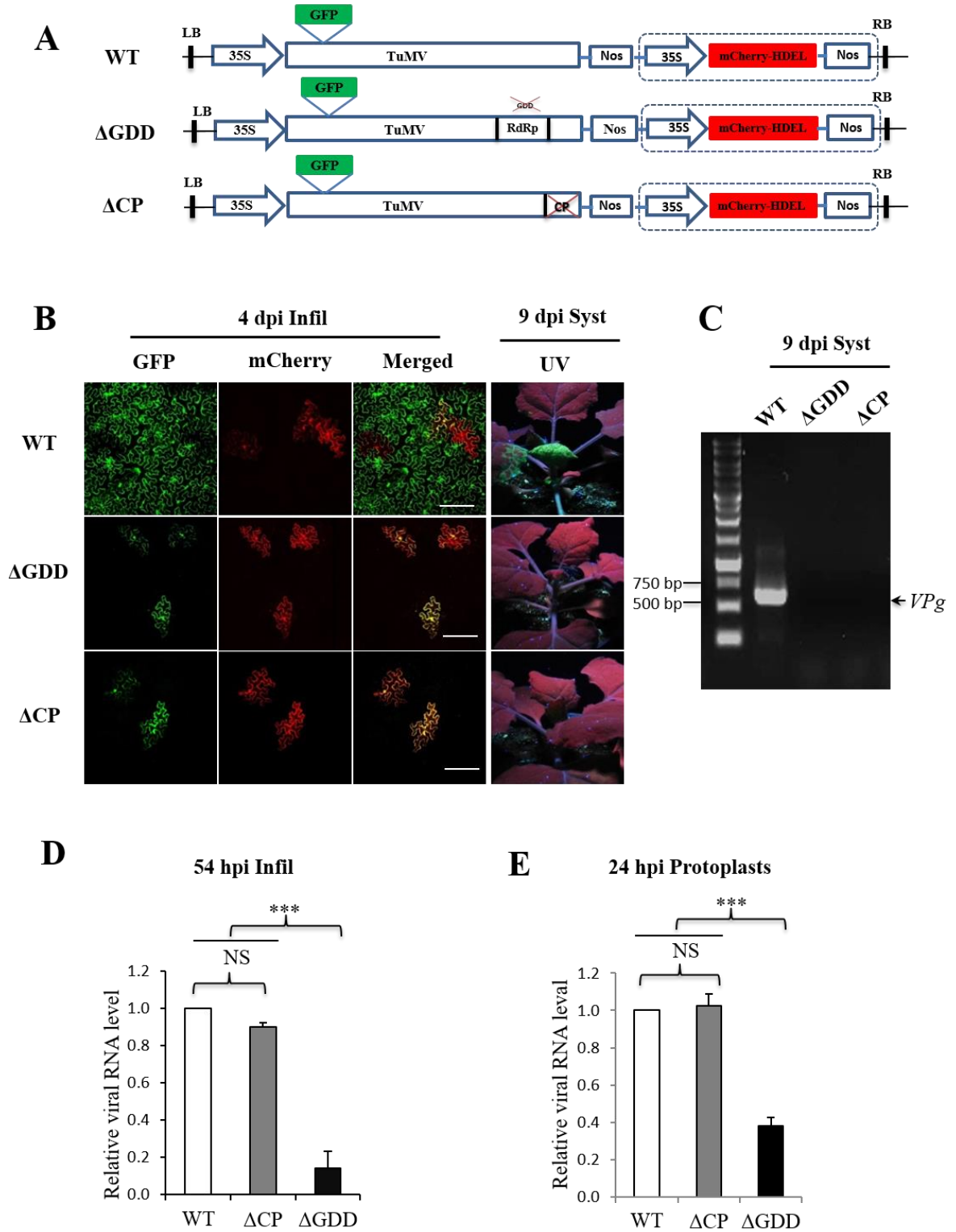


Figure 2.2 CP is required for TuMV cell-to-cell movement but not for viral replication.

(A) Schematic representation of WT virus and viral mutants Δ GDD (deletion of the GDD motif of RdRp from WT virus) and Δ CP (deletion of the CP coding region from WT virus). (B) Analysis of cell-to-cell movement and long-distance movement of WT, Δ GDD and Δ CP in *N. benthamiana* plant. Confocal images are taken at 4 dpi on infiltrated leaf to determine cell-to-cell movement ability. Note that both Δ GDD and Δ CP were restricted in single cells comparing to WT formed large foci. Scale bar = 100 μ m. Long-distance movement was monitored via GFP fluorescence under UV light at 9 dpi. (C) RT-PCR analysis of systemic leaf of inoculated plants at 9 dpi. TuMV specific primers are used to detect viral positive-strand RNA and *NbActin* transcripts were served as internal control. (D) qRT-PCR analysis of viral RNA accumulation of WT or mutants-infiltrated leaves. Total RNA was extracted from agroinfiltrated leaves at 54 hpi and used for RT-qPCR. *mCherry* transcripts were used as normalization control. Error bars represent the standard deviation of three biological replicates. Statistically significant difference was determined by unpaired two-tailed Student's test. (***, $P < 0.001$; NS, Non-significant). (E) qRT-PCR analysis of viral RNA accumulation of WT or mutants-infected protoplasts at 24 hpi. Total RNA was extracted from transfected protoplasts at 24 hpi and was subjected to qRT-PCR. *NbActin* was used as normalization control. Error bars represent the standard deviation of three biological replicates. Statistically significant difference was determined by unpaired two-tailed Student's test. (***, $P < 0.001$; NS, Non-significant).

2.3.3 The core domain and C-terminus of CP are critical for TuMV cell-to-cell movement, whereas the N-terminal amino acids 6-50 are dispensable for viral movement and virion assembly

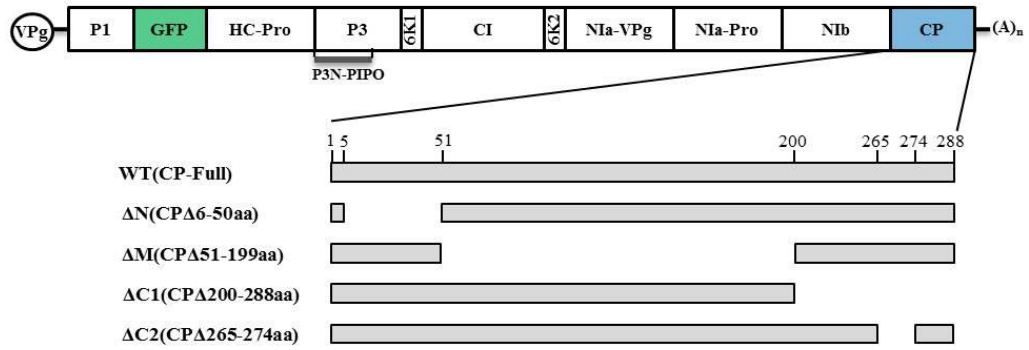
To determine which domain of CP plays an important role on TuMV cell-to-cell movement, I constructed four CP truncated mutants CP Δ 6-50aa (Δ N), CP Δ 51-199aa (Δ M), CP Δ 200-288aa (Δ C1) and CP Δ 265-274aa (Δ C2), where CP amino acid residues 6 to 50, 51 to 199, 200 to 288 and 265 to 274 were deleted, respectively (Fig 2.3A).

Agroinfiltration infection assay showed both the WT virus and the Δ N mutant could systemically infect the *N. benthamiana* plants at 9 dpi and that green fluorescence was clearly observed in the upper new leaves under UV light (Fig 2.3C). However, Δ M, Δ C1 and Δ C2 failed to infect *N. benthamiana* systemically since no green fluorescence was observed under UV light at 9 dpi (Fig 2.3C), neither Δ M, Δ C1 nor Δ C2-inoculated plants developed any detectable symptoms for up to 35 days (Fig 2.3D). Total RNA was extracted from the upper new leaves at 9 and 35 dpi and subjected to RT-PCR with TuMV specific primers. No viral RNA was detected in the upper new leaves of Δ M, Δ C1 or Δ C2-inoculated plants (Fig 2.3E). The fact that Δ M, Δ C1 and Δ C2 fail to establish systemic infection lead me to speculate that these truncated mutants might exhibit abnormal cell-to-cell movement ability. The inoculated *N. benthamiana* leaves were then subjected to confocal microscopy at 4 dpi. WT virus induced large foci of green fluorescence throughout the inoculated leaf area (Fig 2.3B). In contrast, infection by Δ GDD, Δ M, Δ C1 or Δ C2 was restricted to the primarily infected cells emitting both green and red fluorescence signals, indicating amino acids 51-199, 200-288 and 265 to 274 of CP are critical for TuMV cell-to-cell movement (Fig 2.3B).

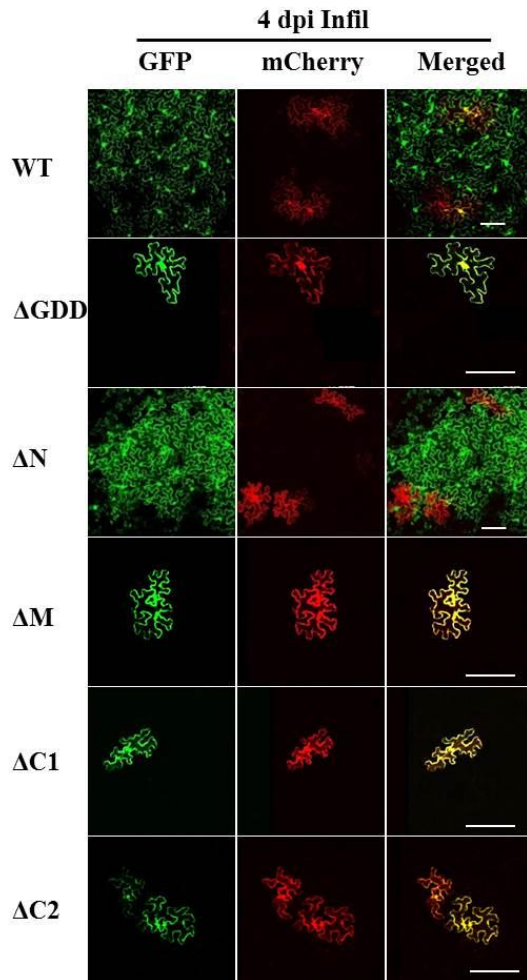
Interestingly, the mutant Δ N systemically infected the *N. benthamiana* plants (Fig 2.3C and D) and showed the ability to move intercellularly as the WT virus (Fig 2.3B). These results demonstrated that the N-terminal region from amino acids 6 to 50 of CP is dispensable for TuMV cell-to-cell movement and long-distance movement. To determine whether Δ N can form virions in the infected plant cells, crude virion preparations were obtained from the *N. benthamiana* protoplasts transfected with Δ N or the upper new

leaves of the *N. benthamiana* agroinfiltrated with ΔN . TEM with negative staining visualized morphologically typical TuMV virions (around 600 to 1000 nm long and 15-20 nm wide, flexuous and filamentous) in both samples (Fig 2.4A). I also verified the presence of viral CP and viral RNA by western blot assay and RT-PCR in both the crude virion preparations (Fig 2.4B and C). These results indicate that the N-terminal amino acids 6 to 50 of CP are not required for TuMV virion assembly.

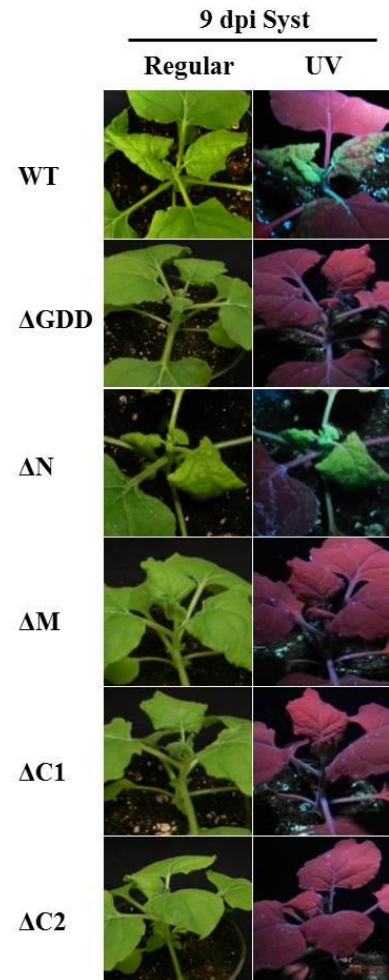
A



B



C



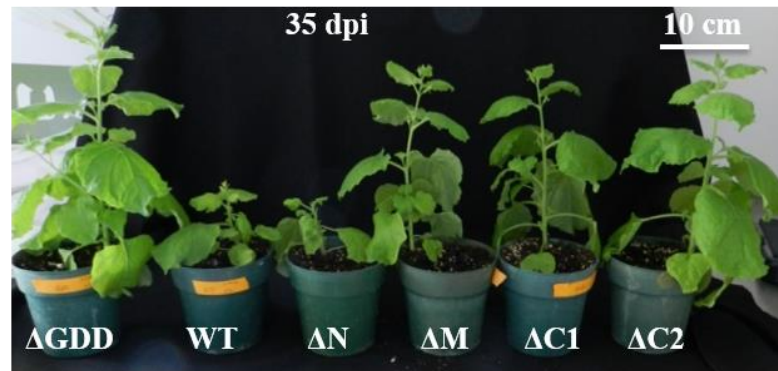
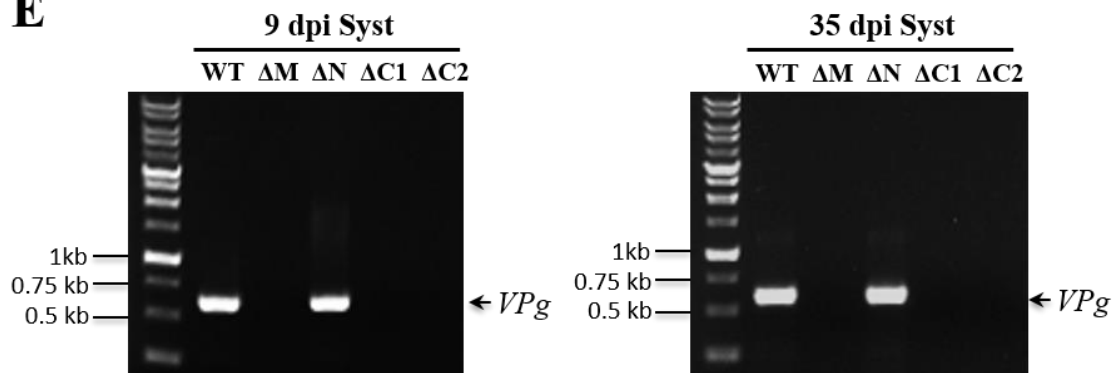
D**E**

Figure 2.3 Effects of truncated mutations of CP on TuMV cell-to-cell movement and long-distant movement.

(A) Schematic representation of truncated CP mutants. (B) Analysis of cell-to-cell movement of truncated CP mutants. Confocal images were taken from infiltrated leaves at 4 dpi. Scale bar = 100 μ m. (C) Analysis of systemic infection of truncated CP mutants. The long-distance movement was monitored by visualization of GFP fluorescence under UV light at 9 dpi. (D) Phenotypes of *N. benthamiana* plants infected by truncated CP mutants at 35 dpi. Scale bar = 10 cm. (E) RT-PCR analysis of viral RNA from systemic leaf of *N. benthamiana* plants inoculated by truncated CP mutants at 9 dpi and 35 dpi. TuMV specific primers were used to detect viral positive-strand RNA.

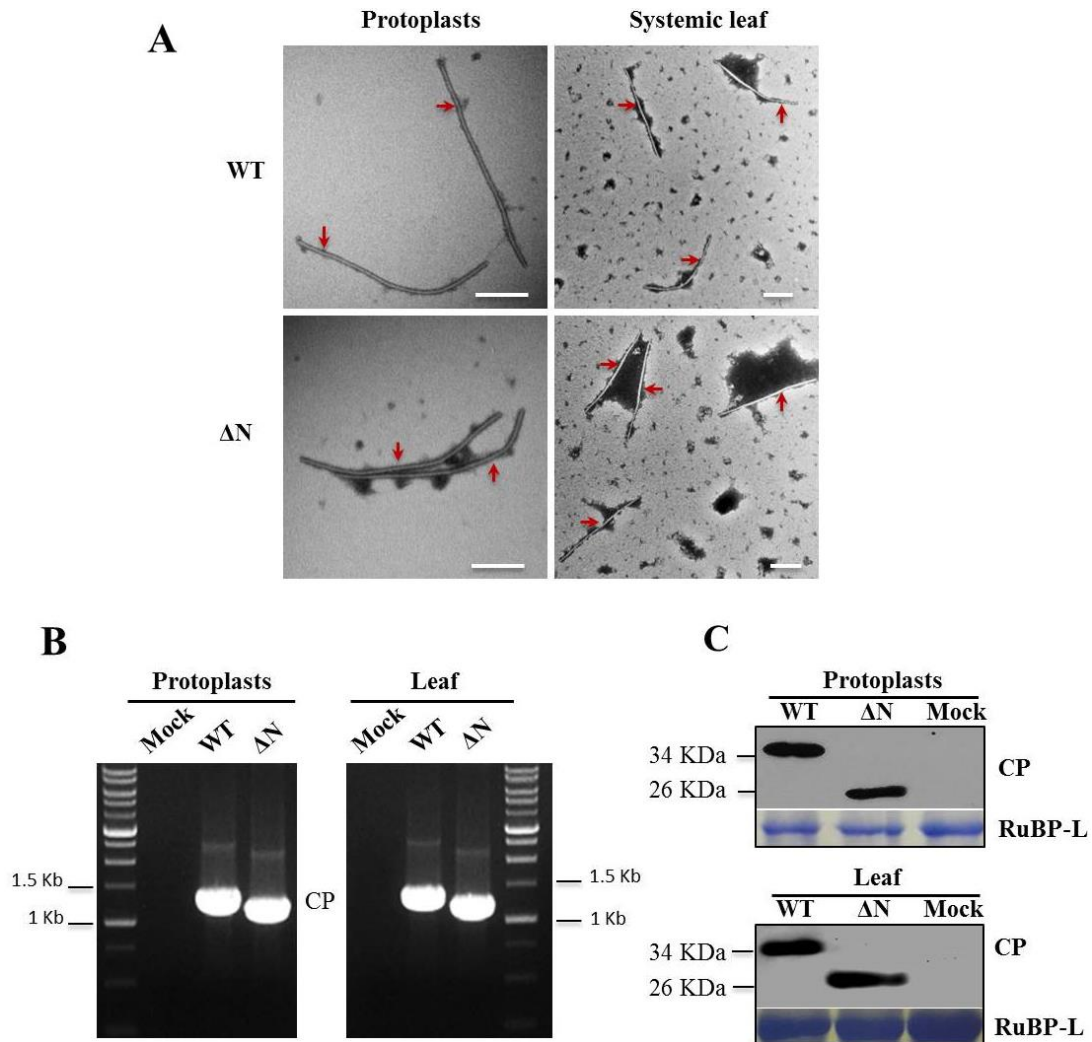


Figure 2.4 The N-terminus of CP is dispensable for TuMV virion assembly.

(A) Analysis of virion assembly ability of ΔN mutant by TEM. Crude virion preparations were obtained from the *N. benthamiana* protoplasts transfected with ΔN at 48 hpi or the upper new leaves of the *N. benthamiana* agroinfiltrated with ΔN at 12 dpi. The preparation was subjected to negative staining and TEM. Scale bar = 200 nm. (B) RT-PCR analysis of viral RNA extracted from ΔN -infected protoplasts of *N. benthamiana* leaves at 48 hpi or from the upper new leaves of *N. benthamiana* plant agroinfiltrated with ΔN at 12 dpi. RT-PCR with TuMV specific primers were used to detect viral positive-strand RNA. (C) Western blot analysis of total proteins extracted from ΔN -infected protoplasts or leaf tissues indicated in (B). Total proteins extracts were probed

with TuMV CP antibody. The Coomassie Brilliant Blue-stained rubisco large subunit (RuBP-L) serves as a loading control.

2.3.4 Identification of amino acids in TuMV CP essential for virus cell-to-cell movement via point mutation analyses

As shown above, the core domain and C-terminus of CP are critical for TuMV intercellular movement. To further determine which amino acids in the core and C-terminus are critical for viral intercellular movement, I first did the protein sequence alignment among seven species in the genus of potyvirus and selected conserved and charged amino acids for substitution with alanine. I generated twelve point mutants and evaluated the effects of those mutants on viral movement and virion assembly (Fig 2.5A).

I found that the point mutants R₁₉₅ A, D₂₅₇ A, E₂₆₅ A, and D₂₇₄ A (designated as group 1 mutants) could systemically infect *N. benthamiana* at 10 dpi, 22 dpi and 35 dpi, and the infected plants showed severe symptoms similar to WT-infected plants (Fig 2.5B and C; Table 2.1). At 4 dpi, these mutants established large infection loci in the inoculated leaf as indicated by green fluorescence under confocal microscopy (Fig 2.5B). These data suggest that substitution of the charged amino acids R₁₉₅, D₂₅₇, E₂₆₅, and D₂₇₄ with alanine does not affect TuMV cell-to-cell and long-distance movement.

Different from WT and group 1 mutants, the point mutants E₂₆₈A, R₂₆₉A and the double mutant ER_{268/269}AA (ER) (designated as group 2 mutants) exhibited a significant delay in the onset of systemic symptoms in inoculated plants at 10 dpi, 22 dpi and 35 dpi (Fig 2.5B and C; Table 2.1). Consistently, I found that the viral RNA level of these mutants was reduced in the inoculated leaf at 4 dpi and in the systemically infected leaf at 10 dpi when compared to that of WT (Fig 2.5D and E). I further examined the CP protein level at 15 dpi in the systemically infected leaf with the mutants, and found the reduced CP level in the *N. benthamiana* plants infected by the mutant E₂₆₈A, R₂₆₉A or ER compared to that in WT-infected plants (Fig 2.6B). As defective intercellular movement might result in the delayed systemic infection, we further examined the cell-to-cell movement ability of the group 2 mutants. At 4 dpi, in the leaf tissue of *N. benthamiana* agroinfiltrated with WT, in addition to the primary infection cell highlighted by double

fluorescence, a bunch of surrounding cells emitted only green fluorescence, indicating a strong ability of WT to move between cells (Fig 2.5B). In contrast, a very limited number of cells emitted green fluorescence in the *N. benthamiana* leaf agroinfiltrated with E₂₆₈A, R₂₆₉A or ER, particularly last two mutants (Fig 2.5B). These results suggest that the amino acid residues E₂₆₈ and R₂₆₉ are critical for efficient viral movement and the delayed onset of systemic symptoms by group 2 mutants could be due to defects in viral cell-to-cell movement.

Among these twelve point mutants, I also found that five mutants R₁₇₈A, R₁₇₈D, D₂₂₂A, D₂₂₂R and the double mutant DR in which Arg (residue 178) and Asp (residue 222) are switched (designated as group 3 mutants) completely lost the ability to move between cells as green fluorescence in the leaf agroinfiltrated with these mutants were restricted in the primary infection cells (Fig 2.5B). No viral RNA was detected in the upper new leaves of the *N. benthamiana* plants agroinfiltrated with the group 3 mutants by qPCR at 10 dpi (Fig 2.5E) and no symptoms could be observed throughout the experimental period (Fig 2.5C). Taken together, the amino acid residues R₁₇₈ and D₂₂₂ are critical for TuMV cell-to-cell movement.

A

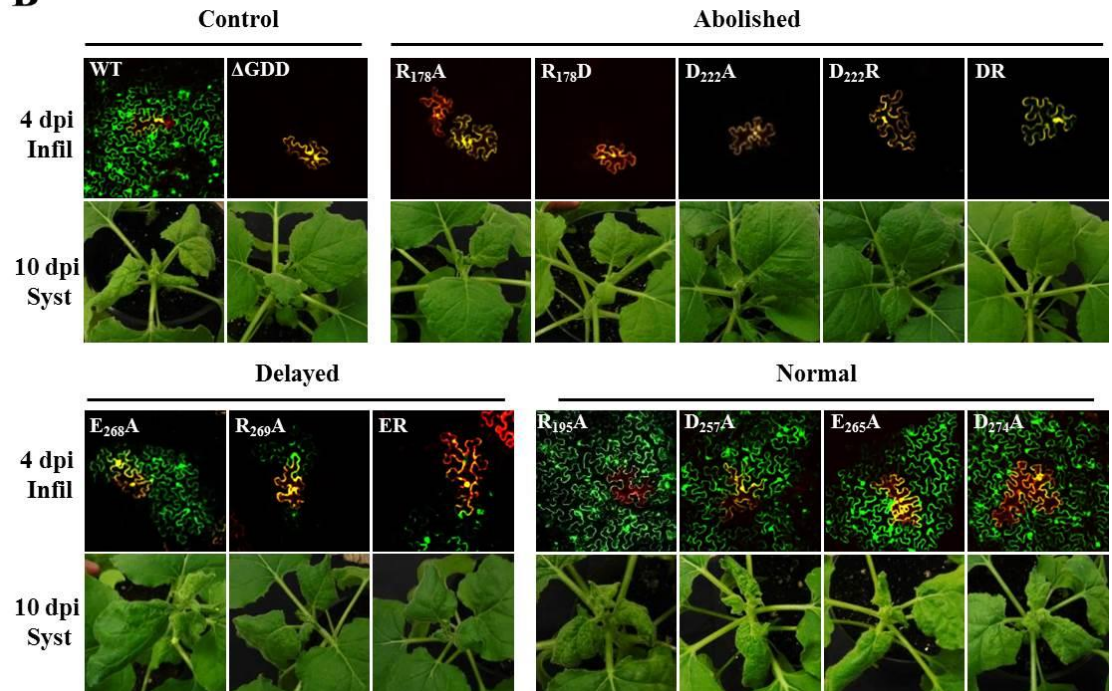
```

TuMV 178 RQIMAHFSDVAEAY IEKRNQDRPYMPRYGLQRNLTDSLARYAFDFYEMTSRTPIR 233
TEV 154 RQIMTHFSDLAEAY IEMRNRRPYMPRYGLQRNITDMSLSRYAFDFYELTSTKTPVR 209
SMV 154 RQIMHHFSDAAEAY IEMRNSESPYMPRYGLLRNLRDRELARYAFDFYEVTSKTPNR 209
PVA 159 RQIMRHFSALAEAY IEMRSREKPYMPRYGLQRNLRDQSLARYAFDFYELITATTPIR 214
WMV 172 RQIMHHFSDAAEAY IEMRNSESPYMPRYGLLRNLRDRELARYAFDFYEVTSKTPNR 227
PPV 205 RQIMAHFSNVAEAY IEKRNYEKAYMPRYGIQRNLTDSLARYAFDFYEMTSSTTPVR 260
TVMV 155 RQIMKHFSNLAEAY IRMRNSEQVYIPRYGLQRGLVDRNLAPFAFDFFEVNGATPVR 210
          **** *  **** *  *  **** *  *  *  **** *  ** *

TuMV 234 AREAHIQMKAALRGANNLFGLDGNVGTTVENTERHTTEDVNRNMHNLGVOGL- 288
TEV 210 AREAHMQMKAALVRNSGTRLFGLDGNVGTAEEDTERHTAHDVNRNMHTLLGVRQ-- 263
SMV 210 AREAIAQMKAALSGVNNKLFGLDGNISTNSEENTERHTARDVNQNMHTLLGMGPQQ 265
PVA 215 AKEAHLQMKAALKNSNTNMFGLDGNVTTSEEDTERHTATDVNRNMHLLGKVGK- 269
WMV 228 AREAIAQMKAALAGINSRFLFGLDGNISTNSEENTERHTARDVNQNMHTLLGMGPPQ 283
PPV 261 AREAHIQMKAALRNQVNRFLFGLDGNVGTQEEEDTERHTAGDVNRNMHNLGMRGV- 315
TVMV 211 AREAHAQMKAALRNSQRMFCLDGSVSGQEEENTERHTVDDVNAQMHHLLGKVGK- 265
          * * *  *****  * * * *  *  *****  * * *  * * * *

```

B



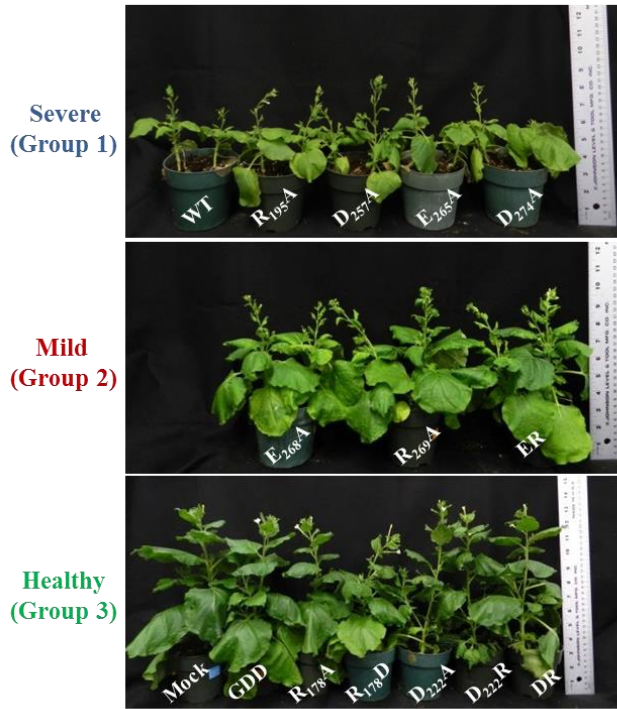
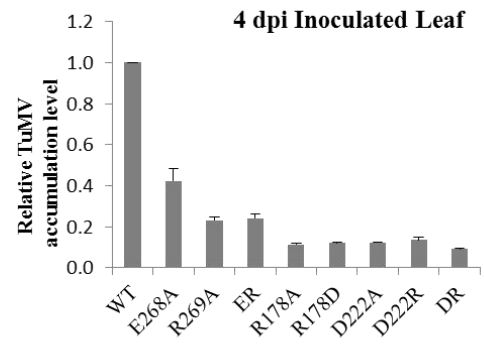
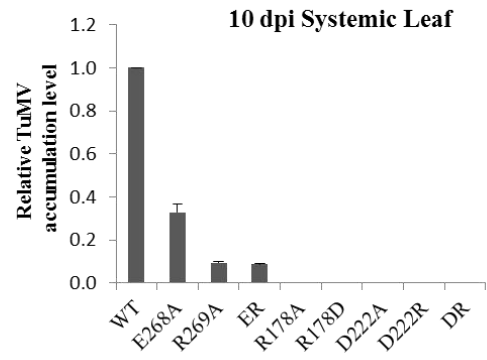
C**D****E**

Figure 2.5 Effects of CP point mutants on TuMV cell-to-cell movement and systemic infection.

(A) Protein sequences alignment of CP derived from various potyviruses. The abbreviated species names and their GenBank accession numbers are as follows: TuMV: *Turnip mosaic virus* (NC_002509); TEV: *Turnip etch virus* (NC_001555); SMV: *Soybean mosaic virus* (FJ807700); PVA: *Potato virus A* (NC_004039); WMV: *Watermelon mosaic virus* (NC_006262); PPV: *Plum pox virus* (NC_001445); TVMV: *Tobacco vein mottling virus* (NC_001768). Asterisks indicate identical residues and amino acids subjected to substitution are colored in green. (B) Analysis of cell-to-cell movement and systemic infection of CP point mutants. Confocal images were taken from infiltrated leaves at 4 dpi. Scale bar = 100 μ m. Images of upper uninfiltrated leaves were taken at 10 dpi. (C) Phenotypes of various CP point mutants-infected *N. benthamiana* plant at 35 dpi. (D) qRT-PCR analysis of viral RNA from the infiltrated leaf of *N. benthamiana* plant inoculated with various CP point mutants at 4 dpi. *NbActin* was used as an internal control. (E) Quantification of viral RNA from systemic leaf from *N. benthamiana* plant inoculated by various CP point mutants at 10 dpi by qRT-PCR. *NbActin* was used as an internal control.

Table 2.1 Effect of TuMV CP point mutants on systemic infection of *N. benthamiana*

Inoculum	Infectivity^a	
	10 dpi	22 dpi
WT	18/18 (100)	18/18 (100)
GDD	0/18 (0)	0/18 (0)
R ₁₉₅ A	18/18 (100)	18/18 (100)
D ₂₅₇ A	18/18 (100)	18/18 (100)
E ₂₆₅ A	18/18 (100)	18/18 (100)
D ₂₇₄ A	18/18 (100)	18/18 (100)
E ₂₆₈ A	16/18 (89)	18/18 (100)
R ₂₆₉ A	10/18 (56)	15/18 (83)
ER	9/18 (50)	14/18 (78)
R ₁₇₈ A	0/18 (0)	0/18 (0)
R ₁₇₈ D	0/18 (0)	0/18 (0)
D ₂₂₂ A	0/18 (0)	0/18 (0)
D ₂₂₂ R	0/18 (0)	0/18 (0)
DR	0/18 (0)	0/18 (0)

^a Infectivity is defined as the number of systemically infected plants/number of inoculated plants. Systemic leaves were examined by symptom appearance, UV light and RT-PCR using TuMV CP specific primers. Results of 3 trials were combined.

2.3.5 Effects of point mutations in TuMV CP on virion assembly

As viral cell-to-cell movement is often correlated with virion assembly (Dolja et al., 1994; Dolja et al., 1995; Seo et al., 2013), I examined if TuMV movement-defective CP mutants could assemble morphologically normal virions.

To determine the effects of point mutations in TuMV CP on virion assembly, I harvested the upper new symptomatic leaves of the *N. benthamiana* plants inoculated with group 1 or 2 mutants at 15 dpi, examined virion assembly using transmission electron microscopy (TEM) with negative staining, and evaluated CP expression using western blot with antibodies against TuMV CP. As shown in Fig 2.6A, group 1 mutants yielded typical flexuous and filamentous virions of potyviruses as WT, and a protein of approximately 34 KDa, corresponding to the predicted size for TuMV CP, was detected in crude virion preparations from group 1 mutants-infected plants (Fig 2.6B). The CP level in the plants inoculated with group 1 mutants was similar to that in WT-infected plants (Fig 2.6B). Interestingly, despite the drastically reduced CP level of group 2 mutants (Fig 2.6B), virions in the crude virus preparation from group 2 mutants-infected plants were morphologically similar to those from WT-infected plants (Fig 2.6B), suggesting group 2 mutants exhibited slow cell-to-cell movement with delayed onset of systemic infection likely independent of virion assembly.

For asymptomatic *N. benthamiana* plants inoculated by group 3 mutants, I checked if they could form regular virion in *N. benthamiana* mesophyll protoplasts. Mesophyll protoplasts were isolated and transfected with infectious clones pCambiaGFP-WT, pCambiaGFP-R₁₇₈A and pCambiaGFP-D₂₂₂A, and crude virion preparations were made and then subjected to western blot and TEM. As expected, the CP protein and typical virions were detected from the sample prepared from the protoplasts transfected with WT (Fig 2.6C and D). However, no virions were found from the protoplasts transfected with the cell-to-cell movement deficient mutants R₁₇₈A and D₂₂₂A (Fig 2.6C). Interestingly, the CP level of R₁₇₈A and D₂₂₂A was very low compared to that of WT (Fig 2.6D). These results suggested that R₁₇₈ and D₂₂₂ are required for TuMV virion assembly and mutations of R₁₇₈ and D₂₂₂ likely affect CP stability.

A

15 dpi Syst

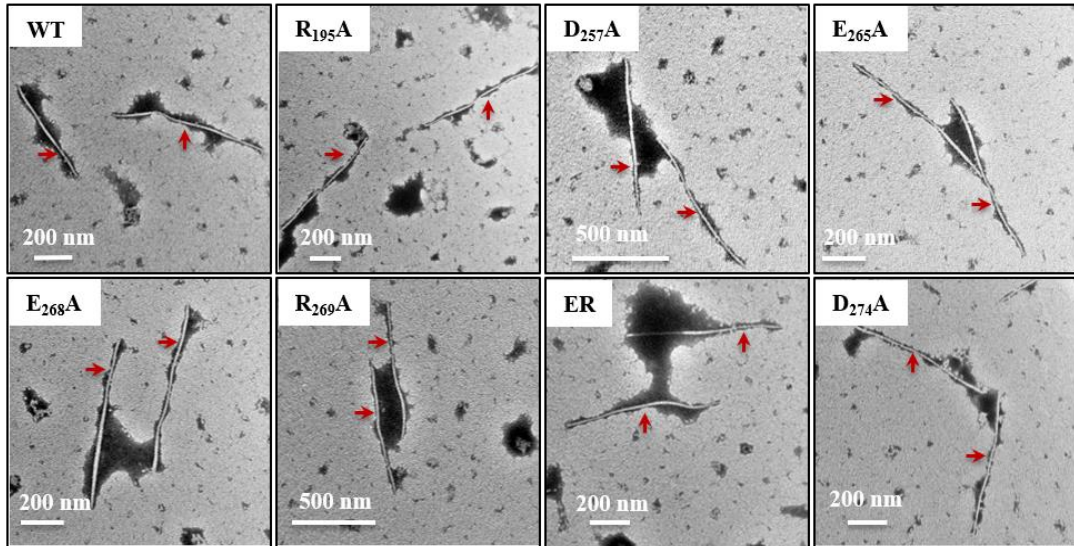
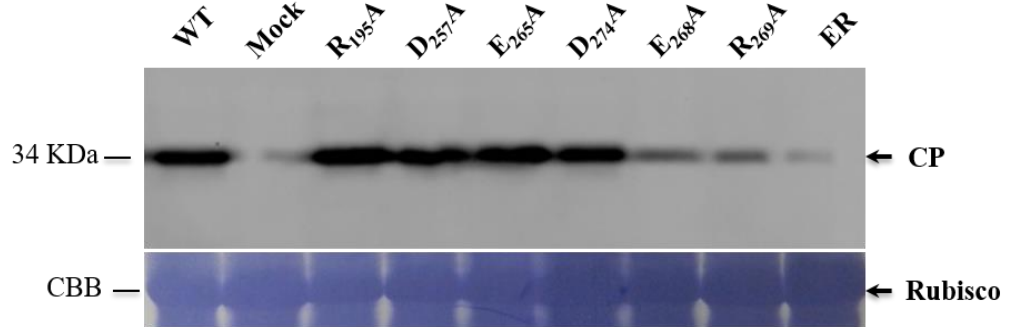
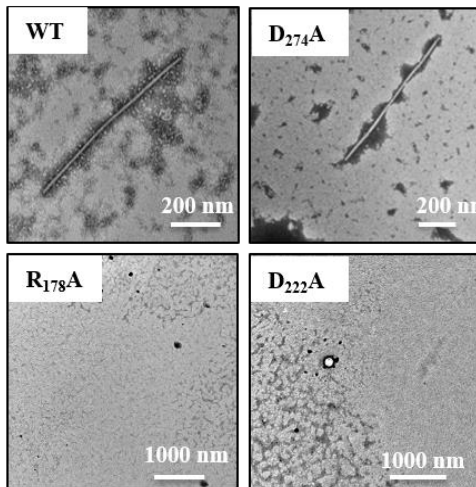
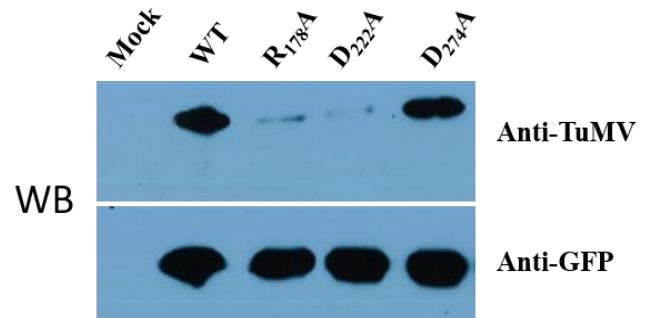
**B****C****D**

Figure 2.6 Effects of point mutations in TuMV CP on virion assembly.

(A) TEM examination of virion assembly of point mutants that can systemically infect *N. benthamiana* plants. Red arrows indicate typical TuMV virions. (B) Western blot analysis of various point mutants that can establish systemic infection of *N. benthamiana* plants. Total proteins extracts from the upper leaf at 15 dpi were probed with TuMV CP antibody. The Coomassie Brilliant Blue-stained rubisco large subunit (RuBP-L) served as a loading control. (C) TEM analysis failed to detect virions in R_{178A} or D_{222A} infected *N. benthamiana* protoplasts. (D) Western blot analysis of TuMV CP in *N. benthamiana* protoplasts transfected with R_{178A} or D_{222A} mutants at 48 hpi. Total proteins extracts were probed with TuMV CP antibody or GFP antibody.

2.3.6 Mapping the domains essential for CP self-interaction

Previous studies showed that CP self-interaction is critical for SMV cell-to-cell movement (Seo et al., 2013). To investigate domains required for TuMV CP self-interaction, I constructed various truncated CP mutants and examined their self-interactions by both Y2H and BiFC analysis. Based on computer-assisted prediction of the secondary structure of TuMV CP, I divided TuMV CP into three fragments and generated five deletion mutants: F1, Δ F1, F3, Δ F3 and M, consisting of amino acid residues 1-50, 51-288, 200-288, 1-199 and 51-199, respectively (Fig 2.7A).

Co-expression of YN-CP/YC-CP, YN-F1/YC-F1, YN- Δ F1/YC- Δ F1, YN- Δ F3/YC- Δ F3 and YN-M/YC-M, respectively, resulted in strong yellow fluorescence in the cytoplasm of *N. benthamiana* epidermal cells at 2 dpi (Fig 2.7B). By contrast, co-infiltration of YN-F3 and YC-F3 resulted in no detectable fluorescence (Fig 2.7B). No fluorescent signal was detected from negative control (co-expression of YN-CP and YC) (data not shown). These data suggest that F1 and M domain contains the CP-CP interaction functional domains, and F3 domain is dispensable for CP self-interaction.

I further conducted Y2H assay. In agreement with BiFC data, yeast cells harboring combinations of CP-AD and CP-BD, F1-AD and F1-BD, Δ F1-AD and Δ F1-BD, Δ F3-AD and Δ F3-BD, M-AD and M-BD, respectively, could grow on the QDO selection medium, whereas yeast cells containing F3-AD and F3-BD could not (Fig. 2.7C). Taken together (Fig 2.7B, C and D), I conclude that F1 (amino acids 1-50) and M (amino acids 51-199) but not F3 (amino acids 200-288) contains the domains required for TuMV CP self-interaction.

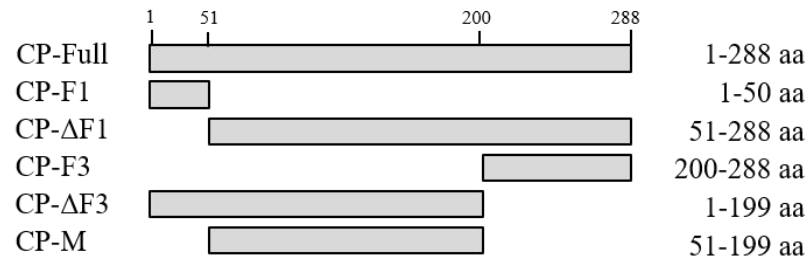
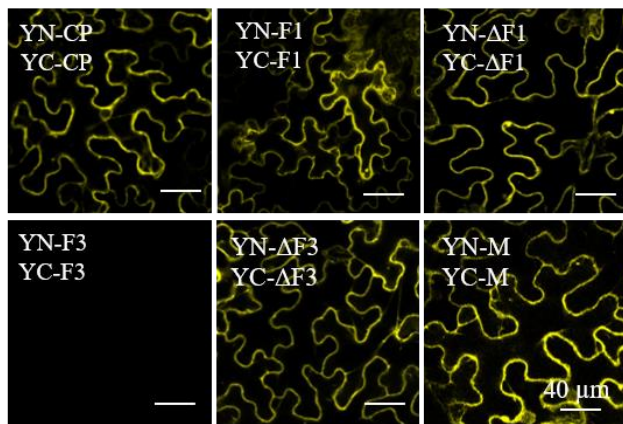
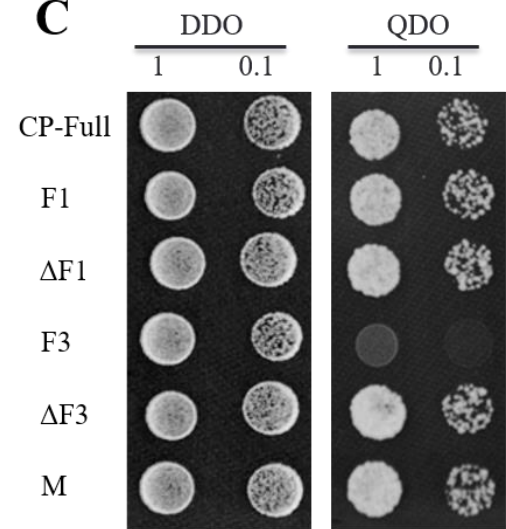
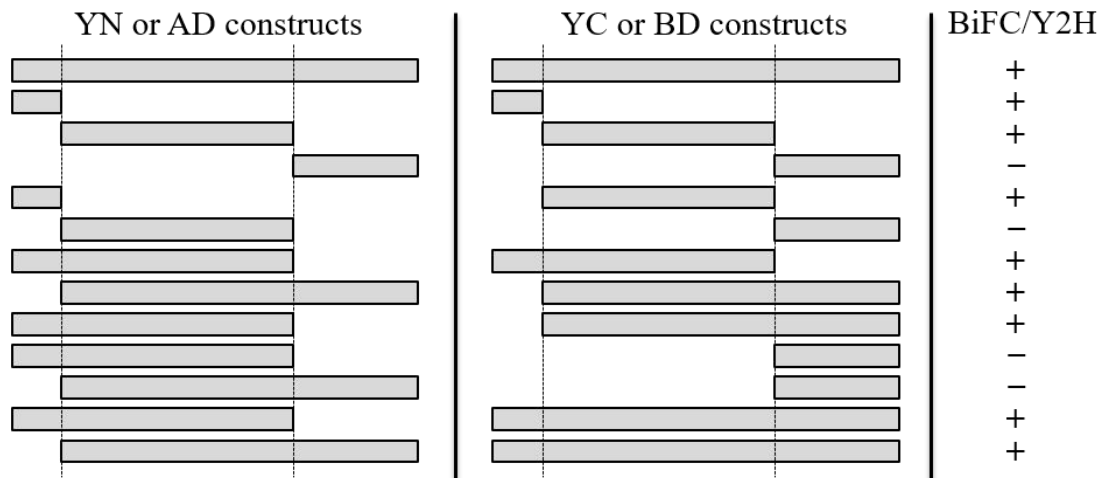
A**B****C****D**

Figure 2.7 Mapping the domains required for TuMV CP self-interaction.

(A) Schematic representation of CP deletion mutants. Full-length CP (CP-full) was divided into five fragments by overlapping PCR. (B) BiFC analysis of CP truncated mutants *in planta*. Strong fluorescence was observed in the *N. benthamiana* leaf co-infiltrated with YN-F1/YC-F1, YN- Δ F1/YC- Δ F1, YN- Δ F3/YC- Δ F3 and YN-M/YC-M, respectively at 48 hpi. No fluorescence was observed when YN-F3 was co-expressed with YC-F3. Combination of YN-CP/YC-CP was served as positive control. Experiments were repeated three times with similar results. Bars are shown. (C) Y2H analysis of CP truncated mutants in yeast. Yeast competent cells co-transformed with bait and prey plasmids were plated on double dropout (DDO) media lacking tryptophan and leucine to test for double transformation, and on quadruple dropout (QDO) media lacking tryptophan, leucine, histidine and adenine, for protein interaction. Yeast co-transformed with AD-CP and BD-CP served as positive control. (D) Summary of Y2H and BiFC analyses. Different combinations tested by Y2H and BiFC were shown. +, fluorescence detected in BiFC analysis or colonies appeared on QDO selection medium in Y2H analysis; -, fluorescence not detected in BiFC experiment or no colonies appeared on QDO selection medium in Y2H analysis.

2.3.7 Characterization of the CP point mutant R_{178A}

As shown above, the point mutation R_{178A} of CP abolished the viral intercellular movement. To understand the possible underlying mechanisms, I first compared the subcellular localization of R_{178A} with wild-type CP (CP_{WT}). The coding regions of CP_{WT} or R_{178A} were cloned into Gateway destination vector pEarlyGate101 to create the transient expression vectors 101-CP_{WT} and 101-R_{178A}. These vectors were agroinfiltrated into *N. benthamiana* leaf cells to express CP_{WT} and R_{178A} and compare their subcellular localization at 48 hpi by confocal microscopy. The mutant R_{178A} and CP_{WT} showed similar subcellular localization that are mainly localized in the cytoplasm (Fig 2.8A).

Because CP self-interaction is required for viral movement (Weber and Bujarski, 2015), and the CP and CI interaction is implicated in potyviral cell-to-cell movement (Wang, 2013a), I investigated if the mutant R_{178A} has the ability to self-interact and interact with CI in yeast and/or *in planta*. As shown in Fig 2.8B and C, that the mutant R_{178A} exhibited normal self-interaction in yeast, and also interacted with CI *in planta*.

Previous studies also suggested that the CP-RNA interaction is indispensable for plant viral movement and potyvirus virion assembly begins near 5'UTR (Wu and Shaw, 1998; Weber and Bujarski, 2015; Serra-Soriano et al., 2017). I thus examined whether the CP mutant R_{178A} can bind to TuMV 5'UTR. Electrophoretic mobility shift assay (EMSA) was performed with an *in vitro* transcribed RNA probe corresponding to the 5'UTR of the TuMV genome (nucleotides 1-231) and the recombinant TuMV CP and CP mutant R_{178A} were expressed and purified from *Escherichia coli*. Indeed, TuMV CP bound to the 5' UTR of TuMV genomic RNA (Fig 2.7D). The EMSA results also showed that the CP mutant R_{178A} can bind to the 5' UTR of TuMV (Fig 2.7D). Therefore, the point mutation R_{178A} does not affect the ability of CP to bind to the 5'UTR of TuMV genomic RNA.

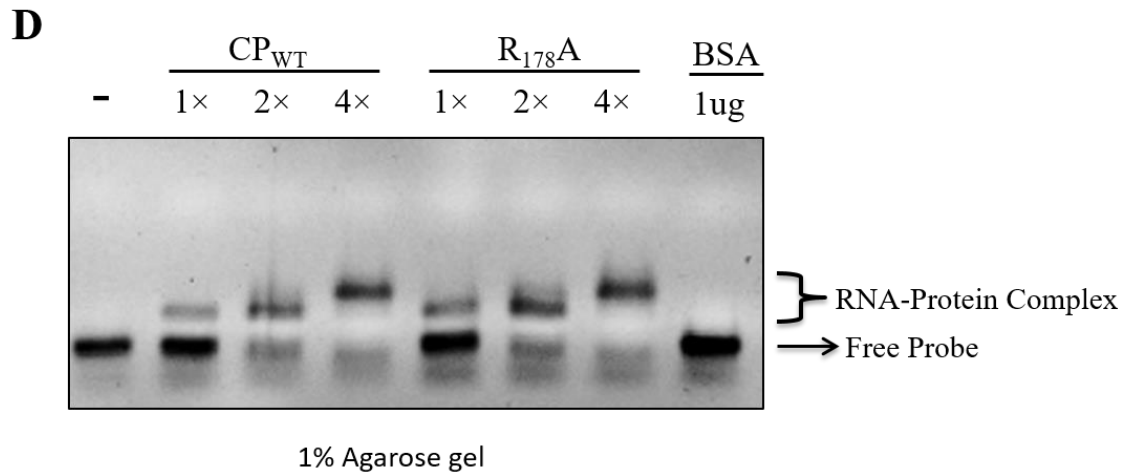
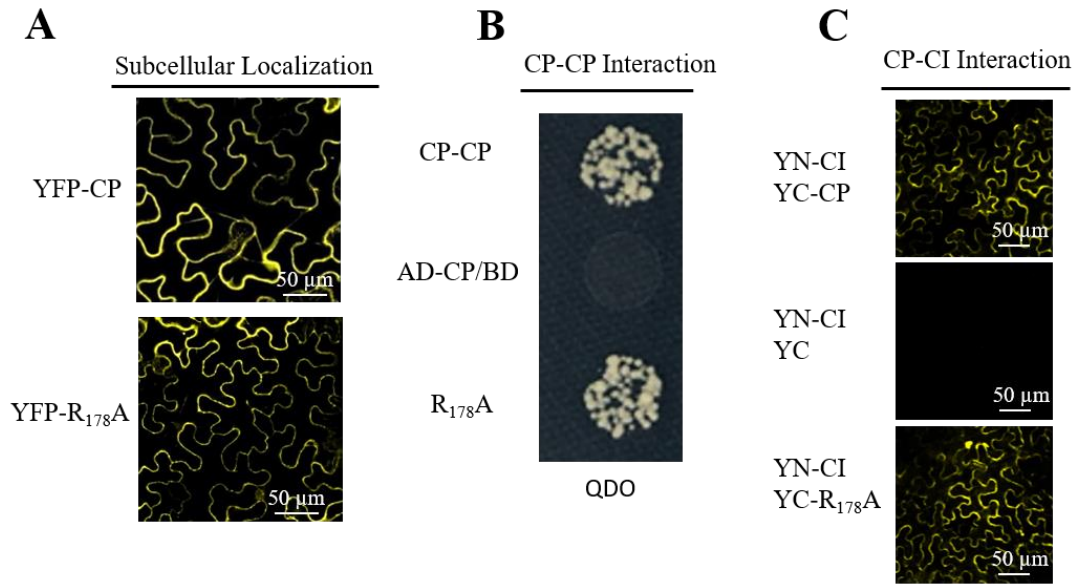


Figure 2.8 The CP point mutant R_{178A} exhibits normal subcellular localization, self-interaction, CI interaction and binding ability with TuMV 5' UTR.

(A) Subcellular localization analysis of wild-type CP and R_{178A}. Agrobacterial cells harboring YFP-CP or YFP-R_{178A} were infiltrated in *N. benthamiana* epidermal cells. Strong fluorescence was detected mainly in the cytoplasm for both constructs at 48 hpi.

(B) Y2H analysis of R_{178A} self-interaction. Yeast competent cells co-transformed with bait and prey plasmids were plated on quadruple dropout (QDO) media for protein interaction. Yeast co-transformed with AD-CP and BD-CP served as positive control. The combination of AD-CP and BD was used as negative control.

(C) BiFC analysis of the CP-CI interaction *in planta*. Strong fluorescence was observed in the *N. benthamiana* leaf co-infiltrated with YN-CI/YC-CP or YN-CI/YC-R_{178A} at 48 hpi. No fluorescence was observed when YN-CI was co-expressed with YC. Experiments were repeated three times.

(D) Electrophoretic gel mobility shift assay of wild-type CP and R_{178A}. RNA probe of 231 bp was synthesized from TuMV 5'UTR and the recombinant CP_{WT} and R_{178A} protein were expressed and purified from *E. coli* BL21 (DE3) cells. RNA transcripts were incubated with increasing amount of purified CP_{WT} or R_{178A} protein, respectively. The RNA-protein mixture was subjected to agarose gel electrophoresis. The positions of bound CP-RNA complexes and free RNA are indicated on the right.

2.3.8 R₁₇₈A is less stable than wild-type CP

Since reduced CP accumulation was observed in *N. benthamiana* mesophyll protoplasts transfected with the TuMV infectious clone mutant R₁₇₈A (Fig 2.6D), I speculated that R₁₇₈A is not stable as wild-type CP. To confirm this assumption, I conducted a transient expression assay to express wild-type CP and the point mutant CP R₁₇₈A using the expression vectors 101-CP_{WT} and 101-R₁₇₈A. At 48 hpi, total protein extracts isolated from the agroinfiltrated leaf were analyzed by immunoblotting using both anti-TuMV and anti-GFP antibodies. The CP mutant R₁₇₈A accumulated at a lower level than wild-type CP (Fig 2.9A and B), suggesting R₁₇₈A is less stable than wild-type CP.

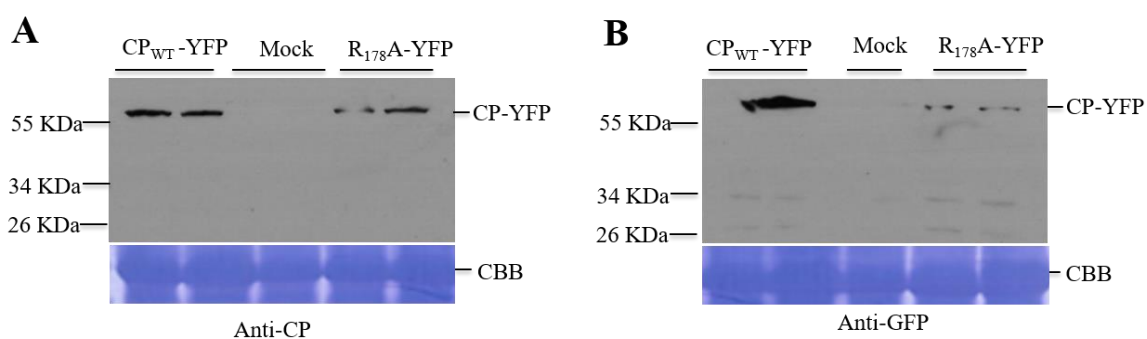


Figure 2.9 R₁₇₈A is less stable than wild-type CP.

(A) Western blot analysis of transient expression of wild-type CP or the CP point mutant R₁₇₈A. Total proteins extracts from inoculated leaf at 2 dpi were probed with TuMV CP antibody. The comparable protein loading was revealed by Coomassie Brilliant Blue staining (CBB). (B) Western blot analysis of transient expression of wild-type CP or the CP point mutant R₁₇₈A. Total proteins extracts from the inoculated leaf at 2 dpi were probed with Anti-GFP antibody. The comparable protein loading was monitored by CBB.

2.4 Discussion

Potyviral CP is a multifunctional protein that has been suggested to play essential roles in the infection process. In this study, I chose TuMV as a model virus to study CP functions. At first, I deleted the CP coding region in a TuMV infection clone and found this CP deletion mutant could replicate in plant cells like the wild-type virus (Fig 2.2D and E), but lost the ability to spread into neighboring cells (Fig 2.2B). I concluded that TuMV CP is not required for viral replication. Therefore, I was concentrated on the elucidation of CP's functional roles related to cell-to-cell movement. For the convenience of study, I divided TuMV CP into three parts, N-terminal domain, core domain and C-terminal domain. I also constructed a plant expression vector containing a TuMV infectious clone tagged by GFP and another separate cassette to express red fluorescent protein. As this vector allows for visualization and detection of primary and secondary infection cells (Fig 2.1), it is a powerful tool to study TuMV cell-to-cell movement mechanisms. I used this vector and examined the effects of TuMV CP deletion and point mutants on TuMV cell-to-cell, long-distance movement and virion assembly.

The role of the N-terminal domain of TuMV CP in viral cell-to-cell movement and virion assembly

Previous studies suggested that the N-terminal domain of potyviral CPs is variable among potyviruses and is exposed on the surface of virus particles (Allison et al., 1985b; Shukla et al., 1988; Dolja et al., 1991). Recently, Zamora and colleagues have, for the first time, reported the cryo-electron microscopy (cryoEM) structure of CP of a potyvirus (*Watermelon mosaic virus*, WMV) at a resolution of 4.0 Å (Zamora et al., 2017). WMV CP has a core domain rich in α helices, a long N-terminal arm, and a C-terminal arm (Zamora et al., 2017). In this study, I report that the N-terminal domain of TuMV CP is dispensable for viral normal cell-to-cell movement, long-distance movement and virion assembly, as deletion of amino acids 6 to 50 of TuMV CP has no negative effect on viral movement in *N. benthamiana* leaf and virion assembly both in *N. benthamiana* leaf and protoplasts (Fig 2.3 and 2.4). My finding is different from an early report in which the ΔN mutant of TEV (CP truncated mutant lacking the N-terminal amino acids 5 to 29)

exhibits slow cell-to-cell movement and fails to establish systemic infection (Dolja et al., 1994). Apparently, although both TEV and TuMV are members of potyviruses, TuMV can manage to tolerate the deletion of the N-terminal domain. Thus, the requirement of the variable N-terminal domain for potyviral cell-to-cell movement and systemic infection might depend from virus to virus.

Indeed, Tatineni and colleagues have recently shown that the N-terminal domain (amino acids 6 to 27) of CP of *Wheat streak mosaic virus* (WMSV), a member of the genus *Tritimovirus* in the family *Poryviridae* is not essential for long-distance movement but required for efficient cell-to-cell movement (Tatineni et al., 2014). Then, the questions are: What is the role of those amino acids in TuMV infection? and, why would TuMV keep those amino acids if they are dispensable for viral movement and virion assembly during the long time evolution? A possible explanation is that the N-terminus of TuMV CP could be required for insect transmission as this is the case for *Tobacco vein mottling virus* (TVMV, the genus: *potyvirus*) and the N-terminal domain of CP is critical for aphid transmission of TVMV (Atreya et al., 1991). In addition, it is also possible that the N-terminal amino acids are involved in other functions in TuMV biology such as determination of host range. Further work is needed to unravel the specific function of the N-terminus of CP.

The role of the core domain of CP in TuMV cell-to-cell and long-distance movement and virion assembly

In this study, I found that the core domain of TuMV CP is indispensable for viral cell-to-cell and long-distance movement and virion assembly (Fig 2.3, 2.5 and 2.6). I further generated various point mutants to substitute charged amino acids in the core domain and to identify key amino acids for viral cell-to-cell movement. I found that point mutations R₁₇₈A, R₁₇₈D, D₂₂₂A and D₂₂₂R and double mutations DR of TuMV CP abolish TuMV cell-to-cell movement in *N. benthamiana* plants (Fig 2.5B), and R₁₇₈A and D₂₂₂A failed to form detectable virions in transfected *N. benthamiana* protoplasts (Fig 2.6C), suggesting these Arg (R) and Asp (D) residues are critical for TuMV intercellular movement and virion assembly. My findings are consistent with Dolja and colleagues'

early work (Dolja et al., 1994) showing that TEV CP mutants containing similar substitutions on charged amino acids in the core domain of CP are defective in cell-to-cell movement and virion formation as well as a recent work by Tatineni et al. demonstrating that the analogous point mutation in tritimoviral CPs also abolishes cell-to-cell movement and virion assembly (Tatineni et al., 2014).

Positively charged arginine residues of CP can interact with negatively charged aspartic acid residues, which may construct a salt bridge crucial for CP assembly and structural stability (Dolja et al., 1991). Interestingly, my double-substitution mutant DR in which Arg (residue 178) and Asp (residue 222) are switched is defective-viral intercellular movement (Fig. 2.5B) and virion assembly (data not shown). Consistently, Dolja et al. reported that a similar DR mutant of TEV is unable to assemble in transfected protoplasts (Dolja et al., 1994). Therefore, the salt bridge model cannot explain these observations. It is possible that these charged amino acid residues are important for timely proper folding upon translation to form the 3D structure. Thus, substitutions of these charged amino acids would affect the functionality of CP.

The role of the C-terminal domain of TuMV CP in viral cell-to-cell movement

Previous studies suggested that the C-terminus of potyviral CP is exposed on the virion surface and possesses a disordered short segment at the very end (Shukla et al., 1988; Zamora et al., 2017). In this study, I found that the C-terminal domain of TuMV CP is required for viral cell-to-cell movement as deletion of amino acids 200 to 288 or 265 to 274 of TuMV CP abolished viral cell-to-cell movement (Fig 2.3B). Furthermore, a single point mutation of CP (the mutants E₂₆₈A and R₂₆₉A) and a double mutant (the mutant ER) compromised the cell-to-cell movement ability of TuMV, leading to a significant delay in the onset of systemic symptoms (Fig 2.5 and Table 2.1). My findings are well in agreement with previous reports that deletion of the C-terminal 17 amino acids of TEV CP resulted in slow cell-to-cell movement (Dolja et al., 1995), and substitution of the amino acid residue R245 or D250 with alanine in the C-terminus of SMV CP disrupted viral cell-to-cell movement (Dolja et al., 1995; Seo et al., 2013). Therefore, the C-terminus of potyviral CP plays a critical role in viral cell-to-cell movement.

Then, how does the C-terminal domain function to support potyviral intercellular movement? It has been suggested that the C-terminus of SMV CP is involved in CP intersubunit interactions, which seems essential for viral cell-to-cell movement (Kang et al., 2006; Seo et al., 2013). Different from this, the C-terminus of TuMV CP is dispensable for CP self-interactions (Fig 2.7), suggesting there exists a different mechanism. Further study is needed to elucidate this. It is possible that the C-terminus of TuMV CP is required for CP-vRNA binding since the C-terminus of WMV CP is positioned at the inner side of WMV viral particles where the direct interaction of CP and vRNA occurs (Zamora et al., 2017). Alternatively, the C-terminus of TuMV CP could be the functional domain for the CP interactions with other key players that regulate TuMV cell-to-cell movement, such as other viral proteins and host factors.

Conclusion remarks

In my study, I found that the movement-defective point mutants R₁₇₈A and D₂₂₂A are unable to form virions in protoplasts. This is also true for several other potyvirus species including TEV, and WSMV (Dolja et al., 1994; Tatineni et al., 2014). It is very tempting to suggest that there is a correlation between virion assembly and potyviral intercellular movement. This leads me to further suggest that virion assembly is essential for potyviral cell-to-cell movement. This assumption contrasts with a recent report by the Laliberte group in which TuMV was suggested to move as VRCs for cell-to-cell movement based on the observations that the motile 6K2-containing vesicles (VRCs) enable vRNA transport to PDs by trafficking along ER/microfilaments and can even pass PD to the neighboring cells (Grangeon et al., 2012a; Grangeon et al., 2013). However, I cannot exclude the possibility that TuMV and related viruses move as RNPs where CP may function through protein-protein and/or protein-RNA interactions involved in the formation and transportation of RNPs intracellularly and further intercellular movement.

It is worth mentioning that although I provide evidence showing that movement-defective mutants exhibit normal subcellular localization, CP-viral protein interaction and RNA binding ability, it still remains unknown why these mutants fail to move intercellularly

and why they cannot form virions. Since host factors are recruited to support viral infection at all stages of the infection process (Wang, 2015), it would be interesting to identify host factors that are involved in potyviral intercellular movement and investigate the mechanistic details of their roles in the viral movement.

In summary, using various TuMV mutants, I have identified the determinants of CP involved in TuMV cell-to-cell movement, long-distance transport and virion assembly. Remarkably, deletion of the N-terminal 46 amino acid residues of CP has no negative effect on TuMV movement and virion assembly, and the C-terminus of CP has no ability to self-interact but plays an essential role in intercellular movement.

2.5 Materials and Methods

2.5.1 Construction of two fluorescent protein-tagged TuMV infectious clone pCBTuMV-GFP//mCherry

The TuMV infectious clone, pCamibaTunos/GFP and the mini-binary vector pCB301 were obtained from Dr. Jean-François Laliberté (Institut National de la Recherche Scientifique) and Dr. David J. Oliver (Iowa State University), respectively. The GFP tagged TuMV infectious clone, pCBTuMV-GFP was constructed by double digestion of pCamibaTunos/GFP with XmaI and ApaI, and then ligation of the TuMV-GFP fragment into the corresponding sites of pCB301. Using a PPV infectious clone tagged with GFP and mCherry-HDEL (Cui and Wang, 2016) as template, I amplified the 35S-mCherry-HDEL-Nos fragment and introduced an ApaI digestion site to this fragment by PCR with primers (ApaI-mCherry-F, TATAGGGCCCATATGTGAACATGG and ApaI-mCherry-R, TATGGGCCCGTCGATCTAGTAA). The amplified fragment was digested with ApaI and then inserted into the ApaI site of pCBTuMV-GFP to generate the TuMV infectious clone pCBTuMV-GFP//mCherry. All the vectors were confirmed by DNA sequencing.

2.5.2 Construction of CP mutants

All the CP mutants constructed in this study for viral replication analysis and virion assembly in protoplasts were based on the TuMV infectious clone pCamibaTunos/GFP. pCBTuMV-GFP//mCherry was used as a parental virus to create the CP mutants for studying viral intercellular movement and virion assembly in plant leaf. To create CP mutants, the CP coding fragment (1342 bp cDNA between MluI and SaII) was amplified by PCR from the parent plasmid pCamibaTunos/GFP using Phusion® High-Fidelity DNA Polymerase (New England BioLabs Inc). The PCR product was then ligated into the pCRBlunt vector (Invitrogen) resulting a recombinant plasmid named pCRBlunt-CP1342, which was used for deletion or introduction of single point or double mutations. Then, the resulting intermediate clones were digested with MluI and SaII and ligated into the corresponding sites of pCamibaTunos/GFP or pCBTuMV-GFP//mCherry.

CP deletion mutants Δ CP, Δ N, Δ M, Δ C1 and Δ C2 were generated by overlap extension PCR using appropriate primers, twelve CP point mutants R₁₉₅A, R₁₇₈A, R₁₇₈D, D₂₂₂A, D₂₂₂R, D₂₅₇A, E₂₆₅A, E₂₆₈A, R₂₆₉A, D₂₇₄A, DR and ER_{268,269} AA were constructed by site-directed mutagenesis using appropriate primers. Restriction enzymes and T4 DNA ligase were purchased from New England BioLabs Inc.

2.5.3 Protoplast isolation and transfection

Four-week-old *N. benthamiana* plants were used for mesophyll protoplast isolation transfection by following the procedure as described previously (Yoo et al., 2007). For PEG mediated transfection, 3×10^5 isolated mesophyll protoplasts were transfected with 30 μ g of plasmid DNA. Plasmid DNAs were extracted using the Maxi Plasmid Kit Endotoxin Free (Geneaid) according to the protocol.

2.5.4 Cell-to-cell movement of TuMV CP mutants

Agrobacterium harboring TuMV CP mutants were inoculated onto four-week-old *N. benthamiana* plants at OD₆₀₀ 0.001. The movement ability of mutants was determined by observing the green fluorescent foci on the agroinfiltrated *N. benthamiana* leaf using a Leica TCS SP2 confocal laser scanning microscope (Leica, Germany) starting at 2 dpi.

2.5.5 Crude virion preparation and electron microscopy

To obtain the crude virion preparation from systemic *N. benthamiana* leaf, 1 g of symptomatic leaves were ground in a mortar and pestle with 150 μ l of potassium phosphate buffer (pH 7.0), containing 0.1% β -mercaptoethanol. Following the centrifugation at 12,000 g for 5 min at 4°C, the supernatant was filtered through a 40 μ m Nylon Cell Strainer (Corning Incorporated, Corning, NY, USA). 50 μ l of chloroform was then added and vortexed for 1 min, the homogenate was then centrifuged at 12,000 \times g for 10 min at 4°C. The aqueous phase was collected and subjected to negative staining.

For crude virion preparation of *N. benthamiana* mesophyll protoplasts, 3×10^5 protoplasts were harvest at 48 or 72 hours post infection (hpi) by centrifugation at 100 \times g for 2 min. 100 μ l of potassium phosphate buffer (pH 7.0) was added to the pellet, followed by the procedure presented above.

Formvar/carbon-coated EM grids (Electron Microscopy Sciences, Hatfield, PA, USA) were incubated with the crude virion preparation for 2 min and stained with 2% phosphotungstic acid (PTA), pH 7.0, for 2 min. Grids were allowed to dry prior examination on the transmission electron microscope (JEM-1200EXII, JEOL Ltd, Japan) operated at 80 kV.

2.5.6 qRT-PCR assay

Total RNA was extracted from *N. benthamiana* leaf tissues or protoplasts using the Plant Total RNA Mini Kit (Geneaid) as instructed. For first-strand cDNA synthesis, 1 μ g RNA was pretreated by DNase I (Invitrogen) as a template, Superscript III reverse transcriptase and an oligo (dT) 12-18 primer (Invitrogen) were used following the manufacturer's instruction. For real-time PCR, primer pairs TuCP-F (5'-GGCACTCAAGAAAGGCAAGG-3') and TuCP-R (5'-CTCCGTCAGTTCGTAATCAGC-3') were used for TuMV detection, the *N. benthamiana actin* reference gene primers *NbActin*-F (5'-GGGATGTGAAGGAGAAGTTGGC-3') and *NbActin*-R (5'-ATCAGCAATGCCCGGAACA-3') were used for normalization. Real-time PCR performed using SsoFast EvaGreen Supermix (Bio-Rad) and CFX96 real-time PCR system (Bio-Rad). The relative gene expression was calculated by Bio-Rad CFX

Manager software. All the results were shown at least three independent biological replicates with corresponding standard errors.

2.5.7 Y2H and BiFC experiments

Yeast two-hybrid experiments were conducted using the Matchmaker two-hybrid system (Clontech). Genes of interest were cloned into Y2H gateway vectors pDEST-GBKT7 and pDEST-GADT7 (Lu et al., 2010) and subsequently co-transformed into yeast cells using the Yeastmaker™ Yeast Transformation System 2 (Clontech) as instructed. Positive protein interactions were selected in synthetically defined medium lacking Leu, Trp, His, and Ade (SD-LWHA).

BiFC assays were carried out to validate protein interactions in *planta*. The CP_{WT} and CP mutant genes were cloned into BiFC gateway vectors p35S-YN or p35S-YC (Lu et al., 2010). Constructs were transiently coexpressed in 3-4 weeks old *N.benthamiana* leaves through agroinfiltration. The YFP fluorescence was excited with an argon laser at 514 nm and emission was captured between 535 and 545 nm. BiFC images were taken by confocal microscopy (Leica TCS SP2) at 48 hours post-inoculation (hpi).

2.5.8 Electrophoretic gel mobility shift assay (EMSA)

The expression and purification of recombinant CPs was performed using the Champion™ pET160 Gateway Expression Kit (Invitrogen). The wild-type CP and R_{178A} were cloned into expression vector pET160-DEST and further transformed into *Escherichia coli* BL21 (DE3) cells. Protein inducing, expression and purification are carried out according to manufacturer instructions (Invitrogen). Protein was verified by SDS-PAGE electrophoresis followed by Coomassie blue staining and western blot.

For *In vitro* transcription, HiScribe T7 High Yield RNA Synthesis Kit (New England Biolabs) was used. RNA probe of 231 bp, corresponding to the 5' UTR of TuMV genome, was synthesized using the following primer pairs: 5' GACGACTAATACGACTCACTATAGGGAA

AAAATATAAAAACTCAAC-3' and 5'-TTGGTTTGCTGTTGGTGATT-3'.

Synthesized RNA was further purified and evaluated by gel electrophoresis and NanoDrop Spectrophotometer.

For EMSA, protein-RNA mixture was set up in a total volume of 20 μ l containing 20 mM Tris-HCl (pH 7.0), 1 mM DTT, 100 mM KCl, 1 mM NaCl, 2 U of RNase inhibitor, 500 ng of RNA probe, and purified recombinant TuMV CPs. The mixture was incubated for 20 min at room temperature, followed by agarose gel electrophoresis.

2.5.9 SDS-PAGE and Western blot analyses

Protein samples were separated on standard SDS-PAGE (12% acrylamide) gel and subsequently either subjected to Coomassie brilliant blue staining (CBB) and destaining or transferred to PVDF membrane (Bio-Rad) using the Trans-Blot SD Semi-Dry Transfer Cell (Bio-Rad).

For Western blot analyse, after transfer, PVDF membranes were either probed overnight at 4°C with polyclonal rabbit anti-TuMV CP antibody (Agdia) or anti-GFP N-terminal antibody (Sigma-Aldrich). The membranes were washed four times with PBST and incubated with horseradish peroxidase-conjugated goat anti-rabbit IgG (Sigma-Aldrich) for two hours at room temperature. After four times washing in PBST, the membranes were treated with Western chemiluminescent HRP substrate (Millipore) and exposed to films in the dark room for visualization.

2.6 References

- Allison, R.F., Sorenson, J.C., Kelly, M.E., Armstrong, F.B., and Dougherty, W.G.** (1985a). Sequence determination of the capsid protein gene and flanking regions of tobacco etch virus: Evidence for synthesis and processing of a polyprotein in potyvirus genome expression. *Proceedings of the National Academy of Sciences* **82**, 3969-3972.
- Allison, R.F., Dougherty, W.G., Parks, T.D., Willis, L., Johnston, R.E., Kelly, M., and Armstrong, F.B.** (1985b). Biochemical analysis of the capsid protein gene and capsid protein of tobacco etch virus: N-terminal amino acids are located on the virion's surface. *Virology* **147**, 309-316.
- Atreya, P.L., Atreya, C.D., and Pirone, T.P.** (1991). Amino acid substitutions in the coat protein result in loss of insect transmissibility of a plant virus. *Proceedings of the National Academy of Sciences* **88**, 7887-7891.
- Benitez-Alfonso, Y., Faulkner, C., Ritzenthaler, C., and Maule, A.J.** (2010). Plasmodesmata: Gateways to Local and Systemic Virus Infection. *Molecular Plant-Microbe Interactions* **23**, 1403-1412.
- Callaway, A., Giesman-Cookmeyer, D., Gillock, E.T., Sit, T.L., and Lommel, S.A.** (2001). The multifunctional capsid proteins of plant RNA viruses. *Annual Review of Phytopathology* **39**, 419-460.
- Cui, H., and Wang, A.** (2016). Plum Pox Virus 6K1 Protein Is Required for Viral Replication and Targets the Viral Replication Complex at the Early Stage of Infection. *J Virol* **90**, 5119-5131.
- Cui, X., Yaghmaiean, H., Wu, G., Wu, X., Chen, X., Thorn, G., and Wang, A.** (2017). The C-terminal region of the Turnip mosaic virus P3 protein is essential for viral infection via targeting P3 to the viral replication complex. *Virology* **510**, 147-155.
- Dolja, V.V., Boyko, V.P., Agranovsky, A.A., and Koonin, E., V.** (1991). Phylogeny of capsid proteins of rod-shaped and filamentous RNA plant viruses: Two families with distinct patterns of sequence and probably structure conservation. *Virology* **184**, 79-86.
- Dolja, V.V., Haldeman, R., Robertson, N.L., Dougherty, W.G., and Carrington, J.C.** (1994). Distinct functions of capsid protein in assembly and movement of tobacco etch potyvirus in plants. *The EMBO Journal* **13**, 1482-1491.
- Dolja, V.V., Haldeman-Cahill, R., Montgomery, A.E., Vandenbosch, K.A., and Carrington, J.C.** (1995). Capsid Protein Determinants Involved in Cell-to-Cell and Long Distance Movement of Tobacco Etch Potyvirus. *Virology* **206**, 1007-1016.
- Grangeon, R., Jiang, J., and Laliberte, J.F.** (2012). Host endomembrane recruitment for plant RNA virus replication. *Curr Opin Virol* **2**, 683-690.
- Grangeon, R., Jiang, J., Wan, J., Agbeci, M., Zheng, H., and Laliberte, J.F.** (2013). 6K2-induced vesicles can move cell to cell during turnip mosaic virus infection. *Front Microbiol* **4**, 351.
- Hipper, C., Brault, V., Ziegler-Graff, V., and Revers, F.** (2013). Viral and cellular factors involved in Phloem transport of plant viruses. *Front Plant Sci* **4**, 154.
- Kang, S.H., Lim, W.S., Hwang, S.H., Park, J.W., Choi, H.S., and Kim, K.H.** (2006). Importance of the C-terminal domain of soybean mosaic virus coat protein for subunit interactions. *J Gen Virol* **87**, 225-229.
- Lu, Q., Tang, X., Tian, G., Wang, F., Liu, K., Nguyen, V., Kohalmi, S.E., Keller, W.A., Tsang, E.W., Harada, J.J., Rothstein, S.J., and Cui, Y.** (2010). Arabidopsis homolog of the yeast TREX-2 mRNA export complex: components and anchoring nucleoporin. *Plant J* **61**, 259-270.
- Lucas, W.J.** (2006). Plant viral movement proteins: agents for cell-to-cell trafficking of viral genomes. *Virology* **344**, 169-184.

- Lucas, W.J., Ham, B.K., and Kim, J.Y.** (2009). Plasmodesmata - bridging the gap between neighboring plant cells. *Trends Cell Biol* **19**, 495-503.
- Ni, P., and Cheng Kao, C.** (2013). Non-encapsidation activities of the capsid proteins of positive-strand RNA viruses. *Virology* **446**, 123-132.
- Seo, J.K., Vo Phan, M.S., Kang, S.H., Choi, H.S., and Kim, K.H.** (2013). The charged residues in the surface-exposed C-terminus of the Soybean mosaic virus coat protein are critical for cell-to-cell movement. *Virology* **446**, 95-101.
- Serra-Soriano, M., Antonio Navarro, J., and Pallas, V.** (2017). Dissecting the multifunctional role of the N-terminal domain of the Melon necrotic spot virus coat protein in RNA packaging, viral movement and interference with antiviral plant defence. *Mol Plant Pathol* **18**, 837-849.
- Shukla, D.D., and Ward, C.W.** (1988). Amino acid sequence homology of coat proteins as a basis for identification and classification of the potyvirus group. *Journal of General Virology* **69**, 2703-2710.
- Shukla, D.D., Strike, P.M., Tracy, S.L., Gough, K.H., and Ward, C.W.** (1988). The N and C Termini of the Coat Proteins of Potyviruses Are Surface-located and the N Terminus Contains the Major Virus-specific Epitopes. *Journal of General Virology* **69**, 1497-1508.
- Tatineni, S., Kovacs, F., and French, R.** (2014). Wheat streak mosaic virus infects systemically despite extensive coat protein deletions: identification of virion assembly and cell-to-cell movement determinants. *J Virol* **88**, 1366-1380.
- Wang, A.** (2013). Molecular isolation and functional characterization of host factors required in the virus infection cycle for disease control in plants. *CAB Reviews* **8**, 1-8.
- Weber, P.H., and Bujarski, J.J.** (2015). Multiple functions of capsid proteins in (+) stranded RNA viruses during plant-virus interactions. *Virus Res* **196**, 140-149.
- Wu, X., and Shaw, J.G.** (1998). Evidence that assembly of a potyvirus begins near the 5' terminus of the viral RNA. *Journal of General Virology* **79**, 1525-1529.
- Yoo, S.D., Cho, Y.H., and Sheen, J.** (2007). Arabidopsis mesophyll protoplasts: a versatile cell system for transient gene expression analysis. *Nat Protoc* **2**, 1565-1572.
- Zamora, M., Méndez-López, E., Agirrezabala, X., Cuesta, R., Lavín, J.L., Sánchez-Pina, M.A., Aranda, M.A., and Valle, M.** (2017). Potyvirus virion structure shows conserved protein fold and RNA binding site in ssRNA viruses. *Science Advances* **3**.

Chapter 3

3 Patellin 3 and 6, two members of the Arabidopsis Sec14-GOLD proteins, interact with both the coat protein (CP) and cylindrical inclusion protein (CI) of *Turnip mosaic virus* and inhibit virus accumulation

3.1 Abstract

A successful viral infection results from complex interaction between an invading virus and a particular host. Molecular identification of host proteins that affect viral infection advances knowledge of the viral infection process and assists in the development of novel antiviral strategies. I used the coat protein (CP) of *Turnip mosaic virus* (TuMV) as bait and conducted a yeast two-hybrid (Y2H) screening for CP-interacting Arabidopsis proteins. I identified several novel protein interactions that could potentially modulate TuMV infection. In this study, I focused on two of the novel CP-interacting partners, PATL3 and PATL6, which are members of the Arabidopsis Patellin protein family that are implicated in membrane trafficking, cytoskeleton dynamics and lipid metabolism. The ability of PATL3 to associate with CP was confirmed by bimolecular fluorescence complementation (BiFC) assay and co-immunoprecipitation (Co-IP) assay *in planta*. The biological significance of PATLs was assayed by TuMV infection of PATLs T-DNA insertion mutants and stable overexpression lines. Knockout of *PATL3* or *PATL6* or both resulted in strongly increased accumulation of TuMV genomic RNA in the inoculated Arabidopsis leaf. A comparative analysis of viral accumulation in protoplasts isolated from wild-type plants or the knockout mutants showed that the absence of PATL3 and PATL6 facilitates viral multiplication, whereas overexpression of PATL3 inhibits TuMV accumulation in Arabidopsis protoplasts. These data suggest that PATL3 and PATL6 negatively regulate TuMV infection in Arabidopsis plants and protoplasts. Interestingly, a subcellular localization study demonstrated that PATL3, but not PATL6 was redistributed to and co-localized with virus replication complexes (VRCs) upon TuMV infection. In addition, the viral protein cylindrical inclusion protein (CI), which presents in VRCs and are critical for TuMV multiplication, interacted with PATL3 both in yeast

and *in planta*. Therefore, I proposed that Arabidopsis protein PATL3 act as a host restriction factor, possibly by targeting TuMV VRCs through its interaction with CI.

3.2 Introduction

Infection by plant viruses causes various symptoms in the infected plants, such as mosaic, stunting, yellowing and necrosis. These altered phenotypes can be explained by the interference of plant physiology and development by the virus. Plant positive-strand RNA viruses can induce the remodelling of host cellular organelles including ER, chloroplasts, peroxisomes, plasma membrane and PD to favor viral genome multiplication and virus movement (Laliberte and Sanfacon, 2010; Revers and Garcia, 2015; Wang, 2015). In the case of potyviruses, virus replication takes place in the 6K2-induced cytoplasmic vesicles referred as the viral replication complex (VRC) that are derived from the ER. The potyviral VRCs are composed of viral RNA, CI, NIa, NIb, P3 as well as various host factors such as heat shock protein 70 (HSP70), poly(A) binding-protein (PABP), eukaryotic initiation factor 4E (eIF4E), elongation factor 1A (eEF1A), DEAD-box RNA helicase RH8 (Ivanov and Makinen, 2012; Wang, 2013b). These host factors are recruited by the virus and physically present in VRCs for promoting viral infection. However, little is known of the host proteins that are present in the VRC with antiviral functions.

In the past decade, a large number of plasma membrane-associated proteins were identified and characterized to be regulators of host-bacteria/fungi interactions by recognizing microbes and subsequently activating signal transduction (Lefebvre et al., 2010; Dormann et al., 2014; Nathalie and Bouhidel, 2014). More recently, a lot of attention was placed on the study of PM-associated proteins in plant virus-host interactions. For example, a PM-associated protein, Remorin (from remora, smaller fish adhering to larger fishes and ships) in relation to its hydrophilicity and membrane location was identified to be a regulator of host-virus interaction and can inhibit *Potato virus X* (PVX) movement (Raffaele et al., 2009).

Turnip mosaic virus (TuMV), a member of the genus *Potyvirus* in the family of *Potyviridae*, was considered to be the second most important virus infecting field-grown

vegetables after *Cucumber mosaic virus* (CMV) (Tomlinson, 1987). The viral coat protein (CP) of plant viruses is a multifunctional protein that is involved in various steps of the virus infection cycle, such as viral RNA transcription, replication, virus movement, virus transmission, activation or suppression of host defenses and symptom development (Callaway et al., 2001; Ni and Cheng Kao, 2013). However, CP-interacting host proteins involved in TuMV infection are largely unknown.

In order to gain more insight into host-TuMV interactions, we attempted to identify the host proteins that interact with TuMV CP. A yeast two-hybrid screening against an Arabidopsis cDNA library was carried out. Among the host proteins identified, I chose two members of the Arabidopsis Patellin family, Patellin 3 (PATL3) and Patellin 6 (PATL6) for further molecular characterization. Knockout of *PATL3* or *PATL6* or both resulted in increased TuMV accumulation in Arabidopsis leaves and protoplasts, whereas stable overexpression *PATL3* inhibited TuMV accumulation in Arabidopsis protoplasts. Interestingly, subcellular localization study showed that a great portion of PATL3 was redistributed to and co-localized with virus replication complexes (VRCs) upon TuMV infection. My data suggest that Arabidopsis protein PATL3 is the host restriction factor that restricts TuMV infection likely by targeting VRCs.

3.3 Results

3.3.1 Identification of TuMV CP-interacting Arabidopsis proteins by Y2H screening

To identify host proteins involved in TuMV infection, I performed a yeast-two-hybrid (Y2H) screening in an Arabidopsis cDNA library (Clontech, Cat# 630487) using TuMV CP as bait. The screening yielded dozens of positive colonies on selective media QDO/X/A (SD/-Leu/-Trp/-Ade/-His supplemented with X- α -Gal and Aureobasidin A). Positive clones were further isolated by using the Easy Yeast Plasmid Isolation Kit (Clontech, Cat# 630467), followed by *E.coli* transformation, plasmid purification and DNA sequencing. Nucleotide sequence analysis revealed that these clones contained cDNA derived from 16 different genes (Table 3.1).

Since Y2H screening can result in false positives, I performed co-transformation experiment to select the true positive interactions. The CDS of TuMV CP was cloned into the Y2H gateway vector pDEST-GBKT7 (BD), termed BD-CP. The full-length CDS of host genes of interest were amplified using Arabidopsis cDNA, fused to pDEST-GADT7 (AD) vector, and co-transformed with BD-CP into competent yeast cells, followed by selection on QDO/X- α -Gal agar plates. This confirmation resulted in the identification of three Arabidopsis proteins that can directly interact with TuMV CP in yeast (Figure 3.1). Of the three host proteins, Patellin 3 (PATL3) and Patlellin 6 (PATL6) are involved in lipid binding and membrane-trafficking events and were also reported to play a negative role on *Alfalfa mosaic virus* (AMV) cell-to-cell movement (Peiro et al., 2014). The other protein is Small nuclear ribonucleoprotein family protein, Sm-like protein (LSM1B), which is involved in RNA binding, RNA splicing and mRNA degradation. LSM1p, the Sm protein encoded by yeast, has been reported to be required for *Brome mosaic virus* (BMV) replication in yeast (Juana Díez, 2000), and LSM1 is used by Hepatitis C virus (HCV) to replicate in human cells (Nicoletta Schellera, 2009).

Table 3.1 TuMV CP-interacting Arabidopsis protein candidates identified by Y2H screening

Gene Locus	Protein Description	Gene Name
AT1G72160	Patellin 3	PATL3
AT3G51670	Patellin 6	PATL6
AT4G04640	ATP synthase gamma chain1	ATPC1
AT3G14080	Small nuclear ribonucleoprotein family protein; Sm-like protein	LSM1B
AT1G02410	Cytochrome c oxidase assembly protein	COX11
AT1G43170	Ribosomal protein 1	RP1
AT1G50460	Hexokinase-like 1	HKL1
AT2G13290	Beta-1,4-N-acetylglucosaminyltransferase family protein	
AT5G52300	Low-temperature-induced 65 KDa protein	LTI65
AT5G16760	Inositol-tetrakisphosphate1-Kinase 1	ITPK1
AT5G11790	N-MYC downregulated-like 2 Protein	NDL2
AT1G01460	Phosphatidylinositol-4-phosphate 5-kinase 10	PIP5K10
AT4G17510	Ubiquitin C-terminal hydroloase3	UCH3
AT5G02790	Glutathione S-transferase family protein L3	GSTL3
AT5G22790	Reticulate-related 1	RER1
AT4G13020	Protein kinase superfamily protein	MHK

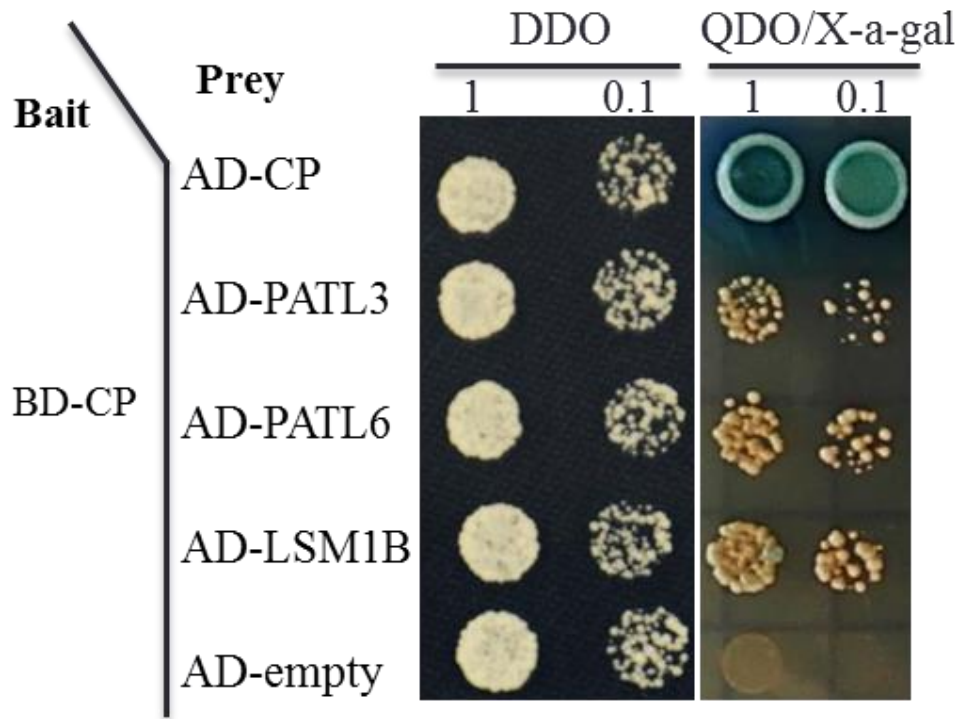


Figure 3.1 PATL3, PATL6 and LSM1B interact with TuMV CP in yeast

Competent yeast cells co-transformed with bait and prey plasmids were plated on double dropout (DDO) media lacking tryptophan and leucine to test for double transformation, and on quadruple dropout (QDO) media lacking tryptophan, leucine, histidine and adenine but supplemented with 40 $\mu\text{g/ml}$ X-a-Gal, for screening for positive protein interactions. Yeast co-transformed with AD-CP and BD-CP served as a positive control and co-transformation of AD-empty and BD-CP was used as a negative control.

3.3.2 PATL3 and PATL6 interact with CP in *N. benthamiana* cells

To determine whether TuMV CP and PATLs interact *in planta*, I conducted a BiFC assay. BiFC Gateway constructs YN-CP (CP fused with the N-terminal half of YFP), YC-CP (CP fused with the C-terminal half of YFP), YN-PATL3 (PATL3 fused with the N-terminal half of YFP), YC-PATL3 (PATL3 fused with the C-terminal half of YFP), YN-PATL6 (PATL6 fused with the N-terminal half of YFP), YC-PATL6 (PATL6 fused with the C-terminal half of YFP) were generated. Co-expression of YN-CP and YC-PATL3, YC-CP and YN-PATL3, YN-CP and YC-PATL6, or YC-CP and YN-PATL6 in *N. benthamiana* epidermal cells via agroinfiltration resulted in strong yellow fluorescence predominantly in the cell periphery (Fig 3.2 A). By contrast, co-expression of YC-CP and YN, or YN-CP and YC, which served as negative controls, did not result in yellow fluorescence (Fig 3.2 A). These results suggest that PATL3 and PATL6 can interact with CP in *N. benthamiana* plant epidermal cells.

To validate the physical interaction between CP and PATL3, I performed a co-immunoprecipitation (Co-IP) assay using a Flag-tagged CP (CP-FLAG) and a hemagglutinin (HA)-tagged PATL3 (PATL3-HA). The leaves of four-week-old *N. benthamiana* plants were agroinfiltrated with CP-FLAG, PATL3-HA or the combination of CP-FLAG with PATL3-HA. Protein extracts from infiltrated leaves were either used directly for western blots for input detection or incubated with anti-Flag M2 affinity gel (Sigma) for Co-IP detection. As shown, both CP and PATL3 were indeed expressed in *N. benthamiana* plant when expressed individually or when co-expressed (Fig 3.2 B). For Co-IP, the beads were washed several times and then analyzed by Western blot with antibodies to FLAG or HA. A strong band corresponding to the predicted molecular mass for PATL3-HA that was co-immunoprecipitated with CP-FLAG was detected using antibodies to HA (Fig 3.2 B), indicating the presence of PATL3-CP complex in the *N. benthamiana* leaf. Taken BiFC and Co-IP results together, I conclude that PATL3 can directly interact with CP *in planta*.

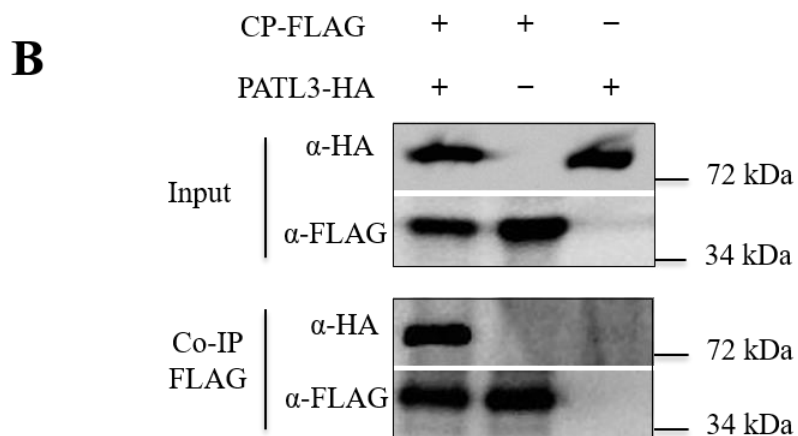
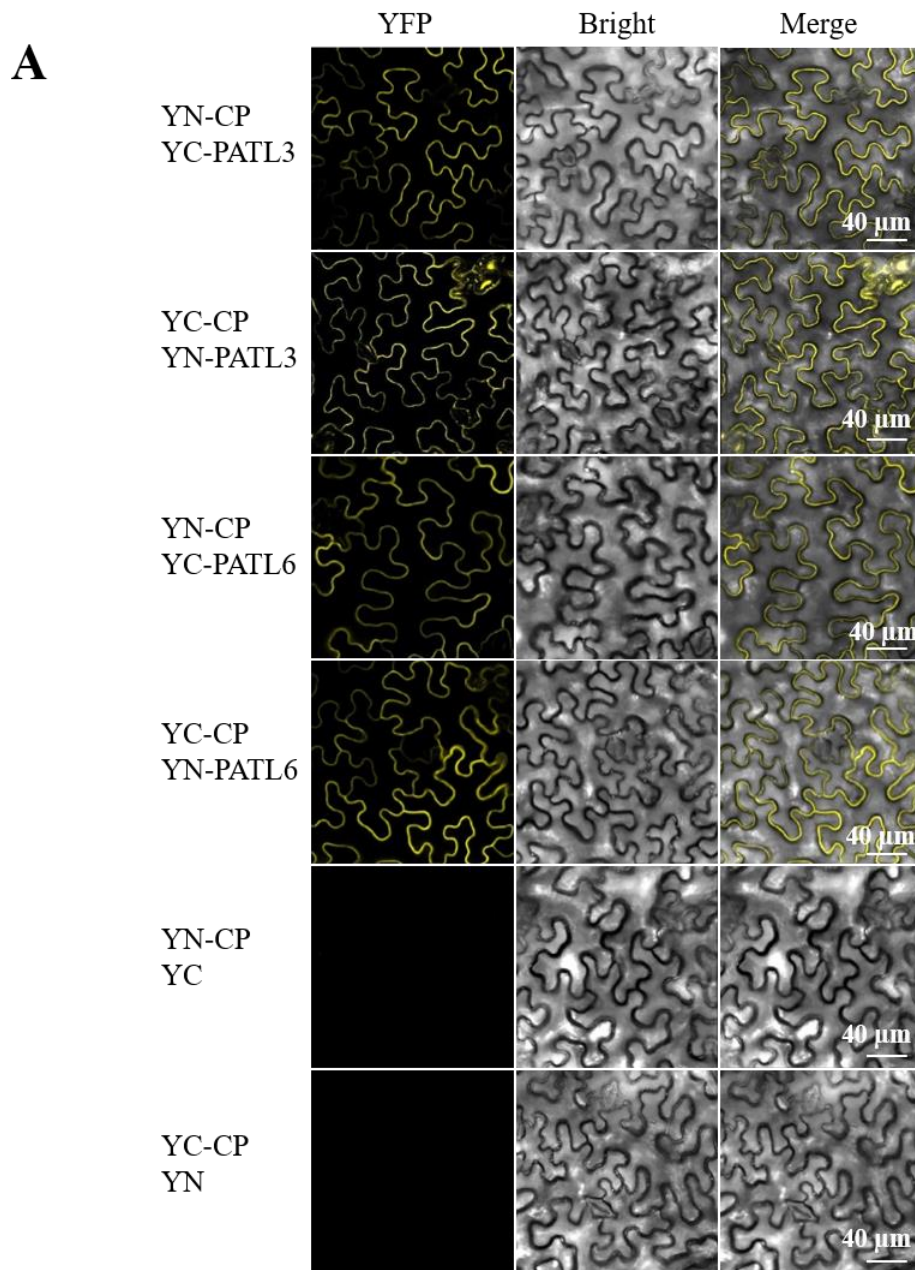


Figure 3.2 PATL3 and PATL6 interact with TuMV CP in *N. benthamiana* cells

(A) BiFC assays of CP interactions with PATL3 and PATL6 *in planta*. Fluorescence was observed in the *N. benthamiana* leaf co-infiltrated with PATL3/CP or PATL6/CP at 48 hpi. The yellow fluorescence results from complementation of the N-terminal part of the YFP fused with CP (YN-CP) by the C-terminal part of the YFP fused with either PATL3 or PATL6 (YC-PATL3 or YC-PATL6), or the complementation of the C-terminal part of the YFP fused with CP (YC-CP) by the N-terminal part of the YFP fused with either PATL3 or PATL6 (YN-PATL3 or YN-PATL6). No fluorescence was observed when CP-YN was co-expressed with unfused C-YFP (YC) or when unfused N-YFP (YN) was co-expressed with YC-CP. The YFP fluorescence (yellow), bright-field and the merged images of the same cells were visualized under a confocal microscope. Experiments were repeated three times with similar results. Bars are shown. (B) Co-immunoprecipitation of TuMV CP with PATL3. CP and PATL3 were fused to FLAG- and HA-tagged expression vectors, respectively. *N. benthamiana* leaves were co-agroinfiltrated with CP-FLAG and PATL3-HA, or infiltrated alone with CP-FLAG or PATL3-HA. Protein extracts were incubated with anti-Flag M2 affinity gel (Sigma). Protein samples before (Input) and after (Co-IP) immunopurification were analyzed by immunoblotting using HA or FLAG antibody.

3.3.3 Isolation of *patl3* and *patl6* single mutants and generation of *patl3patl6* double mutant

Given the physical interaction between PATLs and CP both in yeast and *in planta*, and the involvement of PATL3 and PATL6 in AMV infection (Peiro et al., 2014), I hypothesized that PATL3 and/or PATL6 are involved in TuMV infection.

To test this hypothesis, I used PATLs knockout or knockdown T-DNA insertion mutants. The Arabidopsis T-DNA insertions mutant lines for PATL3 and PATL6 were obtained from the Arabidopsis Biological Resource Center (ABRC) (Fig 3.3A). Homozygous T-DNA insertion lines were identified by two-step PCR genotyping (Fig 3.3B). The resulting homozygous single knockout mutants *patl3* and *patl6*, were confirmed by RT-PCR (Fig 3.3C). Subsequently, I generated a double knockout mutant *patl3patl6* by crossing *patl3* and *patl6* followed by two-step PCR genotyping and RT-PCR analysis of F2 progeny for identification of the homozygous double knockout line (Fig 3.3B and 3C). The single and double mutants obtained showed no visible phenotypes under normal growth conditions (Fig 3.3D).

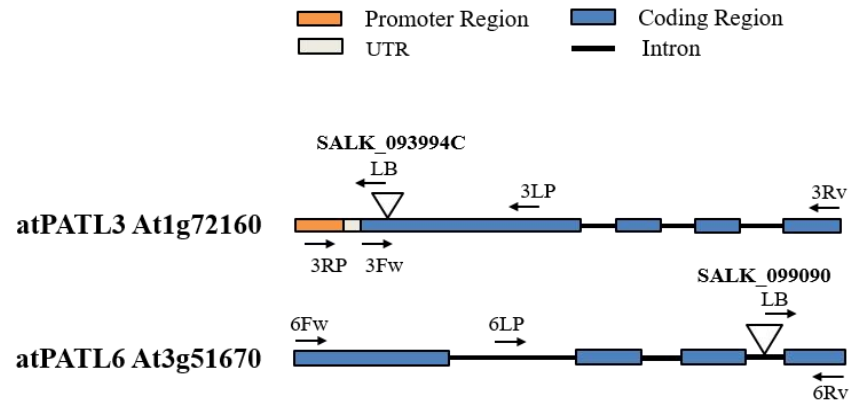
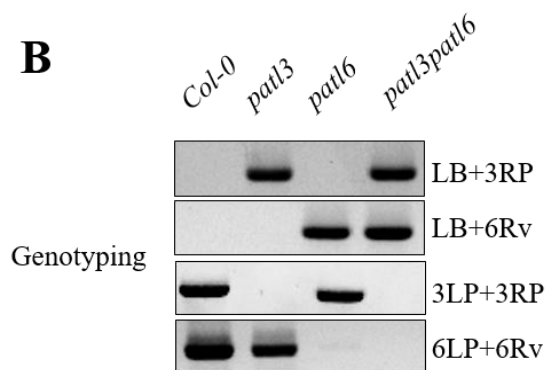
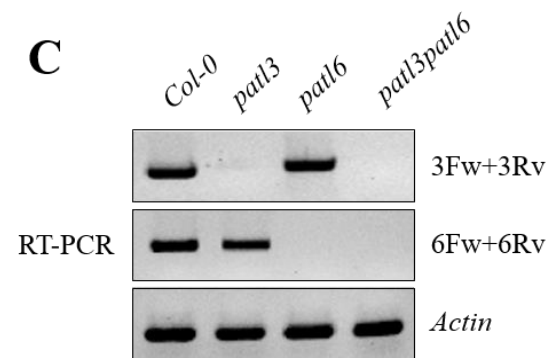
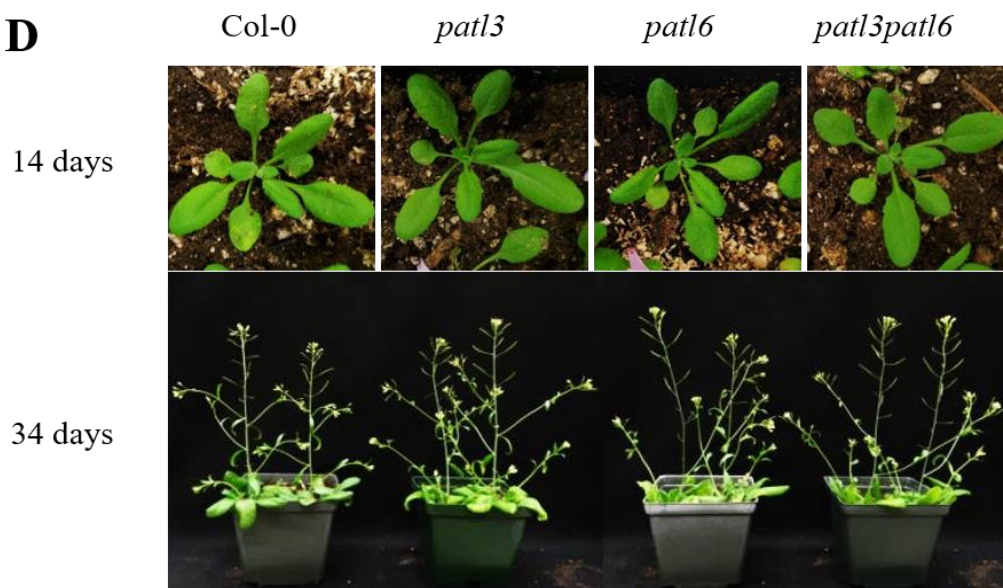
A**B****C****D**

Figure 3.3 Isolation of single and double *patls* T-DNA insertion mutants.

(A) Schematic representation of the PATLs and their T-DNA insertion sites. Inverted triangles indicate the T-DNA insertion sites, and arrows represent the approximate position and orientations of PCR primers. LB, primer specific to the left border of the T-DNA; LP, left genomic primer; RP, right genomic primer. Fw, forward primer; Rv, reverse primer. (B) Genotyping of the Arabidopsis PATLs T-DNA lines for single and double mutants. Primer sets used for genomic PCR are indicated on the right side. (C) RT-PCR analysis showing the absence of mRNA expression of *PATLs* in knockout mutants compared with Col-0 wild-type Arabidopsis. Primers used for RT-PCR are indicated on the right side. *ACTIN2* serves as a control (bottom panel). (D) Fourteen- (top) and thirty four-day-old (bottom) plants of wild-type Columbia-0, and *PATLs* knockout mutants.

3.3.4 Knockout of *PATL3* or *PATL6* or both genes promotes TuMV infection in Arabidopsis

To test the biological impact of *PATLs* knockouts on TuMV infection in Arabidopsis, *PATLs* single and double T-DNA knockout mutants were challenged with TuMV in three independent experiments. For each biological replicate experiment, sixteen individual plants of each mutant line or wild-type Col-0 were mechanically inoculated with TuMV. Total RNA and proteins were extracted from the inoculated leaves at 4 dpi, and viral RNA and CP accumulation were further detected by qRT-PCR and immunoblotting analysis. I found that both viral RNA and viral CP were significantly increased in *patl3*, *patl6* and *patl3patl6* mutants compared with WT plants (Fig 3.4A and B), indicating knockout of *PATL3*, *PATL6* or both promotes TuMV accumulation. At 14 dpi, in comparison with WT plants, the knockout mutant plants *patl3*, *patl6* and *patl3patl6* showed more severe symptoms (Fig 3.4C). Taken together, these data suggest that *PATL3* and *PATL6* negatively regulate TuMV infection in Arabidopsis plants.

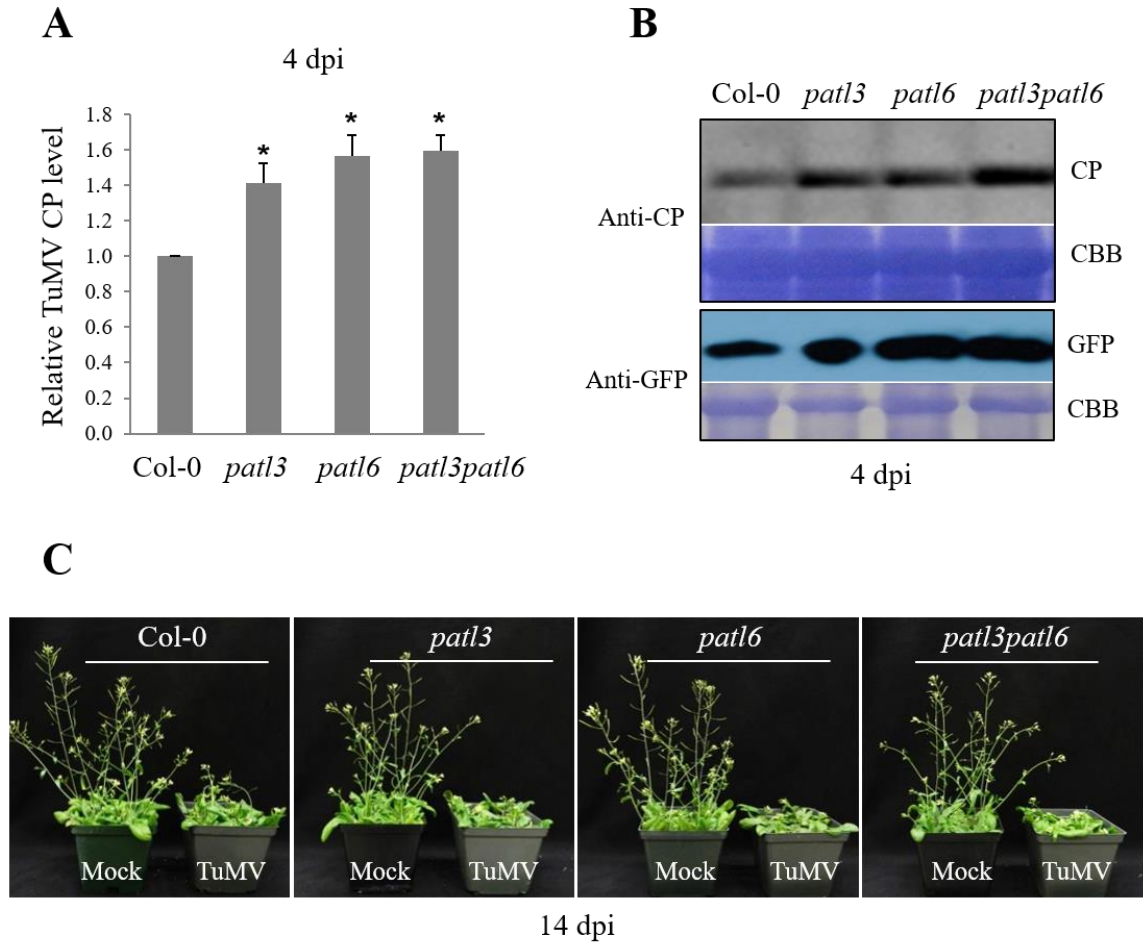


Figure 3.4 TuMV accumulation is enhanced in Arabidopsis Patellin knockouts.

(A) Quantification of TuMV RNA accumulation levels by qRT-PCR analysis from inoculated leaves at 4 dpi. Results are shown as means \pm SD of three biological replicates relative to Col-0 plants and were normalized with *AtActinII* as the internal reference. Asterisks represent a significant difference to Col-0 plants (unpaired two-tailed student's t-test, * $p < 0.05$). (B) Western blot analysis of TuMV CP and GFP accumulation in virus-inoculated leaf of Col-0, *patl3*, *patl6* and *patl3patl6* plants at 4 dpi. The comparable protein loading was monitored by Coomassie Brilliant Blue staining (CBB) (bottom panel). (C) TuMV-induced stunting symptoms in Col-0, *patl3*, *patl6* and *patl3patl6* compared with non-infected controls (Mock) at 14 dpi. Note that TuMV induced more stunted symptoms in *PATLs* knockouts compared to Col-0 plants.

3.3.5 Knockout of *PATL3* or *PATL6* or both facilitates TuMV multiplication in protoplasts

Enhanced viral infection by knockout of *PATL3* and *PATL6* may be through restriction of viral intercellular movement and viral genome replication. To test if viral genome replication is involved, I examined the effect of *PATL3* and *PATL6* knockouts on TuMV multiplication in Arabidopsis protoplasts. Protoplasts were isolated from Col-0, *patl3*, *patl6* and *patl3patl6* mutant plants, respectively, and then transfected with the TuMV infection clone TuMV-GFP using the PEG method (Yoo et al., 2007). qRT-PCR was done at 24 hpt and 48 hpt and immunoblotting was carried out at 48 hpt to monitor viral RNA and CP, respectively. In the control, transfected protoplasts maintained the typical spherical shape and showed high transfection efficiency indicated by green fluorescence at 48 hpt (Fig 3.5A). qRT-PCR results revealed that the viral RNA level in *patl3*, *patl6* and *patl3patl6* protoplasts were significantly increased at both time points tested (Fig 3.5B and C). Consistently, the TuMV CP levels in *patl3*, *patl6* and *patl3patl6* protoplasts were significantly higher than that in the Col-0 sample at 48 hpt (Fig 3.5D). Overall, these results suggest that *PATL3* and *PATL6* inhibit TuMV multiplication in Arabidopsis protoplasts.

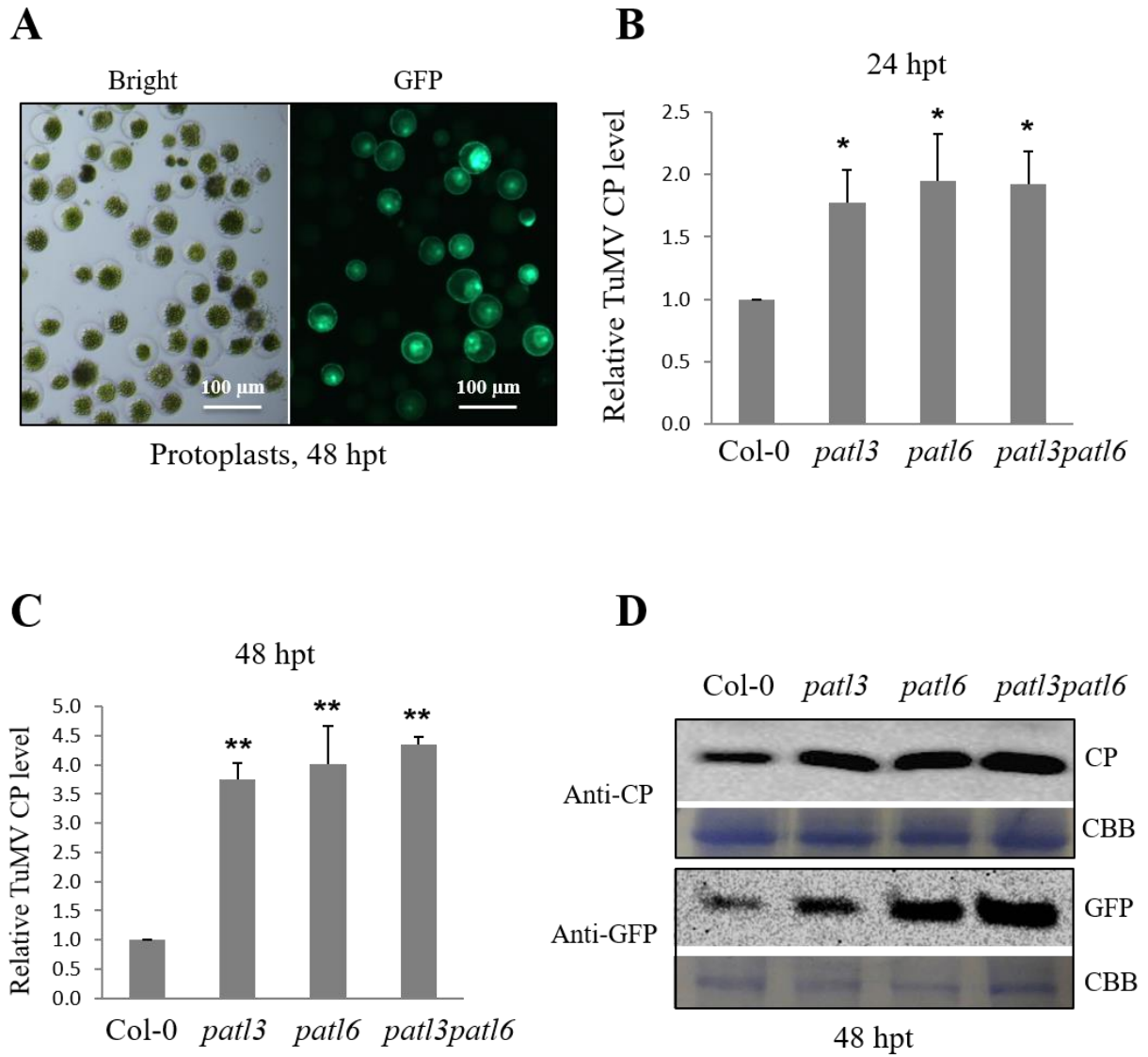


Figure 3.5 Knockout of *PATL3* and *PATL6* promotes TuMV accumulation in Arabidopsis protoplasts.

(A) *A. thaliana* Columbia-0 ecotype (Col-0) protoplasts infected by TuMV-GFP infectious clone. Fluorescence micrograph at 48 hour post-transfection (hpt) shows green fluorescence in the fraction of protoplasts that resulted from TuMV-GFP infection. (B) Quantification of TuMV CP RNA accumulation level by qRT-PCR analysis from protoplasts transfected by TuMV-GFP at 24 hpt. Results are shown as means \pm SD of three biological replicates relative to Col-0 plants and were normalized with *AtActinII* as the internal reference. Asterisks represent a significant difference to Col-0 plants (unpaired two-tailed student's t-test, * $p < 0.05$). (C) Quantification of the TuMV RNA accumulation level by qRT-PCR analysis at 48 hpt. Total RNA was isolated from protoplasts transfected by TuMV-GFP at 48 hpt. Viral RNA was quantified by qRT-PCR with primers specific for the CP coding region. Data were normalized against *AtActinII* mRNA (used as an internal reference). Results are shown as means \pm SD of three biological replicates relative to Col-0 plants. Asterisks represent a significant difference to Col-0 plants (unpaired two-tailed student's t-test, ** $p < 0.01$). (D) Immunoblotting analysis of TuMV CP and GFP accumulated in Col-0, *patl3*, *patl6* and *patl3patl6* at 48 hpt. The bottom panel is a protein gel with Coomassie Brilliant Blue staining (CBB) to show equal protein loading.

3.3.6 Stable overexpression of PATL3 inhibits TuMV accumulation

To investigate the effect of overexpression of PATL3 on TuMV infection in Arabidopsis, I also generated transgenic Arabidopsis lines overexpressing PATL3. The CDS of *PATL3* was cloned into the expression vector pBA-FLAG-4×Myc-DC. Immunoblotting analysis using Myc antibodies was performed to detect the PATL3-FLAG-Myc fusion protein in transgenic lines (Fig 3.6A). RT-PCR further confirmed an increased level of *PATL3* mRNA in the transgenic lines (Fig 3.6A). Protoplasts were isolated from the transgenic lines for transfection assays. The viral protein CP in the wild-type Arabidopsis protoplasts transfected with TuMV-GFP was detected at 36 hpt by immunoblotting analysis (Fig 3.6B). However, it was barely detected in the protoplasts isolated from PATL3 overexpression Arabidopsis plants (Fig 3.6B). These data suggest that overexpression of PATL3 suppresses TuMV multiplication in Arabidopsis protoplasts.

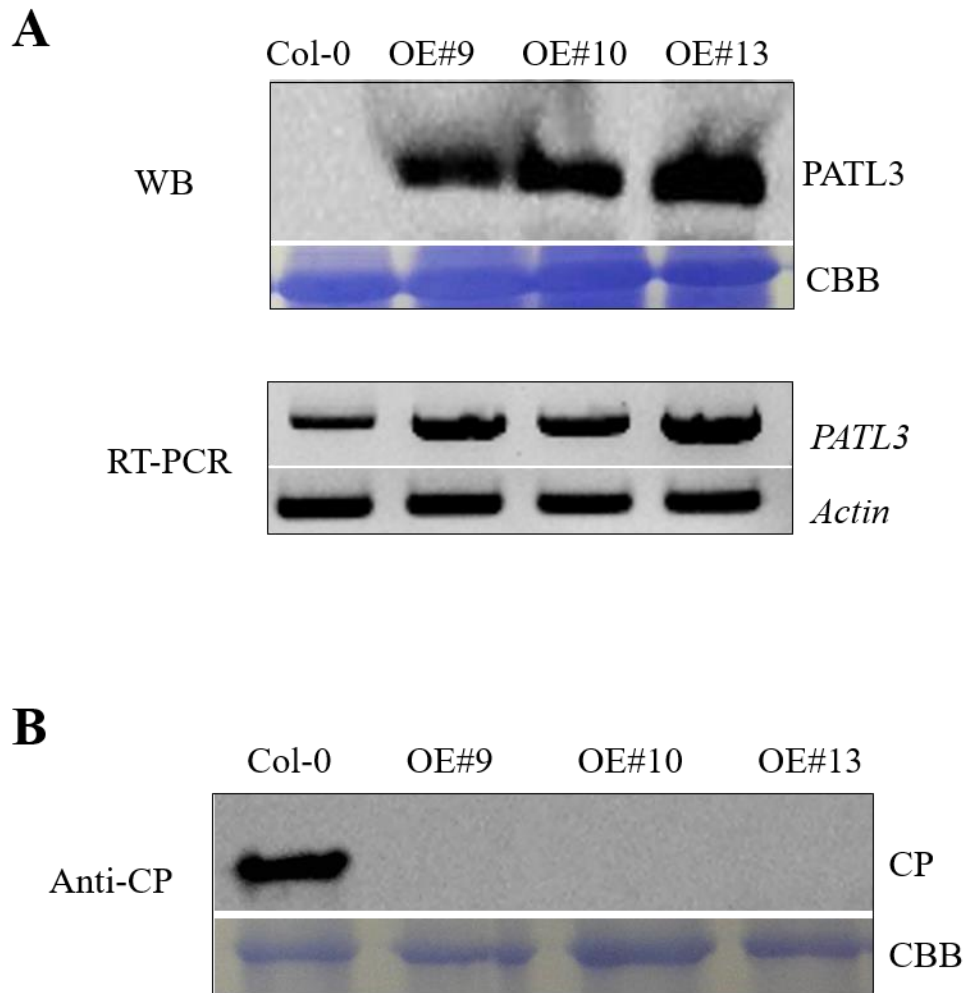


Figure 3.6 Stable overexpression of PATL3 inhibits TuMV accumulation in Arabidopsis protoplasts

(A) Immunoblotting and RT-PCR analysis of three independent PATL3 transgenic overexpression lines. The comparable protein loading was shown by Coomassie Brilliant Blue staining (CBB), and *AtActinII* was used as an internal control for RT-PCR analysis. (B) Immunoblotting analysis of TuMV CP in the protoplasts isolated from wild-type and three independent PATL3 overexpression lines. The comparable protein loading was shown by Coomassie Brilliant Blue staining (CBB).

3.3.7 Subcellular localization of AtPATL3 and AtPATL6 in uninfected and TuMV-infected *N. benthamiana* plants

To explore the possible mechanism by which PATL3 and PATL6 restrict TuMV replication, I determined the subcellular localization of PATL3 and PATL6 in plant cells. PATL3 and PATL6 were fused with GFP (named PATL3-GFP and PATL6-GFP, respectively) and transiently expressed in the *N. benthamiana* leaf by agroinfiltration. Expression of the fusion protein was confirmed by immunoblotting analysis using a rabbit serum raised against the N-terminus of GFP. Confocal microscopy was carried out to subcellularly localize PATL3-GFP and PATL6-GFP. At 48 hpi, both PATL3 and PATL6 were predominantly present in the cell periphery in *N. benthamiana* epidermal cells (Fig 3.7A). This is consistent with the reported data on subcellular localization of PATL3 and PATL6 *in planta* (Peiro et al., 2014).

I further stained the infiltrated leaf with the plasma membrane marker FM4-64. The GFP fluorescence was overlapped with red fluorescence emitted by FM4-64 (Fig 3.7A). These data support that AtPATL3 and AtPATL6 are plasma membrane-associated proteins.

To determine the intracellular localization of PATL3 and PATL6 in the presence of TuMV infection, I co-infiltrated PATL3-GFP or PATL6-GFP with TuMV infectious clone (a TuMV infectious clone without any fluorescent protein tags generated in Wang's lab). Interestingly, in addition to its presence in the cell periphery, PATL3-GFP formed a few large aggregated structures in the cytoplasm in TuMV-infected cells at 3 dpi (Fig 3.7B), suggesting a portion of AtPATL3 was redistributed into the cytoplasm upon TuMV infection. However, no obviously altered distribution pattern was observed for AtPATL6 in TuMV-infected cells.

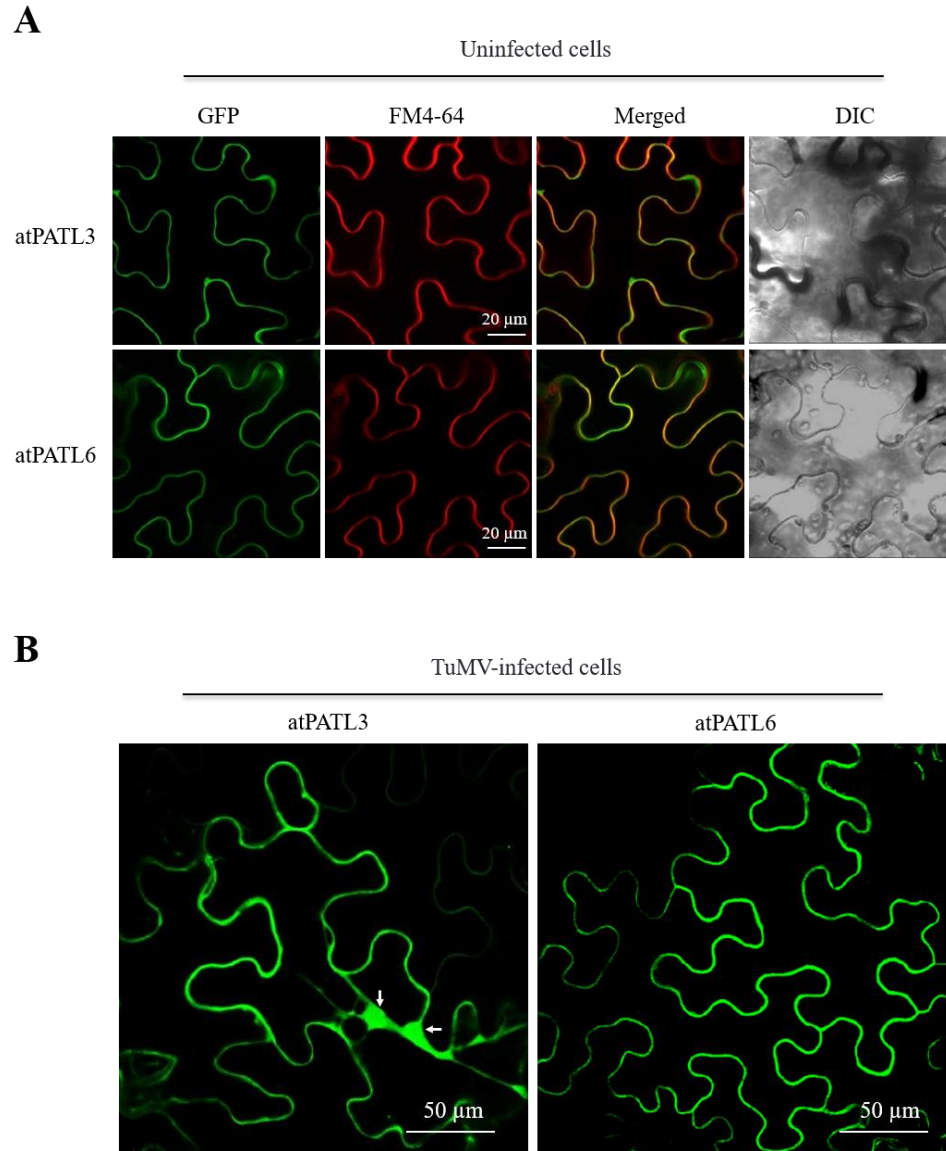


Figure 3.7 Subcellular localization of AtPATL3 and AtPATL6 in uninfected and TuMV-infected *N. benthamiana* epidermal cells.

(A) Subcellular localization of AtPATL3 (top) and AtPATL6 (bottom) in healthy *N. benthamiana* epidermal cells at 2 dpi. *N. benthamiana* leaves were stained with FM4-64, a plasma membrane marker and immediately subjected to confocal microscopy. Scale bars are indicated. (B) Subcellular localization of AtPATL3 (left) and AtPATL6 (right) in TuMV-infected *N. benthamiana* epidermal cells at 3 dpi. PATL3-GFP (left) or PATL6-GFP (right) was co-infiltrated with a TuMV infectious clone. Arrows indicate GFP fluorescence observed in the cytoplasm. Scale bars are indicated.

3.3.8 PATL3, but not PATL6 co-localized with TuMV-induced VRCs

Since TuMV-induced vesicles (globular and cortical aggregates) for virus replication are located in the cytoplasm, I hypothesised that the large aggregated structures of PATL3-GFP found in the cytoplasm upon TuMV infection might be the sites of TuMV VRCs. To test this hypothesis, I employed a TuMV infectious clone tagged by 6K2 fused-mCherry (TuMV-6K2mCherry). TuMV-6K2mCherry was co-agroinfiltrated with PATL3-GFP or PATL6-GFP in the fully expanded leaf of *N. benthamiana*. Under a confocal microscope at 3 dpi, I found that a great portion of PATL3-GFP was co-localized with 6K2-mCherry vesicles in the co-agroinfiltrated leaf (Fig 3.8 A). By contrast, PATL6-GFP remained to be associated with the plasma membrane (Fig 3.8B). It has been well known that the potyviral 6K2 protein induces the formation of the ER-derived vesicles that house VRCs for potyviral replication (Wei and Wang, 2008; Cotton et al., 2009; Wei et al., 2010a). Thus, my data suggest that PATL3, but not PATL6 is redistributed to and co-localizes with VRCs in TuMV-infected *N. benthamiana* epidermal cells.

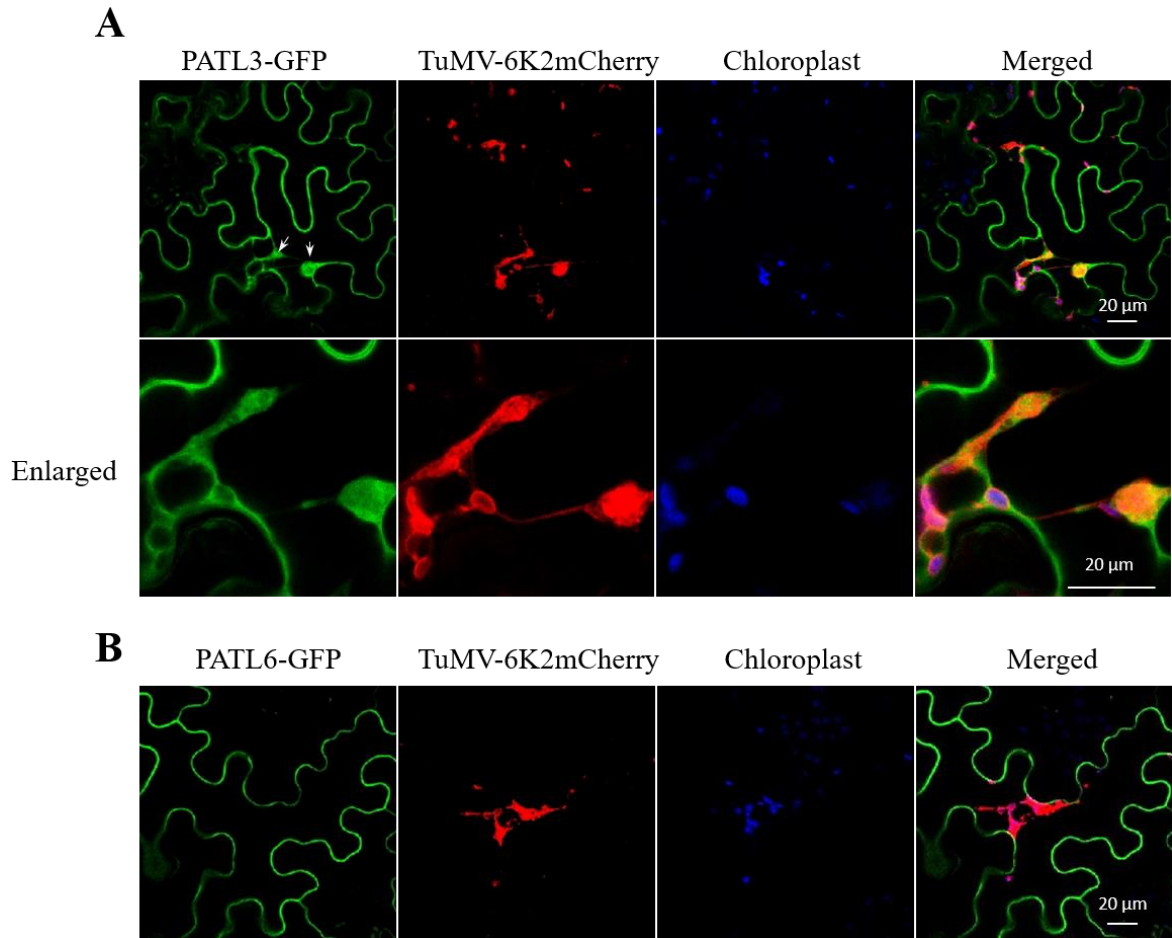


Figure 3.8 PATL3-GFP is recruited to the viral replication complex (VRC) in TuMV-infected *N. benthamiana* epidermal cells.

(A) Co-localization of AtPATL3 with TuMV VRCs (top). PATL3-GFP was co-expressed with a 6K2mCherry tagged TuMV infectious clone and observed under a confocal microscope at 3 dpi. An enlarged view of part of the top panel was presented at the bottom. Scale bars are as indicated. (B) PATL6 does not co-localize with TuMV VRCs. PATL6-GFP was co-expressed with a 6K2mCherry tagged TuMV infectious clone and observed under a confocal microscope at 3 dpi. Scale bars are as indicated.

3.3.9 PATL3 targets the VRC likely through the interaction with CI

To investigate the possible viral interactor of PATL3 that brings PATL3 to the VRC, I conducted Y2H assays to screen for the possible interactions between PATL3 and 11 TuMV viral proteins. The results showed that in addition to the PATL3-CP interaction, PATL3 also interacts with CI in yeast (Fig 3.9A).

To validate the PATL3-CI interaction, I created BiFC Gateway constructs YN-CI (CI fusion with the N-terminal half of YFP), YC-CI (CI fusion with the C-terminal half of YFP), YN-PATL3 (PATL3 fusion with the N-terminal half of YFP), and YC-PATL3 (PATL3 fusion with the C-terminal half of YFP) for BiFC assays in *N. benthamiana*. Co-expression of YN-CI/YC-PATL3 or YC-CI/YN-PATL3 in *N. benthamiana* epidermal cells by agroinfiltration resulted in strong yellow fluorescence predominantly present in the cell periphery Fig 3.9B. As expected, no visible fluorescence was observed in cells co-expressing YN-CI/YC or YC-CI/YN (negative controls) (Fig 3.9B).

I further conducted a co-immunoprecipitation (Co-IP) assay using antibodies against relevant tagged peptides. Four-week-old *N. benthamiana* plant leaves were agroinfiltrated with CI-FLAG, PATL3-HA or the combination of CI-FLAG with PATL3-HA. Protein extracts from infiltrated leaves were either used directly for immunoblotting to confirm the expression of the fusion proteins or incubated with anti-Flag M2 affinity gel (Sigma) for Co-IP detection. Both CI and PATL3 were indeed expressed in *N. benthamiana* plants when expressed alone or co-expressed (Fig 3.9C). For Co-IP, the beads were washed several times and then analyzed by immunoblotting with antibodies to FLAG or HA. A strong signal corresponding to PATL3-HA was detected in the sample co-immunoprecipitated with CI-FLAG (Fig 3.9C), indicating the presence of the PATL3-CI complex in the *N. benthamiana* leaf. Taken together, these data suggest that PATL3 physically interacts with CI *in planta*. Since CI is an essential component of the VRCs of TuMV (Cotton et al., 2009; Wang, 2013b), I proposed that PATL3 is recruited to the VRC through its interaction with CI.

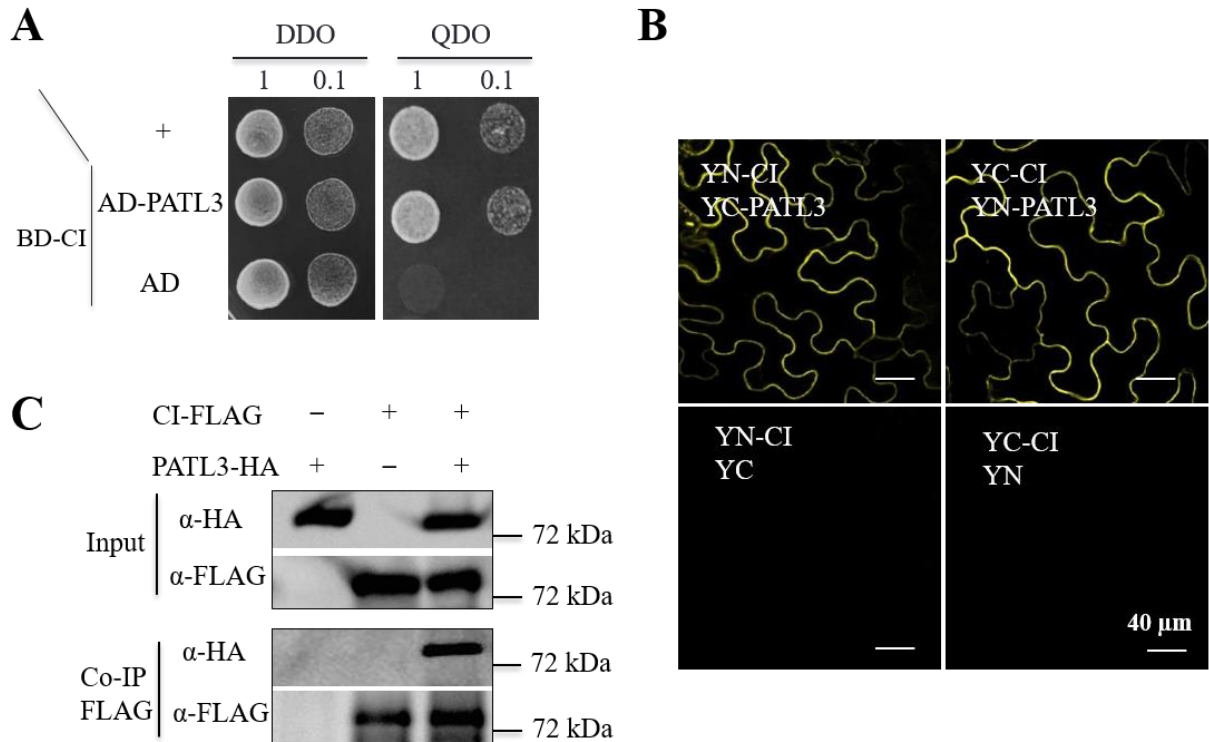


Figure 3.9 PATL3 interacts with TuMV CI in yeast and *in planta*.

(A) Competent yeast cells co-transformed with bait and prey plasmids were plated on double dropout (DDO) media lacking tryptophan and leucine to test for double transformation, and on quadruple dropout (QDO) media lacking tryptophan, leucine, histidine and adenine, for protein interaction. Yeast cells co-transformed with pGBKT7-53 and pGADT7-T, designed as +, served as a positive control and co-transformation of AD and BD-CI was used as a negative control. (B) BiFC assays of the CI-PATL3 interaction *in planta*. Fluorescence was observed in the *N. benthamiana* leaf co-infiltrated with YN-CI/YC-PATL3 or YC-CI/YN-PATL3 at 48 hpi. No fluorescence was observed when co-expressing YN-CI with unfused C-YFP (YC) or N-YFP (YN) with YC-CI. (C) Co-immunoprecipitation of TuMV CI with PATL3. CI and PATL3 were fused to FLAG- and HA-tagged expression vectors, respectively. Protein extracts were incubated with anti-Flag M2 affinity gel (Sigma). Protein samples before (Input) and after (Co-IP) immunopurification were subjected to immunoblotting using HA or FLAG antibody.

3.4 Discussion

As an intracellular parasite, a virus is fully dependent on the host cellular machinery for replication, intracellular and intercellular movement (Daugherty and Malik, 2012; Wang, 2015). On the other hand, during the longtime evolution, plant hosts have evolved multiple resistance mechanisms to defend against viral infection by triggering signal transduction to activate immune responses and/or recruitment of host proteins to interfere with the viral infection processes (Daugherty and Malik, 2012; Coffin, 2013). The CP of potyvirus has been suggested to be implicated in various stages of the viral infection processes, such as viral translation, movement and assembly (Ivanov and Makinen, 2012; Wang, 2013b; Revers and Garcia, 2015). Potyviral CI is a helicase, physically present in the TuMV-induced VRCs and absolutely required for viral replication (Fernandez et al., 1995; Carrington et al., 1998; Gomez de Cedron et al., 2006; Cotton et al., 2009; Wang, 2013b; Deng et al., 2015). In this study, I identified the Arabidopsis Patellin family proteins PATL3 and PATL6 that physically interact with TuMV CP in yeast and *in planta*, and PATL3 also interacts with TuMV CI. I further found that PATLs inhibit TuMV multiplication and PATL3 functions likely by targeting TuMV VRCs through the interaction with CI. Thus, it can be concluded that PATLs are critical for efficient defense against TuMV infection in Arabidopsis plants, likely by their interactions with the viral CP and/or CI.

The Arabidopsis Patellin family comprises six members (PATL1, PATL2, PATL3, PATL4, PATL5 and PATL6). All the six PATLs in Arabidopsis possess a variable N-terminal domain, a Sec14-like domain (homologue to yeast Sec14p) and a C-terminal GOLD domain (Golgi dynamics) (Peterman 2004). Sec14p, originally isolated from a *secretory (Sec)* mutant of yeast, is an essential protein that functions in the formation and exit of vesicles from the trans-Golgi network (Tejosa et al., 2017). To date, proteins with a Sec14 domain are known to be involved in membrane trafficking, lipid metabolism and cytoskeleton dynamic (Peterman et al., 2004; Peiro et al., 2014; Tejosa et al., 2017). The GOLD domain is a conserved domain among p24 protein family that has been shown to be critical for cargo selection and cargo transport from the ER to the Golgi complex and is presumably responsible for protein-protein interaction (Anantharaman and Aravind,

2002). PATL1 is a Sec14-Like protein and localizes to the cell plate during cytokinesis and binds phosphoinositide (Peterman et al. 2004). PATL2 is a phosphoinositide-binding protein and is a substrate of Arabidopsis MPK4 MAP Kinase during septum formation in cytokinesis (Suzuki et al. 2016). PATL family proteins have been reported to function in response to abiotic stresses (Kearns et al., 1998; Monks et al., 2001) and biotic stresses (Kiba et al., 2012; Peiro et al., 2014). Upon abiotic stresses, PATLs can be significantly phosphorylated (Lv et al., 2014; Mattei et al., 2016). In a previous study, PATL3 and PATL6 were suggested to play a negative role in AMV intercellular movement by interfering with the targeting of AMV MP to the PD (Peiro et al., 2014). This prompted me to study the subcellular localization of PATL3 and PATL6. I found that PATL3 and PATL6 are PM-associated proteins as they co-localized with FM4-64, a known PM marker (Fig 3.7A). However, I did not observe obvious PD localization when PATLs were co-expressed with CP or CI (Fig 3.2A and 3.9B). Thus, PATL3 and PATL6 might play a role by interference with the CP-associated movement complex to inhibit the trafficking of the complex to the PD.

In this study, I found that expression of PATL3-GFP in TuMV-infected plant cells disrupted the uniform localization of PATL3-GFP at the plasma membrane and resulted in the formation of PATL3-GFP aggregates in the cytoplasm (Fig 3.7B). Further, by using a 6K2mCherry-tagged TuMV infectious clone, I demonstrated that PATL3, but not PATL6 indeed co-localized with TuMV VRCs upon virus infection (Fig 3.8A). In addition, my protoplast assay showed that knockout of *PATL3* and/or *PATL6* indeed promoted TuMV multiplication (Fig 3.5). Moreover, I found that CI, a viral helicase that is physically present in the VRCs and absolutely required for viral replication, interacts with PATL3 (Fig 3.9). Thus, I propose that PATL3 inhibits TuMV multiplication likely through targeting VRCs via its interaction with CI. However, I cannot exclude the possibility that PATL3 acts as a restriction factor through its interference with TuMV movement, since CP and CI are key players for potyvirus movement.

In summary, my results presented here suggest that the Arabidopsis Patellins family proteins PATL3 and PATL6 physically interact with TuMV CP and play a negative role in TuMV multiplication in Arabidopsis plants and protoplasts. PATL3 targets the VRCs

in the presence of TuMV infection likely through its interaction with CI. Taken together, these findings suggest that PATL3 and PATL6 are novel host restriction factors for potyviral infection. This study also provides strong evidence supporting the critical roles of plasma membrane-associated proteins in defending virus infection.

3.5 Materials and Methods

3.5.1 Plant material and growth conditions

Both the *Nicotiana benthamiana* and *Arabidopsis thaliana* plants were grown in pots with Pro-Mix Mycorrhizae Growing medium under greenhouse conditions with 16 hours light/8 hours dark regime. The relative humidity was set at 70% and temperatures were adjusted to 22 and 18°C during the light and dark periods, respectively.

3.5.2 Y2H and BiFC Assay

Matchmaker Gold Yeast Two-Hybrid System (Clontech) was used to screen and identify CP-interacting Arabidopsis proteins. The Arabidopsis cDNA library was purchased from Clontech (Catalog No. 630487). To make the bait construct, TuMV CP coding sequence (CDS) was amplified from plasmid TuMV-GFP (provided by Dr. Jean-François Laliberté, INRS, Quebec, Canada) and cloned into Y2H gateway vectors pDEST-GBKT7 or pDEST-GADT7 (provided by Dr. Yuhai Cui, AAFC, London, Canada) (Lu et al., 2010).

To test the suitability of CP as bait, we confirmed that CP could be expressed and is not toxic in yeast and CP does not autonomously activate the reporter genes in Y2HGold in the absence of a prey protein, according to the Matchmaker Gold Yeast Two-Hybrid System User Manual (Version No. 092413).

To identify CP-interacting Arabidopsis proteins, Y2H screening was performed essentially combine 1 ml aliquot of Arabidopsis cDNA strain and the bait strain, incubate at 30°C allowing yeast mating (get both bait and prey plasmids in one yeast cell) and subsequently selected on the selective medium DDO/X/A (Double dropout media containing 40 µg/ml X-α-Gal and 200 ng/ml Aureobasidin A). 3-5 days later, blue

colonies grown on DDO/X/A were replica-plated onto higher stringency selective medium QDO/X/A (Quadruple dropout media containing 40 $\mu\text{g/ml}$ X- α -Gal and 200 ng/ml Aureobasidin A). The blue clones grown on QDO/X/A were subjected to plasmid extraction by using the Easy Yeast Plasmid Isolation Kit (Catalog No. 630457, Clontech) and were further transferred into *Escherichia coli*. Plasmid DNA was extracted from overnight-grown *E.coli* and subsequently sequenced. The obtained sequences were used to identify the corresponding interacting genes in the NCBI public database.

To select the genuine positive interactions, co-transformation experiments were conducted. Briefly, the full-length CDS of Arabidopsis genes were amplified from Arabidopsis cDNA, fused to prey vector pDEST-GADT7 (AD), and subsequently co-transformed with BD-CP into yeast competent cells. The resulting yeast cells were plated on selective medium DDO/X- α -Gal agar plates followed by second-round selection on QDO/X- α -Gal agar plates. The combination of pGBKT7-53 and pGADT7-T serves as a positive control, and the pair of the vector BD-CP and the empty construct AD serve as a negative control.

3.5.3 BiFC and Subcellular Localization study

BiFC assays were conducted to validate viral protein-Arabidopsis protein interactions in *planta*. Various Arabidopsis genes are cloned into BiFC vector. A detailed procedure of BiFC assays was described in Chapter 2 Materials and Methods.

For subcellular localization experiment, the *AtPATL3* and *AtPATL6* ORFs were amplified from Arabidopsis cDNA with specific primers designed for Gateway System (Invitrogen) and recombined into binary destination vectors expressing GFP. The infectious clone TuMV-6K2mCherry were obtained from Dr. Jean-François Laliberté, INRS, Quebec, Canada.

All expression vectors were transformed into *Agrobacterium tumefaciens* GV3101 cells. Cultures were then diluted to OD₆₀₀ 0.2 in agro-infiltration buffer (10 mM MES PH 5.6, 10 mM MgCl₂ and 100 μ acetosyringone) and subsequently infiltrated into leaves of 3 to

4 week-old *N.benthamiana* plants. Confocal images were taken at 48 hpi for BiFC study and 72 hpi for subcellular localization study with a Leica TCS SP2 microscope.

3.5.4 Coimmunoprecipitation (co-IP) assay

For Co-IP assay, constructs (pSK-PATL3, pSK-CP and pSK-CI) were transformed into *A. tumefaciens* strain GV3101 and further infiltrated into *N. benthamiana* leaves at OD600 0.4. One gram of leaf tissue was sampled at 60 hpi and frozen in liquid nitrogen. Each sample was ground into fine powder by mortar and pestle and homogenized in extraction buffer (25 mM Tris HCl, pH 7.5, 10% glycerol, 1 mM EDTA, 150 mM NaCl, 10 mM DTT, 2% w/v polyvinylpyrrolidone (PVPP), 0.1% IGEPAL CA-630 (Sigma) and 1×EDTA-free protease inhibitor cocktail (Roche). The homogenate was incubated at 4°C rotating end to end for 30 min and precleared by two centrifugations at 14,000 rpm for 15 min at 4°C. 25 µl anti-Flag M2 affinity gel (Sigma, Catalog Number A2220) per sample washed 3 times with IP buffer (25 mM Tris HCl, pH 7.5, 1mM EDTA, 150 mM NaCl, 10% glycerol, and 0.1% IGEPAL CA-630) were added to 1mL protein extracts and incubated at 4°C rotating end to end for 2 h. Agarose beads were pelleted by centrifugation at 3,000 rpm for 2 min, washed with IP buffer for three times and re-suspended in 5×SDS-PAGE loading buffer. After boiling at 70 °C for 10 min, the protein samples were subjected to western blot. The primary antibodies used in this study were monoclonal anti-FLAG-HRP (Cat No. F3165, Sigma) and polyclonal anti-HA-HRP (Cat No. H6908, Sigma). Anti-mouse antibody conjugated to horseradish peroxidase (Sigma) and anti-rabbit polyclonal antibody conjugated to HRP (Sigma) were used as secondary antibody, respectively. Protein bands were detected using Immobilon Western Chemiluminescent HRP substrate (Kit No. WBKL S00 50, Millipore).

3.5.5 Characterization of T-DNA insertions

The Arabidopsis T-DNA insertion lines for *PATL3* (SALK_093994C) and *PATL6* (SALK_099090) is obtained from Arabidopsis Biological Resource Center (ABRC) at the Ohio State University. The information of these lines is provided on The Arabidopsis Information Resource (TAIR) website (<http://arabidopsis.org>).

The seeds were sown in pots with Pro-Mix Mycorrhizae Growing medium at 4°C for 3 days to break dormancy and subsequently transfer to growth chamber at 24°C with 16 hours light/20°C with 8 hours dark and the relative humidity was set at 70%.

Leaf samples were collected from four-week-old *Arabidopsis* Col-0, *PATL3* (SALK_093994C) and *PATL6* (SALK_099090) plants for genomic DNA extraction according to Edwards *et al.*, (1991) (Edwards et al., 1991). A PCR-based genotyping method was used for determining the T-DNA insertion zygosity described by Salk Institute Genome Analysis Laboratory (<http://signal.salk.edu/tdnaprimers.2.html>). Briefly, a two-step PCR was carried out: LP+RP and LB+RP (LB: primer specific to the left border of T-DNA; LP: left genomic primer; RP: right genomic primer). A PCR product should be detected in the LP+RP reaction for wild-type (Col-0) or heterozygous lines (HZ), no band would be detected for homozygous lines (HM). Nevertheless, a band should be produced in the LB+RP for HM or HZ lines. The identified *PATL3* and *PATL6* HM lines are self-pollinated and allowed to produce seeds. F2 plants were used for confirmation of T-DNA insertion homozygosity and subsequently RT-PCR analysis for determining the full length RNA expression level. To locate the T-DNA insertion site, LB+RP reaction PCR products were purified and sequenced.

3.5.6 Generation of double knockout mutant

The *patl3patl6* double mutant was generated by crossing the homozygous single knockout *patl3* and *patl6* lines and self-pollination of the F1 generation. Of the F2 progeny, individual plants confirmed to be homozygous for *patl3* and heterozygous for *PATL6* were selected for seed collection. The *patl3patl6* double mutant was identified from the F3 generation plants through PCR-based genotyping. RT-PCR analysis was employed to monitor the RNA level of both *PATL3* and *PATL6*.

3.5.7 Generation of *PATL3* transgenic plants

The coding region of *PATL3* was cloned into the binary gateway vector pBA-FLAG-4×Myc-DC (Zhu et al., 2011) using Gateway technology. The construct was introduced into *Agrobacterium tumefaciens* (strain GV3101) and further transformed into

Arabidopsis (Col-0 ecotype) by the floral dip method (Zhang et al., 2006). The resulting Arabidopsis seeds were sowed. Typically 8-10 days after sowing, the seedlings were screened by directly spraying solutions containing 250 mg/liter herbicide Basta. The survival transformants were analyzed by RT-PCR and Western blot to confirm the expression of the transgene. Stable transgenic plants (T3 generation) were used for TuMV infection assay.

3.5.8 Protoplasts isolation and TuMV transfection

Protoplasts isolation and TuMV transfection were essentially as described in Chapter 2 Materials and Methods.

3.6 References

- Anantharaman, R., and Aravind, L.** (2002). The GOLD domain, a novel protein module involved in Golgi function and secretion. *Genome Biology* **3**.
- Callaway, A., Giesman-Cookmeyer, D., Gillock, E.T., Sit, T.L., and Lommel, S.A.** (2001). The multifunctional capsid proteins of plant RNA viruses. *Annual Review of Phytopathology* **39**, 419-460.
- Carrington, J.C., Jensen, P.E., and Schaad, M.C.** (1998). Genetic evidence for an essential role for potyvirus CI protein in cell-to-cell movement. *The Plant Journal* **14**, 393-400.
- Coffin, J.M.** (2013). Virions at the gates: receptors and the host-virus arms race. *PLoS Biol* **11**, e1001574.
- Cotton, S., Grangeon, R., Thivierge, K., Mathieu, I., Ide, C., Wei, T., Wang, A., and Laliberte, J.F.** (2009). Turnip mosaic virus RNA replication complex vesicles are mobile, align with microfilaments, and are each derived from a single viral genome. *J Virol* **83**, 10460-10471.
- Daugherty, M.D., and Malik, H.S.** (2012). Rules of engagement: molecular insights from host-virus arms races. *Annu Rev Genet* **46**, 677-700.
- Deng, P., Wu, Z., and Wang, A.** (2015). The multifunctional protein CI of potyviruses plays interlinked and distinct roles in viral genome replication and intercellular movement. *Virol J* **12**, 141.
- Dormann, P., Kim, H., Ott, T., Schulze-Lefert, P., Trujillo, M., Wewer, V., and Huckelhoven, R.** (2014). Cell-autonomous defense, re-organization and trafficking of membranes in plant-microbe interactions. *New Phytol* **204**, 815-822.
- Edwards, K., Johnstone, C., and Thompson, C.** (1991). A simple and rapid method for the preparation of plant genomic DNA for PCR analysis. *Nucleic Acids Research* **19**, 1349.
- Fernandez, A., Lain, S., and Garcia, J.A.** (1995). RNA helicase activity of the plum pox potyvirus CI protein expressed in *Escherichia coli*. Mapping of an RNA binding domain. *Nucleic Acids Research* **23**, 1327-1332.
- Gomez de Cedron, M., Osaba, L., Lopez, L., and Garcia, J.A.** (2006). Genetic analysis of the function of the plum pox virus CI RNA helicase in virus movement. *Virus Res* **116**, 136-145.
- Ivanov, K.I., and Makinen, K.** (2012). Coat proteins, host factors and plant viral replication. *Curr Opin Virol* **2**, 712-718.
- Juana Díez, M.I., Masanori Kaido, and Paul Ahlquist.** (2000). Identification and characterization of a host protein required for efficient template selection in viral RNA replication. *Proc. Natl. Acad. Sci* **97**, 3913-3918.
- Laliberte, J.F., and Sanfacon, H.** (2010). Cellular remodeling during plant virus infection. *Annu Rev Phytopathol* **48**, 69-91.
- Lefebvre, B., Timmers, T., Mbengue, M., Moreau, S., Herve, C., Toth, K., Bittencourt-Silvestre, J., Klaus, D., Deslandes, L., Godiard, L., Murray, J.D., Udvardi, M.K., Raffaele, S., Mongrand, S., Cullimore, J., Gamas, P., Niebel, A., and Ott, T.** (2010). A remorin protein interacts with symbiotic receptors and regulates bacterial infection. *Proc Natl Acad Sci U S A* **107**, 2343-2348.
- Lu, Q., Tang, X., Tian, G., Wang, F., Liu, K., Nguyen, V., Kohalmi, S.E., Keller, W.A., Tsang, E.W., Harada, J.J., Rothstein, S.J., and Cui, Y.** (2010). Arabidopsis homolog of the yeast TREX-2 mRNA export complex: components and anchoring nucleoporin. *Plant J* **61**, 259-270.
- Lv, D.W., Subburaj, S., Cao, M., Yan, X., Li, X., Appels, R., Sun, D.F., Ma, W., and Yan, Y.M.** (2014). Proteome and phosphoproteome characterization reveals new response and defense mechanisms of *Brachypodium distachyon* leaves under salt stress. *Mol Cell Proteomics* **13**, 632-652.

- Mattei, B., Spinelli, F., Pontiggia, D., and De Lorenzo, G.** (2016). Comprehensive Analysis of the Membrane Phosphoproteome Regulated by Oligogalacturonides in *Arabidopsis thaliana*. *Front Plant Sci* **7**, 1107.
- Nathalie, L.-C., and Bouhidel, K.** (2014). Plasma membrane protein trafficking in plant-microbe interactions: a plant cell point of view. *Front Plant Sci* **5**, 735.
- Ni, P., and Cheng Kao, C.** (2013). Non-encapsidation activities of the capsid proteins of positive-strand RNA viruses. *Virology* **446**, 123-132.
- Nicoletta Schellera, L.B.M., Rui Pedro Galãoa, Ashwin Charic, Mireia Gime' nez-Barconsa, Amine Noueiryd, Utz Fischer, Andreas Meyerhansb, and Juana Díeza.** (2009). Translation and replication of hepatitis C virus genomic RNA depends on ancient cellular proteins that control mRNA fates. *PNAS* **106**, 13517–13522.
- Peiro, A., Izquierdo-Garcia, A.C., Sanchez-Navarro, J.A., Pallas, V., Mulet, J.M., and Aparicio, F.** (2014). Patellins 3 and 6, two members of the Plant Patellin family, interact with the movement protein of Alfalfa mosaic virus and interfere with viral movement. *Mol Plant Pathol* **15**, 881-891.
- Peterman, T.K., Ohol, Y.M., McReynolds, L.J., and Luna, E.J.** (2004). Patellin1, a novel Sec14-like protein, localizes to the cell plate and binds phosphoinositides. *Plant Physiol* **136**, 3080-3094; discussion 3001-3082.
- Raffaele, S., Bayer, E., Lafarge, D., Cluzet, S., German Retana, S., Boubekour, T., Leborgne-Castel, N., Carde, J.P., Lherminier, J., Noirot, E., Satiat-Jeunemaitre, B., Laroche-Traineau, J., Moreau, P., Ott, T., Maule, A.J., Reymond, P., Simon-Plas, F., Farmer, E.E., Bessoule, J.J., and Mongrand, S.** (2009). Remorin, a solanaceae protein resident in membrane rafts and plasmodesmata, impairs potato virus X movement. *Plant Cell* **21**, 1541-1555.
- Revers, F., and Garcia, J.A.** (2015). Molecular biology of potyviruses. *Adv Virus Res* **92**, 101-199.
- Tejosa, R., Rodriguez-Furlanb, C., Adamowskic, M., Sauerd, M., Norambuenab, L., and Frimlc, J.** (2017). PATELLINS are regulators of auxin-mediated PIN1 relocation and plant development in *Arabidopsis thaliana*. *J Cell Sci* **jcs-204198**.
- Tomlinson, J.A.** (1987). Epidemiology and control of virus diseases of vegetables. *Annals of Applied Biology* **110**, 661-681.
- Wang, A.** (2013). Molecular isolation and functional characterization of host factors required in the virus infection cycle for disease control in plants. *CAB Reviews* **8**.
- Wang, A.** (2015). Dissecting the molecular network of virus-plant interactions: the complex roles of host factors. *Annu Rev Phytopathol* **53**, 45-66.
- Yoo, S.D., Cho, Y.H., and Sheen, J.** (2007). *Arabidopsis* mesophyll protoplasts: a versatile cell system for transient gene expression analysis. *Nat Protoc* **2**, 1565-1572.
- Zhang, X., Henriques, R., Lin, S.S., Niu, Q.W., and Chua, N.H.** (2006). Agrobacterium-mediated transformation of *Arabidopsis thaliana* using the floral dip method. *Nat Protoc* **1**, 641-646.
- Zhu, H., Hu, F., Wang, R., Zhou, X., Sze, S.H., Liou, L.W., Barefoot, A., Dickman, M., and Zhang, X.** (2011). *Arabidopsis* Argonaute10 specifically sequesters miR166/165 to regulate shoot apical meristem development. *Cell* **145**, 242-256.

Chapter 4

4 General discussion and future directions

Plant viruses are one of the major pathogens that threaten global food security. Approximately 47% of current crop epidemics are caused by plant viruses. The vast majority of known plant viruses are positive-sense single-stranded (+ss) RNA viruses (Sanfaçon, 2005). After entry into a plant cell, the invading (+ss) RNA virus undergoes viral particle disassembly, viral genome translation, formation of the viral replication complex (VRC), viral genome multiplication and viral genome encapsidation (Wang, 2013b; Revers and Garcia, 2015). Different from animal viruses, the progeny plant viruses must manage to penetrate through the rigid cell wall to enter into the neighbouring cells. Such viral intercellular movement mainly take places in mesophyll and epidermal cells through plasmodesmata (PDs), and further to establish their systemic infection. Subsequently the virus moves from the mesophyll via bundle sheath cells, phloem parenchyma and companion cells into phloem sieve elements (SEs) where it is passively transported to and unloaded at the distant tissues following the source-to-sink flow of photoassimilates (Hipper et al., 2013; Wang, 2015). Clearly, viral intercellular movement through the PD is a key step for the virus to establish a successful infection. A better understanding of this step may assist in the development of novel strategies to control viral diseases.

4.1 Requirement of coat protein (CP) for potyviral cell-to-cell movement

Since PDs are only ~30-50 nm in diameter, they only allow small molecules to diffuse between cells (Brunkard et al., 2013). The PD size exclusion limit (SEL) is estimated to be about 1 kDa (Brunkard et al., 2013). Therefore, PD regulates the intercellular movement of macromolecules and macromolecular complexes such as viral particles. It is well established that viral cell-to-cell movement via the PD requires coordinated action of virus-encoded movement proteins (MP), other required viral proteins and host factors (Schoelz et al., 2011; Wang, 2015). Despite the agricultural and scientific importance of potyviruses as the largest group of known plant viruses, how potyviruses move

intercellularly is still not well understood. Potyviruses have a relatively small genome (approximately 10 kb) that encodes fewer than a dozen proteins (Ivanov et al., 2014; Revers and Garcia, 2015). It has been suggested that several potyviral proteins might be involved in cell-to-cell movement, including CP, CI, P3N-PIPO, VPg and HC-Pro (Wang, 2013b; Revers and Garcia, 2015). Among them, CP is believed to be a multifunctional protein that plays key roles in the viral infection cycle as well as virus-host interplay (Wang, 2013b; Revers and Garcia, 2015). My PhD project aimed to investigate the role of CP in viral cell-to-cell movement and, to identify host proteins that interact with potyviral CP and further characterize their biological effects in viral infection.

In the present study, I chose *Turnip mosaic virus* (TuMV) as a model virus and developed a double fluorescent protein-tagged system that can monitor the intercellular movement of TuMV from the primarily infected cells to the secondarily infected cells (Fig 2.1). I found that deletion of TuMV CP, the mutant virus lost the ability to move between cells (Fig 2.2), suggesting the essential role of CP in intercellular movement. My protoplast infection assay revealed that the CP-deletion mutant could replicate as efficiently as the wild-type virus (Fig 2.2), indicating CP is not required for TuMV replication. These data imply that TuMV CP mainly functions as a basic unit of the capsid shell of the viral particle and as an essential component of the movement complex.

Potyviral replication is carried out by the potyviral VRC that is associated with 6K2-induced vesicles (Cotton et al., 2009; Revers and Garcia, 2015). Grangeon and colleagues showed that the 6K2 vesicles of TuMV that contain NIb (the viral RNA-dependent RNA polymerase) and viral RNA can move between cells (Grangeon et al., 2013). The intercellular movement of the 6K2 vesicles only occurs in the TuMV-infected cells, suggesting that potyviral cell-to-cell movement can be independent of the virions but requires assistance from other viral proteins. Since I did not observe any intercellular movement of the TuMV CP-deletion mutant virus which retains the full ability to replicate, it would be interesting to determine if and how CP assists in cell-to-cell movement of the 6K2 vesicles.

4.2 Role of CP in TuMV cell-to-cell movement

To further address how CP participates in TuMV cell-to-cell movement, I introduced various deletion and point mutations into the CP coding region of the TuMV infectious clone. The results presented in Chapter 2 suggest that the C-terminus of TuMV CP is a domain essential for TuMV cell-to-cell movement. This is consistent with the findings that the C-termini of TEV CP and SMV CP are crucial for SMV cell-to-cell movement (Dolja et al., 1995; Seo et al., 2013). Since the C-terminus of potyviral CP is exposed on the virions surface (Shukla et al., 1988; Zamora et al., 2017), I speculate that this region is the functional domain that interacts with key factors that are crucial for TuMV intercellular movement, such as various viral proteins and host cellular factors. Further experiments will be necessary to determine whether CP cell-to-cell movement deficient mutants are truly not capable to interact with these key movement factors.

In Chapter 2, I also identified two key amino acid residues located in the core domain of CP that are indispensable for TuMV cell-to-cell movement (Fig 2.5). I further investigated how the cell-to-cell movement deficient mutant R_{178A} failed to move from the primarily infected cells to the neighboring cells. Although I demonstrated that R_{178A} exhibits normal subcellular localization, self-interaction, CI interaction and RNA binding ability (Fig 2.8), I could not exclude the possibility that R_{178A} could fail to interact with other viral proteins and/or host cellular factors with diverse functional roles such as providing a driving force for TuMV movement.

I did find that R_{178A} could not form virions in protoplasts (Fig 2.6), and this is consistent with the findings in TEV and SMV that movement-defective CP mutants were not able to form virions at a detectable level by TEM (Dolja et al., 1994; Seo et al., 2013). Thus, I suggest that there is a correlation between assembly defects and intercellular movement defects among potyviruses, and this raise the possibility that TuMV could move as virions from one cell to another. Furthermore, I showed that R_{178A} is less stable than wild-type CP (Fig 2.9), it would be very interesting to clarify the relationship between CP protein stability and TuMV intercellular movement.

4.3 Role of Patellins in TuMV infection

In the past decades, host-virus interactions have been a hot research area in the field of virology (Daugherty and Malik, 2012; Wang, 2015). A large number of host proteins have been identified and characterized as the viral protein interactors and play an important role in plant virus infection (Wang, 2015; Nagy, 2016). Despite that CP is a multifunctional viral protein and essential player in potyvirus infection, little is known about host proteins that bind to TuMV CP. By using Y2H screen against Arabidopsis cDNA library, I identified 16 host proteins candidates that interact with TuMV CP in yeast (Table 3.1). To our knowledge, this is the first list reporting host protein candidates interact with TuMV CP in yeast and, this report provides valuable information for researchers to better understanding potyvirus-host interactions.

In Chapter 3 I reported Patellin 3 and Patellin 6, two novel Arabidopsis proteins, physically bind to both TuMV CP and CI (Fig 3.1, 3.2 and 3.9). These interactions occur in the cell periphery in the absence of TuMV infection (Fig 3.7). However, upon TuMV infection, a portion of PATL3 but not PATL6 was redistributed to TuMV-induced vesicles which housing potyvirus replication (Fig 3.7 and 3.8). Since CI was reported physically present in TuMV VRCs (Cotton et al., 2009), I speculate PATL3 could target to the VRC through the interaction with CI. Further experiments will be necessary to clarify whether PATL3-CI interactions are relocated within VRCs upon TuMV infection. The interactions between Patellins and CP/CI appear significant as PATL3 and PATL6 inhibit TuMV multiplication in the biological impact analysis (Fig 3.4, 3.5 and 3.6). However, the mechanism by which Patellins inhibit TuMV infection remains unknown and need to be clearly defined.

One possibility is that PATL3, CP and CI could form a tripartite complex since PATL3 could interact with both CP and CI, and PATL3 could disrupt the CP-CI interactions which are critical for TuMV infection (Wang, 2013b; Revers and Garcia, 2015). The second possibility is that PATL3 targets to VRCs and disrupts VRCs assembly. This may be clarified by the comparison of VRCs in wild-type Arabidopsis and PATL3 knockout/overexpression lines upon TuMV infection by using ultrastructural analysis

through TEM. Since PATLs are reported to be involved in membrane trafficking (Peterman et al., 2004; Peiro et al., 2014), another possibility is that PATL3 inhibits TuMV intracellular movement by interfering intracellular movement of viral proteins and/or VRCs. In addition, although I did not detect obvious PD localization when PATLs and CP/CI were co-expressed (Fig 3.2 and 3.9), I cannot exclude the possibility that PATLs inhibit TuMV infection through interference with viral cell-to-cell movement. Lastly, it is reported that PATLs can be significantly phosphorylated upon abiotic stress (Hsu et al., 2009; Cerny et al., 2011; Lv et al., 2014; Mattei et al., 2016), future research needs to be directed to investigate the phosphorylation status of PATLs upon potyvirus infection and further to clarify the relationship between PATLs phosphorylation and TuMV infection.

4.4 Reference

- Brunkard, J.O., Runkel, A.M., and Zambryski, P.C.** (2013). Plasmodesmata dynamics are coordinated by intracellular signaling pathways. *Curr Opin Plant Biol* **16**, 614-620.
- Cerny, M., Dycka, F., Bobal'ova, J., and Brzobohaty, B.** (2011). Early cytokinin response proteins and phosphoproteins of *Arabidopsis thaliana* identified by proteome and phosphoproteome profiling. *J Exp Bot* **62**, 921-937.
- Cotton, S., Grangeon, R., Thivierge, K., Mathieu, I., Ide, C., Wei, T., Wang, A., and Laliberte, J.F.** (2009). Turnip mosaic virus RNA replication complex vesicles are mobile, align with microfilaments, and are each derived from a single viral genome. *J Virol* **83**, 10460-10471.
- Daugherty, M.D., and Malik, H.S.** (2012). Rules of engagement: molecular insights from host-virus arms races. *Annu Rev Genet* **46**, 677-700.
- Dolja, V.V., Haldeman, R., Robertson, N.L., Dougherty, W.G., and Carrington, J.C.** (1994). Distinct functions of capsid protein in assembly and movement of tobacco etch potyvirus in plants. *The EMBO Journal* **13**, 1482-1491.
- Dolja, V.V., Haldeman-Cahill, R., Montgomery, A.E., Vandenbosch, K.A., and Carrington, J.C.** (1995). Capsid Protein Determinants Involved in Cell-to-Cell and Long Distance Movement of Tobacco Etch Potyvirus. *Virology* **206**, 1007-1016.
- Grangeon, R., Jiang, J., Wan, J., Agbeci, M., Zheng, H., and Laliberte, J.F.** (2013). 6K2-induced vesicles can move cell to cell during turnip mosaic virus infection. *Front Microbiol* **4**, 351.
- Hipper, C., Brault, V., Ziegler-Graff, V., and Revers, F.** (2013). Viral and cellular factors involved in Phloem transport of plant viruses. *Front Plant Sci* **4**, 154.
- Hsu, J.L., Wang, L.Y., Wang, S.Y., Lin, C.H., Ho, K.C., Shi, F.K., and Chang, I.F.** (2009). Functional phosphoproteomic profiling of phosphorylation sites in membrane fractions of salt-stressed *Arabidopsis thaliana*. *Proteome Sci* **7**, 42.
- Ivanov, K.I., Eskelin, K., Lohmus, A., and Mäkinen, K.** (2014). Molecular and cellular mechanisms underlying potyvirus infection. *J Gen Virol* **95**, 1415-1429.
- Lv, D.W., Subburaj, S., Cao, M., Yan, X., Li, X., Appels, R., Sun, D.F., Ma, W., and Yan, Y.M.** (2014). Proteome and phosphoproteome characterization reveals new response and defense mechanisms of *Brachypodium distachyon* leaves under salt stress. *Mol Cell Proteomics* **13**, 632-652.
- Mattei, B., Spinelli, F., Pontiggia, D., and De Lorenzo, G.** (2016). Comprehensive Analysis of the Membrane Phosphoproteome Regulated by Oligogalacturonides in *Arabidopsis thaliana*. *Front Plant Sci* **7**, 1107.
- Nagy, P.D.** (2016). Tombusvirus-Host Interactions: Co-Opted Evolutionarily Conserved Host Factors Take Center Court. *Annu Rev Virol* **3**, 491-515.
- Peiro, A., Izquierdo-Garcia, A.C., Sanchez-Navarro, J.A., Pallas, V., Mulet, J.M., and Aparicio, F.** (2014). Patellins 3 and 6, two members of the Plant Patellin family, interact with the movement protein of Alfalfa mosaic virus and interfere with viral movement. *Mol Plant Pathol* **15**, 881-891.
- Peterman, T.K., Ohol, Y.M., McReynolds, L.J., and Luna, E.J.** (2004). Patellin1, a novel Sec14-like protein, localizes to the cell plate and binds phosphoinositides. *Plant Physiol* **136**, 3080-3094; discussion 3001-3082.
- Revers, F., and Garcia, J.A.** (2015). Molecular biology of potyviruses. *Adv Virus Res* **92**, 101-199.
- Sanfaçon, H.** (2005). Replication of positive-strand RNA viruses in plants: contact points between plant and virus components. *Canadian Journal of Botany* **83**, 1529-1549.
- Schoelz, J.E., Harries, P.A., and Nelson, R.S.** (2011). Intracellular transport of plant viruses: finding the door out of the cell. *Mol Plant* **4**, 813-831.

- Seo, J.K., Vo Phan, M.S., Kang, S.H., Choi, H.S., and Kim, K.H.** (2013). The charged residues in the surface-exposed C-terminus of the Soybean mosaic virus coat protein are critical for cell-to-cell movement. *Virology* **446**, 95-101.
- Shukla, D.D., Strike, P.M., Tracy, S.L., Gough, K.H., and Ward, C.W.** (1988). The N and C Termini of the Coat Proteins of Potyviruses Are Surface-located and the N Terminus Contains the Major Virus-specific Epitopes. *Journal of General Virology* **69**, 1497-1508.
- Wang, A.** (2013). Molecular isolation and functional characterization of host factors required in the virus infection cycle for disease control in plants. *CAB Reviews* **8**.
- Wang, A.** (2015). Dissecting the molecular network of virus-plant interactions: the complex roles of host factors. *Annu Rev Phytopathol* **53**, 45-66.
- Zamora, M., Méndez-López, E., Agirrezabala, X., Cuesta, R., Lavín, J.L., Sánchez-Pina, M.A., Aranda, M.A., and Valle, M.** (2017). Potyvirus virion structure shows conserved protein fold and RNA binding site in ssRNA viruses. *Science Advances* **3**.

Curriculum Vitae

Name Zhaoji Dai

Education

2013-present Ph.D. candidate. Biology
The University of Western Ontario
London, Ontario, Canada

2009-2012 M.Sc. Agronomy
Fujian Agriculture and Forestry University
Fuzhou, Fujian, China

2005-2009 B.Sc. Agronomy
Jiangxi Agricultural University
Nanchang, Jiangxi, China

Honors/Awards

2018 American Society For Virology (ASV) Travel Award

2018 Department of Biology travel award, The University of Western Ontario

2013-2018 Western graduate research scholarship (WGRS)

2017 American Society For Virology (ASV) Travel Award

2017 Department of Biology travel award, The University of Western Ontario

2015 American Society For Virology (ASV) Travel Award

Work experience

2013-2018 Teaching Assistant, Department of Biology, The University of Western Ontario

2013-2018 Research Assistant, Agriculture and Agri-Food Canada

Conference oral presentation

Zhaoji Dai, Mark Bernards, Aiming Wang. (2018) Patellin 3 and 6, two members of the Arabidopsis Sec14-GOLD proteins, interact with both the coat protein (CP) and cylindrical inclusion protein (CI) of *Turnip mosaic virus* and inhibit virus accumulation. The 37th annual meeting of ASV. College Park, MD, USA.

Zhaoji Dai, Mark Bernards, Aiming Wang. (2017) Molecular characterization of *Turnip mosaic virus* coat protein (CP) in cell-to-cell movement, long-distance movement and virion assembly. The 36th annual meeting of ASV. Madison, WI, USA.

Zhaoji Dai, Mark Bernards, Aiming Wang. (2015) Molecular characterization of the viral coat protein (CP) in *Turnip mosaic virus* cell-to-cell movement. The 34th annual meeting of ASV. London, ON, CA.